UNIVERSIDADE FEDERAL DE VIÇOSA

Exploring potential effects of microplastic contamination in Antarctic soils

Caik Oliveira de Miranda
Doctor Scientiae

VIÇOSA - MINAS GERAIS
2024

CAIK OLIVEIRA DE MIRANDA

Exploring potential effects of microplastic contamination in Antarctic soils

Thesis submitted to the Soil Science and Plant Nutrition Graduate Program of the Universidade Federal de Viçosa in partial fulfillment of the requirements for the degree of *Doctor Scientiae*.

Adviser: Jose J Lelis Leal de Souza

Co-advisers: Carlos E G R Schaefer
Esperanza Huerta Lwanga

VIÇOSA - MINAS GERAIS
2024

Ficha catalográfica elaborada pela Biblioteca Central da Universidade Federal de Viçosa - Campus Viçosa

T
M672e
2024

Miranda, Caik Oliveira de, 1995-
Exploring potential effects of microplastic contamination in Antarctic soils / Caik Oliveira de Miranda. – Viçosa, MG, 2024.
1 tese eletrônica (154 f.): il. (algumas color.).

Texto em inglês.
Inclui apêndices.
Orientador: José João Lelis Leal de Souza.
Tese (doutorado) - Universidade Federal de Viçosa, Departamento de Solos, 2024.
Inclui bibliografia.
DOI: https://doi.org/10.47328/ufvbbt.2024.811
Modo de acesso: World Wide Web.

1. Solos - Antártica. 2. Solos - Poluição. 3. Microplásticos. 4. Solos - Geomorfologia. I. Souza, José João Lelis Leal de, 1986-. II. Universidade Federal de Viçosa. Departamento de Solos. Programa de Pós-Graduação em Solos e Nutrição de Plantas. III. Título.

CDD 22. ed. 631.40989

Bibliotecário(a) responsável: Bruna Silva CRB-6/2552

CAIK OLIVEIRA DE MIRANDA

Exploring potential effects of microplastic contamination in Antarctic soils

Thesis submitted to the Soil Science and Plant Nutrition Graduate Program of the Universidade Federal de Viçosa in partial fulfillment of the requirements for the degree of *Doctor Scientiae*.

APPROVED: November 14, 2024.

Assent:

Caik Oliveira de Miranda
Author

Jose Joao Lelis Leal de Souza
Adviser

ACKNOWLEDGMENTS

Agradeço
à minha mãe, Sirley, e meu pai, Adilson, pelo amor, apoio e esforços incondicionais; aos meus orientadores JJ, Carlos e Esperanza, pela confiança, oportunidade, ensinamentos e amizade; à Luana, companheira de vida, por todo amor e paciência nos momentos fáceis e difíceis; aos meus irmãos Leonn, Icaro e Vitor, que sei que posso contar para qualquer coisa; ao Mateus, irmão por escolha; à minha família; aos meus amigos de Viçosa Rafael, Bruno e Saymon, presentes durante toda minha caminhada; aos meus amigos de Viçosa e de Vitória, grande segunda família; aos companheiros e amigos desta e de outras gerações do Terrantar; aos colegas professores, técnicos e estudantes do departamento; à instituição Universidade Federal de Viçosa, ao PPGSNP e ao Departamento de Solos; ao CNPq, pela concessão da bolsa de estudos; à CAPES, pela concessão da bolsa de estudos no exterior; ao Programa Antártico Brasileiro, por proporcionar meios para realização desta pesquisa; to colleagues from the SLM Group of the Wageningen University; a todos não mencionados que contribuíram de alguma forma com a minha jornada do doutorado.

Sem vocês não seria possível.
ini

This study was financed in part by the Coordenação de Aperfeiçoamento de Pessoal de Nível Superior – Brasil (CAPES) – Finance Code 001.
This study was financed in part by the Conselho Nacional de Desenvolvimento Científico e Tecnológico – Brasil (CNPq)

ABSTRACT

MIRANDA, Caik Oliveira de, D.Sc., Universidade Federal de Viçosa, November, 2024. **Exploring potential effects of microplastic contamination in Antarctic soils**. Adviser: Jose Joao Lelis Leal de Souza. Co-advisers: Carlos Ernesto Goncalves Reynaud Schaefer and Esperanza Huerta Lwanga.

Microplastics (MPs; diameter < 5.0 mm) are currently considered ubiquitous contaminants in several environmental matrices around the planet, occurring in a wide range of shapes, sizes, and polymeric compositions. MPs have been recognized as a potential threat to terrestrial ecosystems, in part due to their significant impacts on soil ecosystems. The Antarctic continent is a pristine environment, geographically isolated and dedicated to environmental conservation and scientific studies. Nevertheless, Antarctica has a historical record of anthropogenic pollution, including the presence of MPs in both terrestrial and marine environmental compartments, including soils, which play a crucial role in ecological processes. Despite evidence of MP contamination in Antarctic terrestrial environments, the potential impacts of such contamination on its soils remain largely unknown. This thesis explored the potential impacts of MP presence in Antarctic soils, focusing on evaluating the physical and chemical properties of soils artificially contaminated with MPs and addressing processes driven by freeze-thaw cycles (FTCs). In a first experiment (Chapter I), short-term impacts of contamination by two types of MPs [polyacrylonitrile (PAN) fibers and polyethylene (PE) fragments], added in different concentrations (from 0.001% to 1.0% w w-1), in an Antarctic marine terrace soil were investigated. Rebuilt soil samples in pots were incubated under field conditions for 22 days, with CO2 fluxes monitored every two days. After this period, soil physical and chemical parameters and microbial activity were evaluated. The results showed effects depending on MP type and dose. In general, PAN fibers at high concentrations (0.1%) increased soil porosity and hydraulic conductivity, possibly addressing the observed increase in mean CO2 fluxes. PE fragments did not affect porosity but decreased soil bulk density. The presence of both types of MPs increased soil microbial activity and decreased cation exchange capacity. Potential causes and implications of the observed impacts were discussed. The experimental units from the first experiment were used for a descriptive analysis of thin sections using micromorphological techniques and concepts (Chapter II). Microphotographs evidenced the interaction of MP particles with the soil matrix. PE fragments were observed as part of the soil matrix and clogging pores – corroborating the decrease in hydraulic conductivity – and

frequent vesicular and planar pores were observed in samples containing PAN fibers. Features such as clay capping, the presence of ovoidal peds, and planar/vesicular pores suggest the occurrence of processes related to FTCs, even within the short incubation period. Clay capping features on MP particles suggest a possible interaction with active pedogenetic processes in Antarctic periglacial environments. In a second experiment (Chapter III), the potential for MP vertical migration in three different types of Antarctic soils under successive FTC conditions and cumulative impacts on soil physical parameters (porosity and bulk density) were investigated. Soil columns (12.5 cm) with three layers containing or not containing MPs (0.01% v v-1) in a surface layer (2.5 cm) were prepared. Three types of MPs [PE, polyethylene terephthalate (PET), and polylactic acid (PLA)] were used to evaluate potential selective migration. After 44 days of incubation, with or without FTCs, MPs and soil physical parameters were analyzed. The abundance of MPs in the second (2.5 – 7.5 cm) and third (7.5 – 12.5 cm) layers of the soil columns relative to the surface layer, particle diameter, and soil physical parameters were compared across treatments, soil types, and layers. The results confirmed vertical MP migration, depending on soil type, MP type, and the occurrence of FTCs. The soil with higher porosity and organic matter content (S3) showed higher relative MP abundance in the lower layers of soil columns, but FTCs representatively facilitated particle migration in columns of the most weathered and finer-textured soil (S1). PE particles and smaller diameter particles were more abundant in the lower layers of the columns. FTCs caused soil subsidence, increased (macro) porosity in the surface layer, and compaction of the lower layers of the columns, and MPs decreased soil bulk density in S1 columns subjected to FTCs. Potential processes involved on the observed results were discussed. This thesis demonstrated that MP contamination in soils can affect at short-term scale the microbial activity, and soil physical and chemical properties differently according on MP type and soil type, and that active pedogenetic processes in Antarctic periglacial environments interact with MPs, potentially facilitating their vertical migration. However, future studies are needed to better understand the long-term ecological implications of MP contamination in terrestrial ecosystems of Antarctica.

Keywords: soil pollution; plastic pollution; maritime antarctica; soil micromorphology; freezing and thawing cycles

RESUMO

MIRANDA, Caik Oliveira de, D.Sc., Universidade Federal de Viçosa, novembro de 2024. **Explorando potenciais efeitos da contaminação por microplásticos em solos antárticos**. Orientador: Jose Joao Lelis Leal de Souza. Coorientadores: Carlos Ernesto Goncalves Reynaud Schaefer e Esperanza Huerta Lwanga.

Microplásticos (MPs; diâmetro < 5.0 mm) são atualmente considerados contaminantes ubíquos em diversas matrizes ambientais ao redor do planeta, ocorrendo em diversas formas, tamanhos e composições químicas. MPs têm sido reconhecidos como uma ameaça potencial para ecossistemas terrestres, em parte por proporcionarem impactos significativos à ecossistemas do solo. O continente Antártico é um ambiente pristino, geograficamente isolado e dedicado à conservação ambiental e estudos científicos. Mesmo assim, a Antártica possui registros históricos de poluição antrópica que inclui a presença de MPs em compartimentos ambientais terrestres e marinhos, incluindo os solos, que desempenham papel fundamental em processos ecológicos. Apesar das evidências da contaminação por MPs em ambientes terrestres da Antártica, os potenciais impactos desse tipo de contaminação nos seus solos ainda são amplamente desconhecidos. A presente tese explorou potenciais impactos da presença de MPs em solos antárticos, com foco em avaliar propriedades físicas e químicas de solos artificialmente contaminados com MPs, e abordar processos promovidos pela condição de ciclos de congelamento e descongelamento. Em um primeiro experimento (Capítulo I), foram investigados impactos a curto prazo da contaminação por dois tipos de MPs [fibras de poliacrilonitrila (PAN) e fragmentos de polietileno (PE)], adicionados em diferentes concentrações (de 0.001% a 1.0% w w-1), em um solo de terraço marinho antártico. Amostras de solo reconstruídas em potes foram incubadas em condições de campo por 22 dias, com monitoramento de fluxos de CO2 a cada dois dias, e, após esse período, foram avaliados parâmetros físicos, químicos e atividade microbiana do solo. Os resultados mostraram efeitos dependentes da dose e do tipo de MP. Em geral, fibras PAN em altas concentrações (0.1%) aumentaram a porosidade e condutividade hidráulica do solo, possivelmente justificando um aumento observado nos fluxos médios de CO2. Fragmentos PE não afetaram a porosidade, mas diminuíram a densidade do solo. A presença de ambos os tipos de MPs aumentou a atividade microbiana do solo e reduziu a capacidade de troca catiônica. Potenciais causas e implicações dos impactos observados foram discutidos. As unidades experimentais do primeiro experimento foram utilizadas para a análise descritiva de lâminas delgadas utilizando técnicas

e conceitos de micromorfologia dos solos (Capítulo II). A análise de microfotografias permitiu identificar a interação das partículas de MPs com a matriz do solo. Foi possível observar fragmentos PE como parte da matriz do solo e obstruindo poros – corroborando o decréscimo na condutividade hidráulica – e a presença frequente de poros vesiculares e planares em amostras contendo fibras PAN. Feições como revestimento por argila, presença de peds ovoidais, e poros planares e vesiculares sugerem a ocorrência de processos relacionados a ciclos de congelamento e descongelamento (FTCs), mesmo com o curto período de incubação. Feições de revestimento por argila em partículas de MPs sugerem uma possível interação com processos pedogenéticos atuantes em ambientes periglaciais da Antártica. Em um segundo experimento (Capítulo III), foi investigado o potencial de migração vertical de MPs em três diferentes tipos de solos Antárticos sob condições de sucessivos FTCs e cumulativos impactos em parâmetros físicos do solo (porosidade e densidade do solo). Foram preparadas colunas de solo (12.5 cm) com três camadas contendo ou não a presença de MPs (0.01% v v-1) em uma camada superficial (2.5 cm). Três tipos de MPs [PE, tereftalato de polietileno (PET), ácido polilático (PLA)] foram utilizados para avaliar potencial de migração seletiva. Após incubação de 44 dias submetidos ou não à FTCs, foi realizada análise de MPs e parâmetros físicos do solo. Números de abundância de MPs na segunda (2.5 – 7.5 cm) e terceira (7.5 – 12.5 cm) camadas das colunas de solo relativo à abundância na camada superficial, diâmetro de partículas, e parâmetros físicos do solo foram comparados entre tratamentos, tipos de solo e camada. Os resultados confirmaram a migração vertical de MPs, dependendo do tipo de solo, tipo de MP, e ocorrência de FTCs. O solo com maior porosidade e teor de matéria orgânica (S3) apresentou maiores números de abundância relativa de MPs em camadas inferiores das colunas, mas FTCs facilitaram a migração de partículas de forma mais representativa em colunas do solo mais intemperizado e de textura mais fina (S1). Partículas PE e de menor diâmetro foram mais abundantes nas camadas inferiores das colunas. FTCs causaram subsidência do solo, aumento da porosidade (macro) na camada superficial e compactação de camadas inferiores das colunas. MPs diminuíram a densidade do solo de colunas de S1 que passaram FTCs. Os processos potencialmente envolvidos de acordo com os resultados observados foram discutidos. Nesta tese foi demonstrado que a contaminação por MPs no solo afeta em escala de curto prazo a atividade microbiana, e propriedades físicas e químicas diferenciadamente de acordo com o tipo de MP e tipo de solo, e que processos pedogenéticos ativos em ambientes periglaciais da Antártica interagem com MPs potencialmente facilitando sua migração vertical. Entretanto ressalta-se a necessidade de estudos futuros para

melhor avaliação das implicações ecológicas da contaminação por MPs em ecossistemas terrestres da Antártica a longo prazo.

Palavras-chave: poluição do solo; poluição plástica; antártica marítima; micromorfologia de solos; ciclos de congelamento e descongelamento

SUMMARY

GENERAL INTRODUCTION AND OBJECTIVES 12

CHAPTER I Short-term impacts of polyethylene and polyacrylonitrile microplastics on soil physicochemical properties and microbial activity of a marine terrace environment in Maritime Antarctica 16

1 INTRODUCTION 18

2 MATERIALS AND METHODS 21

2.1 Soil and site description 21

2.2 Microplastic addition and experimental set up 21

2.3 In situ CO_2 flux measurements 23

2.4 Soil analysis 23

2.5 Statistical analysis 24

3 RESULTS 26

3.1 Impacts on soil physical properties 26

3.2 Impacts on soil chemical properties 27

3.3 Impacts on soil respiration and microbial activity 29

3.4 Principal component analysis 30

4 DISCUSSION 31

5 CONCLUSIONS 36

6 ACKNOWLEDGEMENTS 37

7 REFERENCES 38

8 SUPPLEMENTARY MATERIAL FOR CHAPTER I 48

8.1 Supporting figures 48

8.2 Supporting tables 52

CHAPTER II Interactions of microplastics with an Antarctic marine terrace soil revealed by descriptive thin sections analysis 58

1 INTRODUCTION 60

2 MATERIALS AND METHODS 62
2.1 Site and soil descriptions 62
2.2 Microplastics spiking to the soil 63
2.3 Experimental setup 63
2.4 Soil physical properties and thin section analysis 64
3 RESULTS 65
4 DISCUSSION 70
5 CONCLUSIONS 73
6 ACKNOWLEDGMENTS 74
7 REFERENCES 75
8 SUPPLEMENTARY MATERIAL FOR CHAPTER II 83
8.1 Supporting figures 83
8.2 Supporting tables 84
CHAPTER III Microplastic vertical migration and physical properties in Antarctic soils under successive freezing-thawing cycles 90
1 INTRODUCTION 92
2 MATERIALS AND METHODS 96
2.1 Soil description 96
2.2 Experimental set up 97
2.2.1 Microplastics and soil columns preparation 97
2.2.2 Freeze-thaw cycles incubation 98
2.3 MPs analysis: background levels and experimental samples 99
2.3.1 MPs extraction from the soil samples 99
2.3.2 Laser Direct Infrared (LDIR) spectroscopy analysis 100
2.3.3 QA/QC for MPs analysis 101
2.4 Soil physical parameters: porosity and bulk density 101
2.5 Statistical analysis 102

3 RESULTS 104
3.1 Potential for MP vertical migration in Antarctic soils under successive FTCs condition 104
3.2 Impacts of MPs and FTCs on porosity and bulk density of Antarctic soils 107
3.3 MP analysis: background levels 110
4 DISCUSSION 112
4.1 Potential for MPs vertical migration in Antarctic soils under successive FTCs condition 112
4.2 Impacts of MPs and FTCs on physical parameters of Antarctic soils 115
4.3 Background MP levels in three Antarctic soils 116
5 CONCLUSIONS 119
6 ACKNOWLEDGEMENTS 120
7 REFERENCES 121
8 SUPPLEMENTARY MATERIAL FOR CHAPTER III 133
8.1 Section 1 – Supporting Figures and Tables 133
8.1.1 Supporting Figures 133
8.1.2 Supporting Tables 136
8.2 Section 2 – MP analysis control samples 140
8.2.1 Negative control (blank samples) correction 140
8.2.2 Positive control for microplastic analysis: recovery rate 152
FINAL CONSIDERATIONS 154

GENERAL INTRODUCTION AND OBJECTIVES

The Antarctic continent is a pristine and isolated environment that plays a fundamental role in global climate and ecosystem dynamics; therefore it is reserved for environmental conservation and scientific study purposes by the Protocol on Environmental Protection to the Antarctic Treaty (CEP, 1991). Antarctica is vulnerable to environmental impacts resulting from local and global anthropogenic activities (Kejna; Arazny; Sobota, 2013; Tin *et al.*, 2009). Plastic pollution – especially microplastics (MPs; < 5.0 mm) – has been recognized as a significant issue, as MPs have recently been detected as contaminants in several compartments of marine (Munari *et al.*, 2017; Reed *et al.*, 2018; Zhu *et al.*, 2023) and terrestrial environments (Aves *et al.*, 2022; González-Pleiter *et al.*, 2020; Perfetti-Bolaño *et al.*, 2022), including biota (Bessa *et al.*, 2019; Kim *et al.*, 2023). The presence of MPs in soils impacts physical and chemical properties (Ingraffia *et al.*, 2022; Lehmann *et al.*, 2021; Qi *et al.*, 2020), soil fauna and microbiota (Lin *et al.*, 2020; Rillig; Kim; Zhu, 2023; Sun *et al.*, 2022), plant performance (Machado *et al.*, 2019; Qi *et al.*, 2018), and can drive influential processes for climate change (Ren *et al.*, 2020; Rillig *et al.*, 2021; Sunil *et al.*, 2024). In Antarctica, soils perform ecosystem services and regulate terrestrial ecological processes, driving biological, hydrological, chemical and nutrient cycling processes (de Souza *et al.*, 2012; Guo *et al.*, 2018; Lopes *et al.*, 2021; Santamans *et al.*, 2017; Thomazini *et al.*, 2016). Therefore, evidence of MP contamination in Antarctic soils (He *et al.*, 2024; Kukharchyk; Kakareka; Rabychyn, 2024; Perfetti-Bolaño *et al.*, 2022) raises concerns about potential resulting impacts, which have not yet been widely explored.

As a consultative member of the Antarctic Treaty, Brazil is responsible for maintaining regular scientific production, environmental monitoring and risk assessments, and participating in decision-making meetings about activities carried out in the Antarctic continent. In addition to contributing to enriching the understanding of the potential impacts of MP contamination in Antarctic soils, the research carried out in this thesis contributes to the fulfillment of Brazilian responsibilities under the scope of the Antarctic Treaty, strengthening scientific production of the country and fostering initiatives to mitigate and monitor environmental impacts on the continent.

The thesis has three chapters structured in the format of independent scientific papers. According to the context presented, the general objectives of this thesis were:

- Investigate the potential impacts of the presence of microplastics on the microbial activity, physical and chemical properties of marine terrace soil in Maritime Antarctica (Chapter I)
- Evaluate the interaction of microplastics with Antarctic marine terrace soil using soil micromorphology techniques and concepts (Chapter II)
- Verify the potential for vertical migration of microplastics in different Antarctic soils subjected to freezing and thawing cycles (Chapter III)
- Evaluate the impacts of the presence of microplastics on the physical properties of different Antarctic soils in subjected to freezing and thawing cycles (Chapter III)

References

AVES, Alex R. *et al.* First evidence of microplastics in Antarctic snow. Cryosphere, [*s. l.*], v. 16, n. 6, p. 2127–2145, 2022.

BESSA, Filipa *et al.* Microplastics in gentoo penguins from the Antarctic region. Scientific Reports, [*s. l.*], v. 9, n. 1, p. 1–7, 2019.

CEP, (Committee of Environmental Protection). Protocol on Environmental Protection to the Antartic Treaty. Antarctic Treaty: [*s. n.*], 1991.

DE SOUZA, José João L.L. *et al.* Hydrogeochemistry of sulfate-affected landscapes in Keller Peninsula, Maritime Antarctica. Geomorphology, [*s. l.*], v. 155–156, p. 55–61, 2012.

GONZÁLEZ-PLEITER, Miguel *et al.* First detection of microplastics in the freshwater of an Antarctic Specially Protected Area. Marine Pollution Bulletin, [*s. l.*], v. 161, n. October, p. 1–6, 2020.

GUO, Yudong *et al.* Direct and indirect effects of penguin feces on microbiomes in Antarctic ornithogenic soils. Frontiers in Microbiology, [*s. l.*], v. 9, n. APR, 2018.

HE, Jianuo *et al.* Record of microplastic deposition revealed by ornithogenic soil and sediment profiles from Ross Island, Antarctica. Environmental Research, [*s. l.*], v. 262, 2024.

INGRAFFIA, Rosolino *et al.* Polyester microplastic fibers affect soil physical properties and erosion as a function of soil type. Soil, [*s. l.*], v. 8, n. 1, p. 421–435, 2022.

KEJNA, Marek; ARAZNY, Andrzej; SOBOTA, Ireneusz. Climatic change on King George Island (West Antarctica) in the years 1948– 2011. Polish Polar Research, [*s. l.*], v. 34, n. 2, p. 213–235, 2013.

KIM, Youmin *et al.* Microplastics in gastrointestinal tracts of gentoo penguin (Pygoscelis papua) chicks on King George Island, Antarctica. Scientific Reports, [*s. l.*], v. 13, n. 1, p. 1–11, 2023.

KUKHARCHYK, T I; KAKAREKA, S V; RABYCHYN, K O. Microplastics in Soils of the Thala Hills, East Antarctica. [*s. l.*], v. 57, n. 3, p. 502–512, 2024.

LEHMANN, Anika *et al.* Microplastics have shape- and polymer-dependent effects on soil aggregation and organic matter loss – an experimental and meta-analytical approach. Microplastics and Nanoplastics, [*s. l.*], v. 1, n. 1, p. 1–14, 2021.

LIN, Dunmei *et al.* Microplastics negatively affect soil fauna but stimulate microbial activity: insights from a field-based microplastic addition experiment. Proceedings of the Royal Society B: Biological Sciences, [*s. l.*], v. 287, n. 1934, 2020.

LOPES, Davi do Vale *et al.* Hydrogeochemistry and chemical weathering in a periglacial environment of Maritime Antarctica. Catena, [*s. l.*], v. 197, n. June 2020, p. 104959, 2021.

MACHADO, Anderson Abel de Souza *et al.* Microplastics Can Change Soil Properties and Affect Plant Performance. Environmental Science and Technology, [*s. l.*], v. 53, n. 10, p. 6044–6052, 2019.

MUNARI, Cristina *et al.* Microplastics in the sediments of Terra Nova Bay (Ross Sea, Antarctica). Marine Pollution Bulletin, [*s. l.*], v. 122, n. 1–2, p. 161–165, 2017.

PERFETTI-BOLAÑO, Alessandra *et al.* Occurrence and Distribution of Microplastics in Soils and Intertidal Sediments at Fildes Bay, Maritime Antarctica. Frontiers in Marine Science, [*s. l.*], v. 8, n. February, 2022.

QI, Yueling *et al.* Impact of plastic mulch film debris on soil physicochemical and hydrological properties. Environmental Pollution, [*s. l.*], v. 266, p. 115097, 2020.

QI, Yueling *et al.* Macro- and micro- plastics in soil-plant system: Effects of plastic mulch film residues on wheat (Triticum aestivum) growth. Science of the Total Environment, [*s. l.*], v. 645, p. 1048–1056, 2018.

REED, Sarah *et al.* Microplastics in marine sediments near Rothera Research Station, Antarctica. Marine Pollution Bulletin, [*s. l.*], v. 133, 2018.

REN, Xinwei *et al.* Effects of microplastics on greenhouse gas emissions and the microbial community in fertilized soil. Environmental Pollution, [*s. l.*], v. 256, 2020.

RILLIG, Matthias C. *et al.* Microplastic fibers affect dynamics and intensity of CO2 and N2O fluxes from soil differently. Microplastics and Nanoplastics, [*s. l.*], v. 1, n. 1, p. 1–11, 2021.

RILLIG, Matthias C.; KIM, Shin Woong; ZHU, Yong Guan. The soil plastisphere. Nature Reviews Microbiology, [*s. l.*], 2023.

SANTAMANS, Anna C. *et al.* Soil features in rookeries of Antarctic penguins reveal sea to land biotransport of chemical pollutants. PLOS ONE, [*s. l.*], v. 12, n. 8, p. e0181901, 2017.

SUN, Yuanze *et al.* Deciphering the Mechanisms Shaping the Plastisphere Microbiota in Soil. mSystems, [*s. l.*], v. 7, n. 4, 2022.

SUNIL, Syama *et al.* Microplastics and climate change: the global impacts of a tiny driver. [*S. l.*]: Elsevier B.V., 2024.

THOMAZINI, A. *et al.* Geospatial variability of soil CO2-C exchange in the main terrestrial ecosystems of Keller Peninsula, Maritime Antarctica. Science of the Total Environment, [*s. l.*], v. 562, p. 802–811, 2016.

TIN, T. *et al.* Impacts of local human activities on the Antarctic environment. Antarctic Science, [*s. l.*], v. 21, n. 1, p. 3–33, 2009.

ZHU, Wenbin *et al.* Microplastics in Antarctic krill (Euphausia superba) from Antarctic region. Science of the Total Environment, [*s. l.*], v. 870, n. January, p. 161880, 2023.

CHAPTER I

Short-term impacts of polyethylene and polyacrylonitrile microplastics on soil physicochemical properties and microbial activity of a marine terrace environment in Maritime Antarctica[1]

[1] The content of this chapter is a full reproduction of the article published in the journal Environmental Pollution, under the Digital Object Identifier (DOI): https://doi.org/10.1016/j.envpol.2024.123791

ABSTRACT

Evidence of microplastic (MP) pollution in Antarctic terrestrial environments reinforces concerns about its potential impacts on soil, which plays a major role in ecological processes at ice-free areas. We investigated the effects of two common MP types on soil physicochemical properties and microbial responses of a marine terrace from Fildes Peninsula (King George Island, Antarctica). Soils were treated with polyethylene (PE) fragments and polyacrylonitrile (PAN) fibers at environmentally relevant doses (from 0.001% to 1% w w^{-1}), in addition to a control treatment (0% w w^{-1}), for 22 days in a pot incubation experiment under natural field conditions. The short-term impacts of MPs on soil physical, chemical and microbial attributes seem interrelated and were affected by both MP dose and type. The highest PAN fiber dose (0.1%) increased macro and total porosity, but decreased soil bulk density compared to control, whereas PE fragments treatments did not affect soil porosity. Soil respiration increased with increasing doses of PAN fibers reflecting impacts on physical properties. Both types of MPs increased microbial activity (fluorescein diacetate hydrolysis), decreased the cation exchange capacity but, especially PE fragments, increased Na^+ saturation. The highest dose of PAN fibers and PE fragments increased total nitrogen and total organic carbon, respectively, and both decreased the soil pH. We discussed potential causes for our findings in this initial assessment and addressed the need for further research considering the complexity of environmental factors to better understand the cumulative impacts of MP pollution in Antarctic soil environments.

Keywords: fibers, fragments, soil pollution, soil health, Antarctic soil, Fildes Peninsula

1 INTRODUCTION

Microplastic (MP) pollution is a consequence of inappropriate use and disposal of plastics and a recognized global environmental concern as it becomes widespread in several marine and terrestrial ecosystems (Campanale *et al.*, 2022; Horton *et al.*, 2017; Lebreton; Egger; Slat, 2019), posing potential risks to living organisms (Khalid *et al.*, 2021; Ma *et al.*, 2023; Yang *et al.*, 2021). MP occurrence in terrestrial environments is more representative in areas of high population density and intensive anthropic activities, but it can also reach remote regions (Büks; Kaupenjohann, 2020). Field research and atmospheric/oceanic modeling have shown that global dispersion can support the occurrence of MPs in areas with low population density in coastal and high-altitude areas, from low to high latitudes (Evangeliou *et al.*, 2020; Godoy *et al.*, 2022; Isobe *et al.*, 2017; Lusher *et al.*, 2015; Onink *et al.*, 2019). Hence, despite geographic isolation, low human occupation, and protection under international law, the Antarctic continent is not exempt from MP pollution (Rota *et al.*, 2022).

Plastic pollution has been reported in Antarctica since the 1980s (van Franeker; Bell, 1988), and has become the most common and enduring evidence of past and recent human activities at some coastal Antarctic sites (Bargagli; Rota, 2023). Most debris reported from islands around continental Antarctica are historic remnants of man-made debris since the beginning of human exploration, increasing recognition and concern over its impact on marine birds and seals (Convey; Barnes; Morton, 2002). Recently, MPs have been detected in several compartments of the Antarctic marine (Kelly *et al.*, 2020; Munari *et al.*, 2017; Suaria *et al.*, 2020) and terrestrial (Aves *et al.*, 2022; González-Pleiter *et al.*, 2020; Perfetti-Bolaño *et al.*, 2022) environments, including the biota inhabiting these ecosystems (Bergami *et al.*, 2020; Bessa *et al.*, 2019; Fragão *et al.*, 2021). External sources of MP contamination by long-distance transport are usually considered (González-Pleiter *et al.*, 2020; Isobe *et al.*, 2017; Lozoya *et al.*, 2022), but it is evident that the highest concentrations of MPs in Antarctica occur near anthropic activities (Lacerda *et al.*, 2019; Munari *et al.*, 2017).

Coastal research stations act as localized sources of MPs for water and marine sediments, especially fibers originating from washing clothes (Cincinelli *et al.*, 2017; Munari *et al.*, 2017), and wind action can contribute to their dispersion and deposition with snow in inland terrestrial environments (Aves *et al.*, 2022; González-Pleiter *et al.*, 2020). The Fildes Peninsula (King George Island) hosts six permanent scientific bases and the sole airport of South Shetlands Islands, therefore the anthropic pressure is enormous (Lu *et al.*, 2012) and includes the

widespread presence of MPs (Lozoya *et al.*, 2022). The Peninsula was subject of the first assessment of soil MPs in Antarctica, which suggested land use and occupation as the main sources of MP fragments (Perfetti-Bolaño *et al.*, 2022). Human occupation in Antarctica occurs mainly in ice-free areas of periglacial environments, which represent less than 0.5% of the continent's area (Brooks *et al.*, 2019). In these sensitive environments, soil acts as the main mediator of terrestrial ecological processes in Antarctica, mediating the cycling of nutrients and chemical, hydrological, and biological processes (Lopes *et al.*, 2021; Simas *et al.*, 2007; Thomazini *et al.*, 2015a).

However, MPs can change soil properties and may affect their ability to perform multifunctional ecosystem functions (Chia *et al.*, 2022; Qiu *et al.*, 2022; Wan *et al.*, 2023). MPs impacts soil physical properties such as aggregation, bulk density, porosity, and water dynamics (Machado *et al.*, 2018; Qi *et al.*, 2020; Zhang; Zhang; Li, 2019), as well as soil chemical properties, such as soil pH, nutrient availability and adsorption reactions (Boots; Russell; Green, 2019; Li; Liu, 2022; Zhang *et al.*, 2020). Consequently, MPs triggers responses in the soil microbiota (Rillig *et al.*, 2021; Zhao; Lozano; Rillig, 2021). Furthermore, as MPs are heterogeneous contaminants, their effects on soil properties are different in relation to shape, size, polymeric composition and concentration (Lehmann *et al.*, 2021; Wan *et al.*, 2023). For example, PE MPs tend to decrease soil pH (Boots; Russell; Green, 2019; Yu *et al.*, 2020) and microbial activity (Fei *et al.*, 2020) while polypropylene (PP) MPs present an opposite behavior (Liu *et al.*, 2017; Zhao; Lozano; Rillig, 2021). Alternatively, fibers often promote negative impacts on soil structure but other shapes do not have such obvious responses (Lehmann *et al.*, 2021).

The effects of MPs are also dependent on soil type and environmental conditions. Inherent soil characteristics affect the interaction between MPs and natural soil particles, which tend to be more efficient in soils with higher clay and organic matter contents (Guo *et al.*, 2022; Ingraffia *et al.*, 2022; Liang *et al.*, 2021). The exposure of MP polluted soils to different temperature and moisture conditions also mediates the effects on soil properties such as aggregation, microbial activity and organic matter decomposition (Liang *et al.*, 2019; Lozano *et al.*, 2021a; Zhang; Zhang; Li, 2019). In general, periglacial soils of Maritime Antarctic coastal areas are poorly weathered, poorly structured and coarse (Bockheim, 2014), being constantly subject to physical (e.g. cryoturbation) (Chaves *et al.*, 2017; Michel *et al.*, 2014), biological and chemical dynamics (e.g. ornithogenic influence) (Guo *et al.*, 2018; Lopes *et al.*, 2021; Simas *et al.*, 2007). However, despite the evidence of MPs occurring in terrestrial environments of Maritime Antarctica

(González-Pleiter *et al.*, 2020; Perfetti-Bolaño *et al.*, 2022), potential impacts on their soils are still largely unknown.

Here we used well-established soil physical, chemical, and microbial response parameters to perform the first exploratory assessment of potential disturbances caused by the presence of two usual MP types (PAN fibers and PE fragments) in an Antarctic marine terrace bare soil on the Fildes Peninsula (King George Island, Maritime Antarctica) through a pot experiment under field conditions. Field experimentation was prioritized to account for actual daily temperature and moisture variations, which drive microbial metabolism and nutrient cycling in Antarctic soils (Pires *et al.*, 2017; Thomazini *et al.*, 2020), seeking to provide insights and guide further research based on representative natural conditions. With this experimental setup we expected that significant impacts on soil properties would be observed on a short-term scale and the effects would be distinct for the different MP types (polymer and shape) and applied doses.

2 MATERIALS AND METHODS

2.1 Soil and site description

The tested soil was sampled in February 2022 on the Fildes Peninsula, Maritime Antarctica (62º13'S; 58º57'W), in a marine terrace environment susceptible to flooding by ice melt drainage streams, with sparse mossy vegetation, approximately 50 m from the coastline and 13 m a.s.l. (Figure S1). This area was selected for the experiment because this type of environment is susceptible to MP contamination in Antarctica, both by the runoff of fresh meltwater streams and by coastal maritime influence (González-Pleiter *et al.*, 2020; Perfetti-Bolaño *et al.*, 2022). Fildes Peninsula is one of the main entrances for ships and airplanes to the Maritime Antarctica region, and a major hub of anthropic activities. Soils in the study area are mostly formed by transported sediments of basaltic and andesitic origin, resulting from periglacial and isostatic uplift processes (Michel *et al.*, 2014), which are common conditions on marine terraces in the Maritime Antarctic region (López-Martínez *et al.*, 2012). The clay mineralogy in the area is predominantly composed of chlorites, micas and smectites (Pelayo *et al.*, 2022). The experiment was performed during the Antarctic summer (Zacharias; Setzer, 2004), in February and March 2022. The actual mean daily air temperature in the area ranged between -1.1 and 5.5 ºC, with cumulative liquid precipitation of 16.4 mm distributed over 13 days, cumulative snow precipitation of 4 cm distributed over 3 days, and mean UVB radiation index of 1 and maximum of 3 (Chilean meteorological service – station 950001).

The soil (~ 25 kg) was sampled with a hoe and a metal trowel at a 0-15 cm depth, in the transition between a poorly structured sandy surface horizon, and a clayey subsurface horizon with a stronger developed structure of plastic consistency and characteristic features of occurrence of expansive clays (Figure S1). After sampling, the soil was sieved in the field at ambient temperature through a 2 mm mesh to remove granules and pebbles, and the fraction that passed through the sieve was used for the experiment. The physical and chemical characteristics of the soil used in the experiment are presented in Table S1.

2.2 Microplastic addition and experimental set up

The experiment tested the effect of two types of MPs: polyacrylonitrile (PAN) fibers and polyethylene (PE) fragments (Figure S2). PE is primarily used in single-use plastic packaging and is one of the most common polymeric composition of MPs found in coastal environmental samples, where fragments are generally high in low density polymers like PE (Erni-Cassola *et*

al., 2019; Hale *et al.*, 2020; Koutnik *et al.*, 2021). Fibers are the most common shape found even in Antarctic ecosystems (Fragão *et al.*, 2021; González-Pleiter *et al.*, 2020; Hale *et al.*, 2020), where PAN fibers, used as synthetic wool for clothing, have been found in Antarctic biota (Bessa *et al.*, 2019) and shown high toxicity for soil nematodes (*C. elegans*) (Kim *et al.*, 2020). The PAN fibers were obtained by manually cutting 100% "Mollet" acrylic threads (Círculo S/A, São Paulo, Brazil; product No. 781), with mean size of 2818 µm (± 1193 µm; min = 635 µm, max = 5463 µm; n = 55). The virgin PE fragments were acquired from Bianquímica (São Paulo, Brazil; product No. MLB1282396142), with mean size of 407 µm (± 369 µm; min = 31 µm, max = 2644 µm; n = 205). Both MP types were microwaved for 3 min (500 W) to minimize the risk of microbial contamination (Machado *et al.*, 2019), and stored in sterilized glass bottles until their addition to the soil. Microwaving did not cause visible damage or melting of the MPs according to a stereomicroscope inspection.

Fragment doses were 0.01, 0.1 and 1.0% wet weight, and fiber doses were 0.001, 0.01 and 0.1% wet weight, so that the soil presented minimal differences in volume with MP particles effectively blended to the soil matrix (Machado *et al.*, 2018). The doses were calculated by wet weight since the experiment was set up in situ without access to drying oven resources. This range of doses has been widely reproduced in experiments with soil MPs, which can cause noticeable changes in soil properties (Colzi *et al.*, 2022; Li; Liu, 2022; Pignattelli; Broccoli; Renzi, 2020). Considering real conditions found in environmental samples of highly polluted sites (Fuller; Gautam, 2016; Scheurer; Bigalke, 2018; Wang *et al.*, 2020), these doses simulate the worst future scenarios of MP pollution in Antarctic terrestrial environments (Perfetti-Bolaño *et al.*, 2022).

The MPs were weighed (± 0.001 g) and mixed at the predetermined doses with 3 kg of soil in a 100 L polyethylene bag by vigorous stirring supported by a metal spatula. After mixing, each experimental unit was prepared with 700 g of spiked wet soil, which were stored without compaction in conical polypropylene pots (h = 8 cm, upper diameter = 11 cm, lower diameter = 9.5 cm) with bottom holes (3 mm diameter) to allow water percolation. The soil moisture during the experiment set up was 27%. Four replicates for each treatment plus the control (without MP addition) were prepared, totaling 28 experimental units that were partially buried in the same soil sample site, side by side, in random positions, to simulate real field conditions (Figure S1E). After 22 days, the pots were removed and stored frozen until the analyses were carried out. To minimize the risks of contaminating the Antarctic environment and deep soil layers, each experimental unit was covered with a holed plastic lid allowing gas

exchange and the entry of precipitation water, and had its bottom covered with permeable paper. In addition, a soil layer (~3 cm) immediately in contact with the experimental units (~0.7 m^2) was collected after the experiment and transported to the laboratory for further disposal.

2.3 In situ CO_2 flux measurements

To estimate the microbial activity, the CO_2 emissions (μmol m^{-2} s^{-1}) were measured on the soil surface of the experimental units using an automated soil CO_2 flux system LI-8100A portable analyzer (LI-COR Biosciences, Lincoln, USA) coupled to a dynamic automatic survey chamber. The cylindrical chamber (854.2 cm^3; base area 83.7 cm^2) was positioned in PVC collars (10 cm in diameter) previously inserted in the upper part of each experimental unit. The flux measurements lasted 45 s, with pre- and post- purges of 10 s, and the CO_2 concentrations were recorded inside the chamber at intervals of 1 s. The CO_2 emission data were collected with three measurement replicates for each experimental unit. Fifteen data collection events were carried out in total, and the average of daily measurements was used to calculate the mean CO_2 flux for each treatment throughout the experiment. The soil temperature was measured in each experimental unit using a digital thermometer (± 0.1ºC) at each data collection event. Since soil temperature is one of the most influential variables related to CO_2 fluxes (Carvalho *et al.*, 2013; Thomazini *et al.*, 2020), a correlation analysis (r, Pearson) was performed on the daily data of these two variables to assess whether changes in CO_2 fluxes derived from fluctuations in soil temperature.

2.4 Soil analysis

The physical and chemical properties of the soil were determined by methods according to (Embrapa, 2017); described in detail in Table S2).

After thawing, undisturbed subsamples were obtained from each experimental unit using a volumetric cylinder, while the remaining soil from the samples was air-dried. The undisturbed samples are representative of the newly formed structure in the experimental units during the experiment. The soil bulk density was determined by the volumetric cylinder method, while the particle density was assessed by the volumetric flask method, and the total soil porosity was calculated using the indirect method through the ratio of the latter values. The hydraulic conductivity in a saturated medium was determined by the induced flow method, with a constant head of 2 cm. The soil microporosity was assessed using a tension table at –6 kPa, and the soil macroporosity was determined by the difference between micro and total soil porosity.

The physical analyzes were carried out in three replicas, since the fourth undisturbed sample replica was intended for the production and analysis of thin sections (which is subject of another study).

Soil pH was determined in distilled water with a glass electrode in a 1:2.5 suspension (w v^{-1}). The potential acidity ($H^+ + Al^{3+}$) was extracted by 1M ammonium acetate solution at pH 7. Exchangeable cations (Ca^{2+}, Mg^{2+}, and Al^{3+}) were extracted with 1 M KCl solution and the available P (AP), Na^+ and K^+ were extracted with Mehlich-1 extractor. The elemental concentrations in the extracts were determined by atomic absorption (Ca^{2+}, Mg^{2+}, and Al^{3+}), flame emission spectrometry (K^+ and Na^+) and photocolorimetry (AP). From these results, the cation exchange capacity (CEC) was calculated. The total organic carbon (TOC) content was determined by titration after wet oxidation with potassium dichromate (Yeomans; Bremner, 1988), and the total nitrogen (TN) content was determined by sulfuric acid digestion followed by Kjeldahl distillation (Bremner, 1960). The C:N ratio was calculated on a mass basis. The general microbial activity of the soil was assessed in 1 g of dry soil by the hydrolysis of fluorescein diacetate (FDA) method, optimized by (Green; Stott; Diack, 2006).

2.5 Statistical analysis

The effects of the treatments on soil parameters were evaluated by the analysis of variance (ANOVA) on a factorial design, considering the MP type, MP dose and the interaction of the two factors as a source of data variation. In this case, only the doses shared between the two MP types were considered (0.01 and 0.1%) as categorical variables. Then, one-way ANOVAs were performed on linear models for the separate PE fragments or PAN fibers treatments, and the treatments were differentiated from the control by grouping the means when ANOVA was significant according to Fisher's least significant difference test. Model residuals were verified for ANOVA assumptions of normality and homogeneity of variance. Since they did not meet ANOVA assumptions, statistical inferences on mean CO_2 flux and soil temperature data were supported by the Kruskal-Wallis test, with the same post hoc test for grouping means. A multivariate principal component analysis (PCA) was performed to evaluate relationships between the response parameters based on effects caused by the treatments, whereas the variables coordinates were used to assess correlations with the principal components (Abdi; Williams, 2010). The data suitability for PCA was verified using the Bartlett sphericity test and the Shapiro Wilk normality test. A significance level of 0.05 was considered for all tests, and all statistical analyses and graphs were achieved in R environment (R 4.2.2 with Rstudio

2021.09.0 interface). Linear models were achieved with the lm function, ANOVA with the anova function, and Kruskal-Wallis test with the kruskal.test function, from the R base package. Fisher's least significant difference test was achieved with the LSD.test function from the "*agricolae*" package. PCA was performed using the prcomp function with scaled data on treatment means, and the package "*factoextra"* was used to extract the variables coordinates and generate the variables correlation plot. Packages "*dplyr*", "*Rmisc*", "*ggplot2*" and "*ggthemes*" were used for data manipulation and graphs.

3 RESULTS

3.1 Impacts on soil physical properties

Except for the total porosity, all soil physical parameters presented a significant dose-dependent response regardless of the MP type, but only total and macroporosity presented a significant type-dependent response, apart from the dose (Table S3). The interaction effect was significant for the soil bulk density and macroporosity. PE fragments caused significant differences only for soil bulk density and hydraulic conductivity (Table S5). All PE fragment treatments decreased soil bulk density by approximately 6% compared to the control, regardless of the dose (Figure 1B). The 0.01 and 1% PE fragments doses decreased the hydraulic conductivity up to 94% compared to the control (Figure 1A). PAN fibers caused significant differences in all physical parameters depending on the applied doses (Table S5, Figure 1). Macroporosity decreased up to 25% compared to the control when PAN fibers doses were equal or lower than 0.01% and increased by up to 17% when treated with the 0.1% dose (Figure 1E). The soil total porosity was affected in the same way as macroporosity, but to a lesser extent, and decreased up to 5% compared to the control when PAN fiber doses were equal or below 0.01% (Figure 1C). Soil bulk density was only affected by the 0.1% dose of PAN fibers, decreasing by up to 6% compared to the control. Hydraulic conductivity did not differ from the control at the 0.1% PAN fibers dose but decreased it by up to 97% at the 0.01% dose.

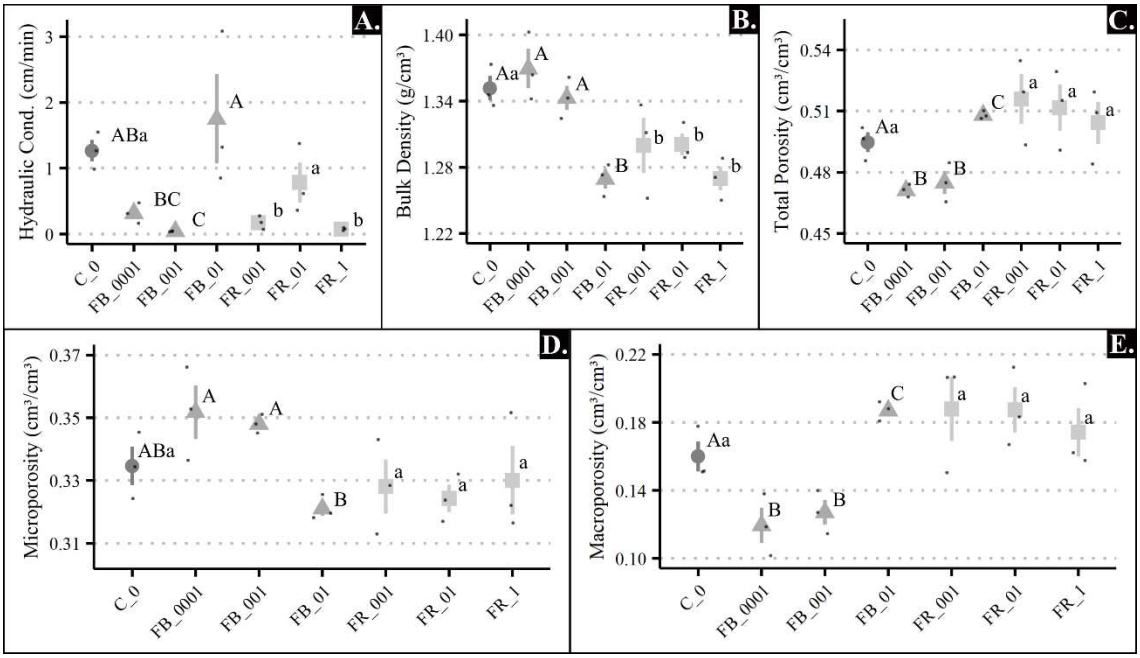

Figure 1. Effects of MP treatments on soil physical properties: A. saturated hydraulic conductivity; B. soil bulk density; C. soil total porosity; D. microporosity; E. macroporosity. Treatments are shape and color coded in grayscale, from darkest to lightest: control (C, circle); fibers (FB, triangle); and fragments (FR, square). Means with the same letters belong to the same group, by Fischer's LSD ($\alpha = 0.05$).

3.2 Impacts on soil chemical properties

The MP doses and types affected differently soil chemical properties. Soil pH, TN and C:N ratio presented a significant dose-dependent response, regardless of the MP type. The TN, C:N ratio, Na^+ and sodium saturation presented a significant type-dependent response, regardless of the dose (Table S4). The interaction effect between MP type and dose was significant for Ca^{2+}, Na^+, AP and TN.

Among the soil chemical parameters evaluated, only Mg^{2+}, K^+ and $H^+ + Al^{3+}$ contents were not significantly affected by the PAN fibers or PE fragments treatments (Table S6; Figures 2 and 3). For PAN fibers treatments, the significant effects on pH, AP, TN, C:N ratio, Na^+ and sodium saturation were different according to the dose, but the significant effects observed for Ca^{2+} and CEC were the same regardless of the applied dose. The significant effects caused by PE fragments also differed according to the dose for pH, TOC, C:N ratio, CEC, Na^+ and sodium saturation, but did not differ according to the dose for Ca^{2+}.

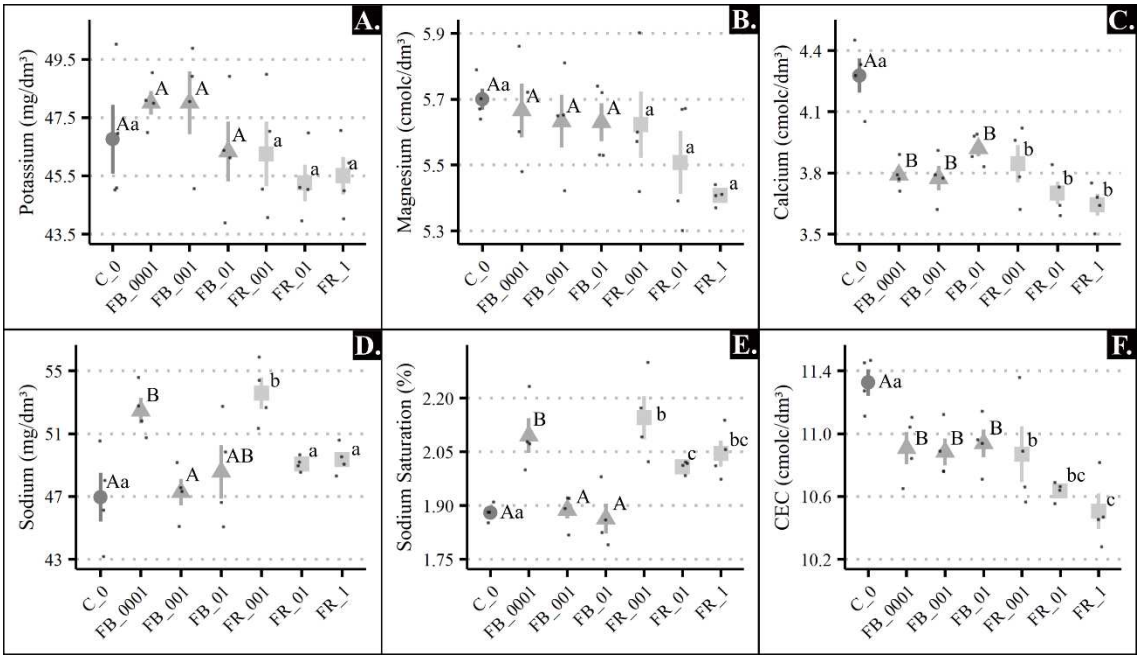

Figure 2. Effects of MP treatments on soil chemical properties: A. K^+; B. Mg^{2+}; C. Ca^{2+}; D. Na^+; E. sodium saturation; F. CEC. Treatments are shape and color coded in grayscale, from darkest to lightest: control (C, circle); fibers (FB, triangle); and fragments (FR, square). Means with the same letters belong to the same group, by Fischer's LSD ($\alpha = 0.05$).

The Ca^{2+} contents decreased by up to 12% compared to the control for any PAN fibers treatment, and by up to 15% for any PE fragments treatment (Figure 2C). CEC decreased by up to 4% for any PAN fiber treatment compared to the control, and by up to 7% for the 1% dose of PE fragments (Figure 2F). Both MP types induced similar behavior on pH, Na^+ and sodium saturation – low doses increased pH and Na^+, while high doses decreased the pH and caused non-significant changes in the exchangeable Na^+ levels (Figures 2D, 2E and 3D). Only PAN fibers treatments significantly increased the AP levels by increasing doses (Figure 3E). PAN fibers caused a significant increase in TN contents up to 84% compared to the control at a 0.1% dose (Figure 3B), and the PE fragments significantly increased the TOC contents by up to 130% compared to the control at a 1% dose (Figure 3A). Thus, the highest concentrations of the two types of MPs had opposite effects on the C:N ratio – PAN fibers at 0.1% decreased C:N ratio by up to 66%, while PE fragments at 1% increased it by up to 91% compared to the control (Figure 3C).

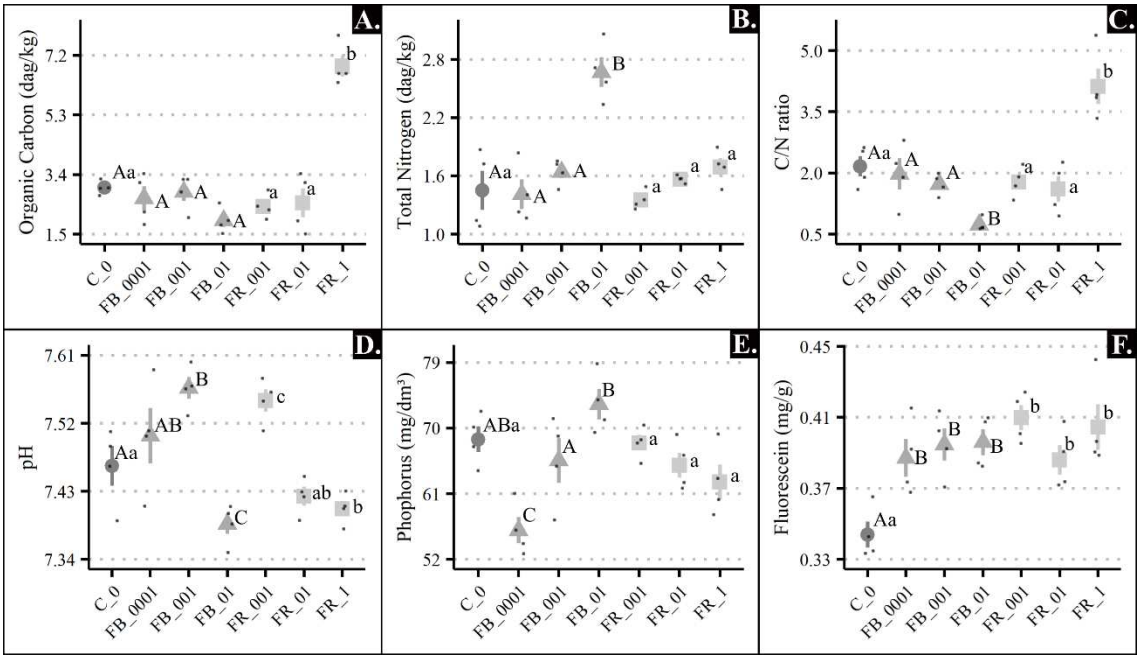

Figure 3. Effects of MP treatments on soil chemical properties: A. TOC; B. TN; C. C:N ratio; D. soil pH; E. AP; F. FDA (fluorescein released). Treatments are shape and color coded in grayscale, from darkest to lightest: control (C, circle); fibers (FB, triangle); and fragments (FR, square). Means with the same letters belong to the same group, by Fischer's LSD ($\alpha = 0.05$).

3.3 Impacts on soil respiration and microbial activity

Effects of PAN fibers were significant on mean CO_2 fluxes and different for the tested doses, increasing the CO_2 fluxes as the dose increased, resulting in fluxes up to 20% higher for the 0.1% PAN fibers treatment compared to the control (Table S7, Figure 4A). Alternatively, PE fragments treatments did not significantly affect mean CO_2 fluxes. The treatments did not cause significant effects on mean soil temperature (Table S7, Figure 4B), and no significant correlation ($r = -0.16$) was observed between soil temperature and mean CO_2 fluxes. No significant effects on soil microbial activity measured by FDA hydrolysis depending on MP dose, MP type or on the interaction between the two factors were observed (Table S4). However, both PE fragments and PAN fibers treatments caused significant effects on FDA hydrolysis (Table S6). Regardless of the dose, FDA hydrolysis increased by up to 18% for PE fragments treatments and by up to 15% for PAN fibers treatments compared to the control (Figure 3F).

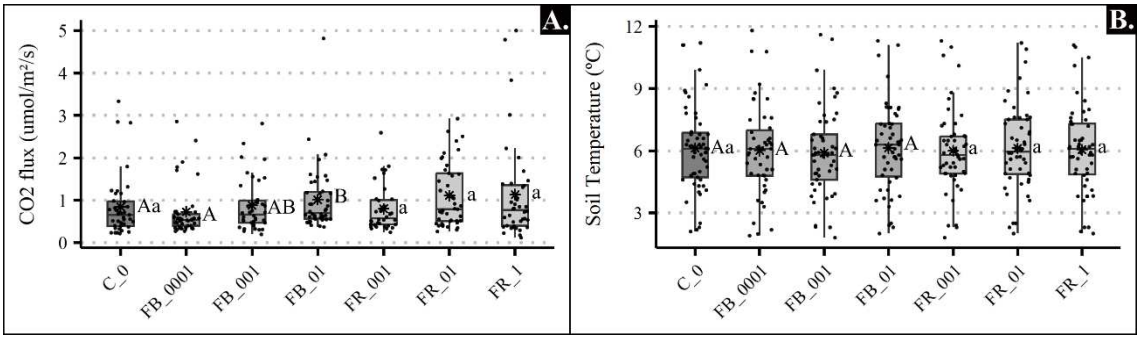

Figure 4. Effects of MP treatments on mean soil CO_2 fluxes (A.), mean soil temperature (B.) during the 22 days incubation period. Treatments are color coded in grayscale, from darkest to lightest: control (C); fibers (FB); and fragments (FR). Means with the same letters belong to the same group, by Fischer's LSD ($\alpha = 0.05$).

3.4 Principal component analysis

Five principal components (PC1 to PC5) had eigenvalues greater than 1, although PC1 (38%) and PC2 (29%) cumulatively explained 67% of the data variance (Table S8) and were addressed in the variable correlation plot (Figure S3). PC1 shows a strong correlation with porosity (0.83) and macroporosity (0.88), and an expected strong negative correlation with bulk density (-0.95) and microporosity (-0.86). Mean CO_2 fluxes (0.83) are also strongly positive correlated with PC1, and consequently with porosity, but pH (-0.72), Mg^{2+} (-0.76) and K^+ (-0.95) presented a strong negative correlation, although the latter two did not show significant differences between treatments. PC2 was positively correlated with hydraulic conductivity (0.92), Ca^{2+} (0.77), AP (0.77) and CEC (0.71), but negatively correlated with sodium saturation (0.74). PC3 (14%), PC4 (9%) and PC5 (6%) cumulatively explained 29% of the data variance (Table S8) but did not show high correlations with any variables, except Na^+ and PC3 (-0.73), which may indicate high random data variability associated with uncontrolled field conditions.

4 DISCUSSION

This study showed that MPs affect soil attributes on an Antarctic marine terrace, according to their type and dose. Except for total porosity, all physical parameters were significantly affected by MP dose, although for soil bulk density and macroporosity the influence of doses was dependent on the MP type. However, total porosity exclusively depended on MP type, and was not significantly affected by PE fragments. These results contradict the findings of (Lozano *et al.*, 2021b), who suggested little influence of MP concentration on soil aggregation, and discrepancies may rely on the different soil types tested. Antarctic marine terrace soils of the Fildes Peninsula present a weakly developed structure with high sand content and presence of expansive clays (Michel *et al.*, 2014), and soils with these characteristics are strongly susceptible to MP impacts on soil aggregation and hydraulic properties (Guo *et al.*, 2022; Ingraffia *et al.*, 2022). Therefore, the inherent physical characteristics of the soil tested here may enhance the aggregating or disaggregating effect of MP particles incorporation at increasing levels, since this is little expected from their natural condition of unconsolidated constituents (Bockheim, 2014). Even so, specific impacts considering MP types separated are influenced by the applied dose (Lozano *et al.*, 2021b), which was corroborated by this study and several others (Liu *et al.*, 2017; Machado *et al.*, 2018; Zhang *et al.*, 2020).

PAN fibers affected soil structure, which led to pronounced changes in soil porosity and saturated hydraulic conductivity, but PE fragments physically interacted with the soil matrix more harmoniously and presented no significant changes in soil porosity. PAN fibers seem to obstruct macropores at low doses ($\leq 0.01\%$), decreasing soil macroporosity and the hydraulic conductivity related to it (Centeno *et al.*, 2020). MP fibers are known to decrease aggregation and aggregate stability by creating fracture points or decreasing cohesion (Ingraffia *et al.*, 2022; Lozano *et al.*, 2021b; Zhang; Liu, 2018), and can favor the contact between MP particles rather than between soil particles at high concentrations (Guo *et al.*, 2022; Machado *et al.*, 2018). Therefore, the 1% PAN fibers treatment decreased the microporosity probably reflecting a poor aggregation, but increased macroporosity by creating interconnected pores between the fiber particles. However, increasing macroporosity didn't increased the hydraulic conductivity, since these pores formed by MP particles are less efficient to conduct water than the natural ones, due to the hydrophobicity of MPs and their ability to bind soil particles/aggregates (Guo *et al.*, 2022). Since no significant effects on soil porosity were observed in PE fragment treatments, the replacement of natural soil pores by inefficient pores formed between plastic particles (Guo *et al.*, 2022) probably addresses the decrease in hydraulic conductivity. It is also unlikely that

the decrease in soil bulk density by PE fragments treatments was promoted by significant changes in soil structure, but rather by their lower density (~ 0.95 g cm^{-3}) compared to soil mineral particles (~ 2.65 g cm^{-3}) and PAN fibers (~ 1.18 g cm^{-3}).

Our results on soil physical properties are in line with the hypothesis of shape dissimilarity – the more dissimilar the shape of a contaminant in relation to the matrix, the greater the impacts promoted on the surrounding environment (Rillig *et al.*, 2019). The absence of vegetation and roots in the tested soil may have amplified this effect, increasing the impacts of linear shaped fibers on soil physical properties. This hypothesis has often been corroborated in studies assessing the impacts of MP fibers on soil aggregation, although the chemical composition and particle size seem to affect the soil aggregation directly or indirectly (Lehmann *et al.*, 2021; Lozano *et al.*, 2021b; Machado *et al.*, 2018).

Soil aggregation and water dynamics can modulate microbial functions and vice versa (Han *et al.*, 2021; Rillig; Muller; Lehmann, 2017; Vu; Ellen Schaumann; Buchmann, 2022), which has frequently been noted among the effects driven by MPs in soils (Liang *et al.*, 2021; Machado *et al.*, 2018; Rillig *et al.*, 2021; Yu *et al.*, 2020). Carbon mineralization by CO_2 emissions is strictly related to microbial metabolism and controls carbon stocks in Maritime Antarctica, where it is sensitive to soil temperature and moisture (Carvalho *et al.*, 2013; Thomazini *et al.*, 2020). Hence, porosity and soil aggregation affect soil respiration by conditioning water and oxygen availability for soil microbiota (Yang; Liu; Zhang, 2019). The daily measurements of soil respiration presented no significant correlation with soil temperature, but mean CO_2 fluxes were strongly associated with the effects of MPs on soil physical properties according to PCA. This suggests that greater microbial activity and CO_2 fluxes were favored by MPs increasing porous spaces, air/water circulation and oxygen diffusivity (Rillig *et al.*, 2021).

The increased microbial activity may also indicate a disturbance caused by the MP addition as a representative source of organic carbon – associated with FDA hydrolysis by PCA – and nitrogen in the low organic matter soil tested. Polyethylene MPs are composed of ~87% carbon which was quantified by the analytical method employed here, contributing to increase TOC levels up to 130% compared to the control at the 1% dose. This input would represent ~8.7 g of PE carbon source and an even greater increase in TOC levels was to be expected, although it is unclear whether the TOC analysis quantified all carbon originating from MPs. As the degradation of PE MPs is unlikely to occur in this short-term scale (Huang *et al.*, 2021; Yang *et al.*, 2023), the representative input of a poorly available carbon source may triggered a

positive priming effect and favored the decomposition of native soil organic matter, contributing to a TOC increase lower than expected. The magnitude of the priming effect is positively correlated with MP degradability (Zhang *et al.*, 2023), but it could be representative in this soil with high relative availability of limiting nutrients (e.g., AP, low C:N ratio).

Nonetheless, PAN fibers comprise ~28% nitrogen, and the 0.1% dose represents a significant input to total soil nitrogen. Therefore, the C:N ratio of soils treated with PE fragments and PAN fibers presented opposite trends, which can lead to changes in the structure of soil microbial communities (Zhang *et al.*, 2014). Although the addition of PAN fibers also represents a carbon input, low C:N ratios tend to increase organic matter decomposition and carbon mineralization in Maritime Antarctic soils (Pires *et al.*, 2017), which may have favored significant increases in CO_2 fluxes. In contrast, the higher carbon input increased C:N ratio in soils treated with 1% PE fragments and could have affected the mineralization rate, causing data variability and no significant differences in mean CO_2 fluxes.

The effects on soil pH were dose-dependent and similar for both PE fragments and PAN fibers, increasing pH at a 0.01% dose but decreasing it above 0.1% dose. Soil pH was strongly negatively related with physical properties and CO_2 fluxes according to PCA, similar to previous reports (Yang; Li; Zhang, 2019). Increasing CO_2 fluxes at MP doses of 0.1% or higher could favor carbonic acid formation, potentially decreasing pH. Furthermore, soil pH regulates and is affected by soil microbiota (Rong *et al.*, 2021; Yang; Liu; Zhang, 2019), playing a key role in shaping the plastisphere community (Feng *et al.*, 2022; Li *et al.*, 2021; Rillig; Kim; Zhu, 2023). Since our treatments affected microbial activity and C:N ratio, the effects observed on soil pH could possibly be linked to impacts on microbial functions. However, further research is encouraged to better address these effects, as soil pH influences biotic processes in the coastal land environments of Maritime Antarctica by affecting soil microbial communities, nutrient cycling and vegetation cover (Park; Ahn; Lee, 2012; Thomazini *et al.*, 2015; Tscherko *et al.*, 2003).

Effects of MPs on pH can be promoted by changes in adsorption and cation exchange dynamics (Boots; Russell; Green, 2019; Feng *et al.*, 2022). Both PE fragments and PAN fibers affected cation exchange dynamics, decreasing CEC compared to the control. The CEC of the studied soil is chiefly composed of Mg^{2+} and Ca^{2+}, so its decrease was mainly caused by impacts on exchangeable contents of these cations. Sorption processes involving MPs are mainly controlled by surface mechanisms, although MPs in the size range of this study have a low

specific surface area (Li; Liu, 2022; Luo *et al.*, 2020; Xu *et al.*, 2019). Despite the negative charge surface at the pH range of the studied soil (Godoy *et al.*, 2019), the lower capacity of MPs to adsorb cations compared to natural soil particles probably address the CEC decrease, which was more representative for the higher dose applied (PE fragments at 1%). MPs decreasing soil adsorptive capacity can affect the mobility and availability of divalent metallic cations (Cao *et al.*, 2023; Feng *et al.*, 2022; Zhang *et al.*, 2020), which could be worrisome in Fildes Peninsula – where soils are historically and continually affected by heavy metals enrichment (Amaro *et al.*, 2015; Lu *et al.*, 2012; Marina-Montes *et al.*, 2020).

Interestingly, sodium saturation increased especially in soils treated with the lowest doses of both MP types, which indicate a greater presence of Na^+ ions in the soil exchange complex. The Na^+ ion is easily leachable as it has a larger hydrated radius and fewer specific interaction with soil-charged particles than divalent cations, although characteristics of soil porosity and pH also affect soil sorption dynamics in the presence of MPs (Luo *et al.*, 2020). Our results demonstrated a selective interaction of MPs with Na^+ ions, and further investigation into the adsorption behavior under these conditions is needed to better understand this interaction.

Otherwise, MPs adsorptive functions do not seem to be a main factor affecting soil P dynamics, but secondary effects may play a more representative role (Li; Liu, 2022). Changes promoted in soil pH affect phosphate solubilization, which is mainly controlled by mineral or exchangeable calcium sources whithin this pH range (Penn; Camberato, 2019). Impacts of MPs on soil microbiota also affect enzymes that promote P mineralization and availability, which can reflect in AP content (Dong *et al.*, 2021; Feng *et al.*, 2022). Here, only the lowest dose of PAN fibers treatment significantly decreased the soil AP content, which were strongly associated with hydraulic conductivity according to PCA. The effects on AP possibly addressed impacts of PAN fibers on physical and hydrological conditions mediating pH and microbial functions, but specific mechanisms involved need to be further explored accounting to the sources and speciation of P, as coastal areas in Maritime Antarctica are highly affected by the runoff of penguin and marine birds guano (Simas *et al.*, 2007).

Different types and doses of MPs affected Antarctic marine terrace soil properties, but the generalization of the results presented here must be addressed with care. Given the short-term character of our experiment, significant effects on soil physical properties refer to the artificial structure newly built in the experimental units during the incubation period. Nevertheless, periglacial soils are subject to freezing and thawing activity which can induce aggregation over

short periods, even on a scale of days (Van Vliet-Lanoë, 2010). Liquid water infiltrates the soil during snow melting periods and it freezes during sub-zero conditions causing gel-like clays and organic particles to precipitate, promoting cohesion and flocculation into aggregates with voids formed by desiccation crack networks (Campbell; Claridge, 1987; Van Vliet-Lanoë, 2010). These processes are even more evident in summer due to increased liquid water availability and more frequent freeze-thaw cycles driven by daily temperature fluctuations (Almeida *et al.*, 2017; Chaves *et al.*, 2017), potentially favoring MP particles integration into soil aggregates (Figure S4). Over time, cryoturbation can promote particle movement, fragmentation and sorting along the active layer of permafrost (Bockheim; Tarnocai, 1998). The low temperatures make polymers more brittle and increase susceptibility of MPs to fragment (Chubarenko, 2022). In a scenario of MP pollution, cryoturbation processes could contribute to vertical migration and fragmentation of MPs possibly affecting soil properties at greater depths, which should be further investigated.

Likewise, MPs degradation is not expected to occur in about three weeks and was not assessed in this study, but the addition of recalcitrant organic carbon sources may be sufficient to trigger the disturbance impacts on microbial functions. However, Antarctic hydrocarbon-degrading microorganisms can metabolize carbon from polypropylene MPs when exposed exclusively to this carbon source (Habib et al., 2020). This is plausible to occur in the Fildes Peninsula region due to its history of anthropogenic impacts and prevalent hydrocarbon pollution (Wu *et al.*, 2023). Moreover, Maritime Antarctic environments are vulnerable to climate change (Rosa *et al.*, 2023; Thomazini *et al.*, 2020), which favors soil exposure promoted by glacial retreat and creates new ice-free areas to be colonized by the Antarctic fauna, flora and microbiota (Francelino *et al.*, 2011) affecting soil ecosystems and carbon mineralization (Pires *et al.*, 2017; Simas *et al.*, 2007). The ornithogenic influence, common in Maritime Antarctica coastal areas, accelerate organic matter degradation, mineralization of carbon from recalcitrant sources, and colonization by vegetation (Pires *et al.*, 2017; Simas *et al.*, 2007; Thomazini *et al.*, 2015). As MPs are present in penguin scats (Bessa *et al.*, 2019; Fragão *et al.*, 2021), their interaction with ornithogenic processes is presumable and can contribute to mediate the effects of soil MPs observed here. Therefore, considering the complexity of these multiple environmental factors is needed and encouraged in future assessments to better understand the ecological and long-term consequences of MP pollution in these ecosystems.

5 CONCLUSIONS

We reported impacts of PAN fibers and PE fragments MPs on several physical, chemical and microbial attributes of an Antarctic marine terrace soil in a short-term pot experiment under field conditions. PAN fibers significantly affected soil porosity and hydraulic conductivity, but PE fragments did not change soil porosity. Both MP types increased microbial activity regardless of the dose, but only the highest PAN fibers dose (0.1%) increased CO_2 fluxes, compared to the control, when soil porosity increased. The addition of PE and PAN at high doses (1% and 0.1%, respectively) represented a significant input of C and N to the soil with low organic matter content, affecting the C:N ratio. Soil pH increased at low doses and decreased at high doses for both MP types, while CEC decreased with the addition of PAN fibers regardless of dose but decreased with increasing doses of PE fragments. PE fragments and PAN fibers showed specific effects that remain unclear on exchangeable Na^+ and AP contents, respectively. The effects on soil properties observed here are likely interrelated and foster further investigation. Complex environmental factors should be considered to better address their causes and long-term ecological implications, including the interaction of MPs with Antarctic soil microbiota under climate change conditions and co-contamination with heavy metals and/or organic pollutants, besides to cumulative effects on environments undergoing ornithogenesis and cryoturbation dynamics.

6 ACKNOWLEDGEMENTS

The present work was carried with the support of the following Brazilian research agencies: National Council for Research and Development (Conselho Nacional Desenvolvimento Científico e Tecnológico – CNPq) and Coordination for the Improvement of Higher-Level Personnel (Coordenação de Aperfeiçoamento de Pessoal de Nível Superior – CAPES). This study was conducted within activities of project TERRANTAR/PERMACLIMA, financed by CNPq and the Brazilian Ministry of Science, Technology and Innovation – MCTI, under the scope of Brazilian Antarctic Program (PROANTAR). The authors thank the support of the Brazilian Ministries of Science, Technology and Innovation (MCTI), Environment (MMA) and Inter-Ministry Commission for Sea Resources (CIRM).

7 REFERENCES

ABDI, Hervé; WILLIAMS, Lynne J. Principal component analysis. **Wiley Interdisciplinary Reviews: Computational Statistics**, [*s. l.*], v. 2, n. 4, p. 433–459, 2010.

ALMEIDA, Ivan C.C. *et al.* Long term active layer monitoring at a warm-based glacier front from maritime Antarctica. **Catena**, [*s. l.*], v. 149, p. 572–581, 2017.

AMARO, Eduardo *et al.* Assessing trace element contamination in Fildes Peninsula (King George Island) and Ardley Island, Antarctic. **Marine Pollution Bulletin**, [*s. l.*], v. 97, n. 1–2, p. 523–527, 2015.

AVES, Alex R. *et al.* First evidence of microplastics in Antarctic snow. **Cryosphere**, [*s. l.*], v. 16, n. 6, p. 2127–2145, 2022.

BARGAGLI, Roberto; ROTA, Emilia. Microplastic Interactions and Possible Combined Biological Effects in Antarctic Marine Ecosystems. **Animals**, [*s. l.*], v. 13, n. 1, 2023.

BERGAMI, Elisa *et al.* Plastics everywhere: first evidence of polystyrene fragments inside the common Antarctic collembolan Cryptopygus antarcticus. **Biology Letters**, [*s. l.*], v. 16, n. 6, 2020.

BESSA, Filipa *et al.* Microplastics in gentoo penguins from the Antarctic region. **Scientific Reports**, [*s. l.*], v. 9, n. 1, p. 1–7, 2019.

BOCKHEIM, J. G. Antarctic Soil Properties and Soilscapes. *In*: ANTARCTIC TERRESTRIAL MICROBIOLOGY. Berlin, Heidelberg: Springer Berlin Heidelberg, 2014. v. 9783642452, p. 293–315.

BOCKHEIM, J. G.; TARNOCAI, C. Recognition of cryoturbation for classifying permafrost-affected soils. **Geoderma**, [*s. l.*], v. 81, n. 3–4, p. 281–293, 1998.

BOOTS, Bas; RUSSELL, Connor William; GREEN, Dannielle Senga. Effects of Microplastics in Soil Ecosystems: Above and below Ground. **Environmental Science and Technology**, [*s. l.*], v. 53, n. 19, p. 11496–11506, 2019.

BREMNER, J. M. Determination of nitrogen in soil by the Kjeldahl method. **The Journal of Agricultural Science**, [*s. l.*], v. 55, n. 1, p. 11–33, 1960.

BROOKS, Shaun T. *et al.* Our footprint on Antarctica competes with nature for rare ice-free land. **Nature Sustainability**, [*s. l.*], v. 2, n. 3, p. 185–190, 2019.

BÜKS, Frederick; KAUPENJOHANN, Martin. Global concentrations of microplastics in soils - A review. **Soil**, [*s. l.*], v. 6, n. 2, p. 649–662, 2020.

CAMPANALE, Claudia *et al.* Microplastics pollution in the terrestrial environments: Poorly known diffuse sources and implications for plants. **Science of the Total Environment**, [*s. l.*], v. 805, p. 150431, 2022.

CAMPBELL, Iain Bruce; CLARIDGE, Graeme Geoffrey Carré. **Antarctica: soils, weathering processes and environment**. [*S. l.*]: Elsevier, 1987.

CAO, Yanxiao *et al.* Polypropylene microplastics affect the distribution and bioavailability of cadmium by changing soil components during soil aging. **Journal of Hazardous Materials**, [*s. l.*], v. 443, n. PA, p. 130079, 2023.

CARVALHO, Juliana Vanir De Souza *et al.* CO2-C losses and carbon quality of selected Maritime Antarctic soils. **Antarctic Science**, [*s. l.*], v. 25, n. 1, p. 11–18, 2013.

CENTENO, Luana Nunes *et al.* Dominant Control of Macroporosity on Saturated Soil Hydraulic Conductivity at Multiple Scales and Locations Revealed by Wavelet Analyses. **Journal of Soil Science and Plant Nutrition**, [*s. l.*], v. 20, n. 4, p. 1686–1702, 2020.

CHAVES, D. A. *et al.* Active layer and permafrost thermal regime in a patterned ground soil in Maritime Antarctica, and relationship with climate variability models. **Science of the Total Environment**, [*s. l.*], v. 584–585, p. 572–585, 2017.

CHIA, Rogers Wainkwa *et al.* Soil health and microplastics: a review of the impacts of microplastic contamination on soil properties. **Journal of Soils and Sediments**, [*s. l.*], p. 2690–2705, 2022.

CHUBARENKO, Irina. Physical processes behind interactions of microplastic particles with natural ice. **Environmental Research Communications**, [*s. l.*], v. 4, n. 1, 2022.

CINCINELLI, Alessandra *et al.* Microplastic in the surface waters of the Ross Sea (Antarctica): Occurrence, distribution and characterization by FTIR. **Chemosphere**, [*s. l.*], v. 175, p. 391–400, 2017.

COLZI, Ilaria *et al.* Impact of microplastics on growth, photosynthesis and essential elements in Cucurbita pepo L. **Journal of Hazardous Materials**, [*s. l.*], v. 423, n. PB, p. 127238, 2022.

CONVEY, P.; BARNES, D. K.A.; MORTON, A. Debris accumulation on oceanic island shores of the Scotia Arc, Antarctica. **Polar Biology**, [*s. l.*], v. 25, n. 8, p. 612–617, 2002.

DONG, Youming *et al.* Effect of microplastics and arsenic on nutrients and microorganisms in rice rhizosphere soil. **Ecotoxicology and Environmental Safety**, [*s. l.*], v. 211, p. 111899, 2021.

EMBRAPA. **Manual de Métodos de Análise de Solo**. 3ªed. Brasília, DF: [*s. n.*], 2017.

ERNI-CASSOLA, Gabriel *et al.* Distribution of plastic polymer types in the marine environment; A meta-analysis. **Journal of Hazardous Materials**, [*s. l.*], v. 369, n. February, p. 691–698, 2019.

EVANGELIOU, N. *et al.* Atmospheric transport is a major pathway of microplastics to remote regions. **Nature Communications**, [*s. l.*], v. 11, n. 1, 2020.

FEI, Yufan *et al.* Response of soil enzyme activities and bacterial communities to the accumulation of microplastics in an acid cropped soil. **Science of the Total Environment**, [*s. l.*], v. 707, p. 135634, 2020.

FENG, Xueying *et al.* Microplastics change soil properties, heavy metal availability and bacterial community in a Pb-Zn-contaminated soil. **Journal of Hazardous Materials**, [*s. l.*], v. 424, n. PA, p. 127364, 2022

FRAGÃO, Joana *et al.* Microplastics and other anthropogenic particles in Antarctica: Using penguins as biological samplers. **Science of the Total Environment**, [*s. l.*], v. 788, p. 147698, 2021.

FRANCELINO, Marcio Rocha *et al.* Geomorphology and soils distribution under paraglacial conditions in an ice-free area of Admiralty Bay, King George Island, Antarctica. **Catena**, [*s. l.*], v. 85, n. 3, p. 194–204, 2011.

FULLER, Stephen; GAUTAM, Anil. A Procedure for Measuring Microplastics using Pressurized Fluid Extraction. **Environmental Science and Technology**, [*s. l.*], v. 50, n. 11, p. 5774–5780, 2016.

GODOY, Verónica *et al.* The human connection: First evidence of microplastics in remote high mountain lakes of Sierra Nevada, Spain. **Environmental Pollution**, [*s. l.*], v. 311, n. August, 2022.

GODOY, V. *et al.* The potential of microplastics as carriers of metals. **Environmental Pollution**, [*s. l.*], v. 255, 2019.

GONZÁLEZ-PLEITER, Miguel *et al.* First detection of microplastics in the freshwater of an Antarctic Specially Protected Area. **Marine Pollution Bulletin**, [*s. l.*], v. 161, n. October, p. 1–6, 2020.

GREEN, V. S.; STOTT, D. E.; DIACK, M. Assay for fluorescein diacetate hydrolytic activity: Optimization for soil samples. **Soil Biology and Biochemistry**, [*s. l.*], v. 38, n. 4, p. 693–701, 2006.

GUO, Yudong *et al.* Direct and indirect effects of penguin feces on microbiomes in Antarctic ornithogenic soils. **Frontiers in Microbiology**, [*s. l.*], v. 9, n. APR, 2018.

GUO, Zi Qi *et al.* Soil texture is an important factor determining how microplastics affect soil hydraulic characteristics. **Environment International**, [*s. l.*], v. 165, n. May, p. 107293, 2022.

HALE, Robert C. *et al.* A Global Perspective on Microplastics. **Journal of Geophysical Research: Oceans**, [*s. l.*], v. 125, n. 1, p. 1–40, 2020.

HAN, Shun *et al.* Soil aggregate size-dependent relationships between microbial functional diversity and multifunctionality. **Soil Biology and Biochemistry**, [*s. l.*], v. 154, n. January, 2021.

HORTON, Alice A. *et al.* Large microplastic particles in sediments of tributaries of the River Thames, UK – Abundance, sources and methods for effective quantification. **Marine Pollution Bulletin**, [*s. l.*], v. 114, n. 1, p. 218–226, 2017.

HUANG, Daofen *et al.* Degradation of polyethylene plastic in soil and effects on microbial community composition. **Journal of Hazardous Materials**, [*s. l.*], v. 416, n. May, p. 126173, 2021.

INGRAFFIA, Rosolino *et al.* Polyester microplastic fibers affect soil physical properties and erosion as a function of soil type. **Soil**, [*s. l.*], v. 8, n. 1, p. 421–435, 2022.

ISOBE, Atsuhiko *et al.* Microplastics in the Southern Ocean. **Marine Pollution Bulletin**, [*s. l.*], v. 114, n. 1, p. 623–626, 2017.

KELLY, A. *et al.* Microplastic contamination in east Antarctic sea ice. **Marine Pollution Bulletin**, [*s. l.*], v. 154, n. March, p. 111130, 2020.

KHALID, Noreen *et al.* Linking effects of microplastics to ecological impacts in marine environments. **Chemosphere**, [*s. l.*], v. 264, p. 128541, 2021.

KIM, Shin Woong *et al.* Effects of Different Microplastics on Nematodes in the Soil Environment: Tracking the Extractable Additives Using an Ecotoxicological Approach. **Environmental Science and Technology**, [*s. l.*], v. 54, n. 21, p. 13868–13878, 2020.

KOUTNIK, Vera S. *et al.* Distribution of microplastics in soil and freshwater environments: Global analysis and framework for transport modeling. **Environmental Pollution**, [*s. l.*], v. 274, p. 116552, 2021.

LACERDA, Ana L.d.F. *et al.* Plastics in sea surface waters around the Antarctic Peninsula. **Scientific Reports**, [*s. l.*], v. 9, n. 1, p. 1–12, 2019.

LEBRETON, Laurent; EGGER, Matthias; SLAT, Boyan. A global mass budget for positively buoyant macroplastic debris in the ocean. **Scientific Reports**, [*s. l.*], v. 9, n. 1, p. 1–10, 2019.

LEHMANN, Anika *et al.* Microplastics have shape- and polymer-dependent effects on soil aggregation and organic matter loss – an experimental and meta-analytical approach. **Microplastics and Nanoplastics**, [*s. l.*], v. 1, n. 1, p. 1–14, 2021.

LI, Huan Qin *et al.* Soil pH has a stronger effect than arsenic content on shaping plastisphere bacterial communities in soil. **Environmental Pollution**, [*s. l.*], v. 287, n. January, 2021.

LI, Haixiao; LIU, Le. Short-term effects of polyethene and polypropylene microplastics on soil phosphorus and nitrogen availability. **Chemosphere**, [*s. l.*], v. 291, n. P2, p. 132984, 2022.

LIANG, Yun *et al.* Effects of Microplastic Fibers on Soil Aggregation and Enzyme Activities Are Organic Matter Dependent. **Frontiers in Environmental Science**, [*s. l.*], v. 9, n. April, p. 1–11, 2021.

LIANG, Yun *et al.* Increasing Temperature and Microplastic Fibers Jointly Influence Soil Aggregation by Saprobic Fungi. **Frontiers in Microbiology**, [*s. l.*], v. 10, n. September, p. 1–10, 2019.

LIU, Hongfei *et al.* Response of soil dissolved organic matter to microplastic addition in Chinese loess soil. **Chemosphere**, [*s. l.*], v. 185, p. 907–917, 2017.

LOPES, Davi do Vale *et al.* Hydrogeochemistry and chemical weathering in a periglacial environment of Maritime Antarctica. **Catena**, [*s. l.*], v. 197, n. June 2020, p. 104959, 2021.

LÓPEZ-MARTÍNEZ, Jerónimo *et al.* Periglacial processes and landforms in the South Shetland Islands (northern Antarctic Peninsula region). **Geomorphology**, [*s. l.*], v. 155–156, p. 62–79, 2012.

LOZANO, Yudi M. *et al.* Effects of microplastics and drought on soil ecosystem functions and multifunctionality. **Journal of Applied Ecology**, [*s. l.*], v. 58, n. 5, p. 988–996, 2021a.

LOZANO, Yudi M. *et al.* Microplastic Shape, Polymer Type, and Concentration Affect Soil Properties and Plant Biomass. **Frontiers in Plant Science**, [*s. l.*], v. 12, n. February, p. 1–14, 2021b.

LOZOYA, Juan Pablo *et al.* Stranded Pellets in Fildes Peninsula (King George Island, Antarctica): New Evidence of Southern Ocean Connectivity. **SSRN Electronic Journal**, [*s. l.*], p. 119519, 2022.

LU, Zhibo *et al.* Baseline values for metals in soils on Fildes Peninsula, King George Island, Antarctica: The extent of anthropogenic pollution. **Environmental Monitoring and Assessment**, [*s. l.*], v. 184, n. 11, p. 7013–7021, 2012.

LUO, Yuanyuan *et al.* Distribution characteristics and mechanism of microplastics mediated by soil physicochemical properties. **Science of the Total Environment**, [*s. l.*], v. 726, p. 138389, 2020.

LUSHER, Amy L. *et al.* Microplastics in Arctic polar waters: The first reported values of particles in surface and sub-surface samples. **Scientific Reports**, [*s. l.*], v. 5, n. June, p. 1–9, 2015.

MA, Yan Bo *et al.* Recent advances in micro (nano) plastics in the environment: Distribution, health risks, challenges and future prospects. **Aquatic Toxicology**, [*s. l.*], v. 261, n. April, 2023.

MACHADO, Anderson Abel de Souza *et al.* Impacts of Microplastics on the Soil Biophysical Environment. **Environmental Science and Technology**, [*s. l.*], v. 52, n. 17, p. 9656–9665, 2018.

MACHADO, Anderson Abel de Souza *et al.* Microplastics Can Change Soil Properties and Affect Plant Performance. **Environmental Science and Technology**, [*s. l.*], v. 53, n. 10, p. 6044–6052, 2019.

MARINA-MONTES, C. *et al.* Heavy metal transport and evolution of atmospheric aerosols in the Antarctic region. **Science of the Total Environment**, [*s. l.*], v. 721, p. 1–7, 2020.

MICHEL, Roberto F.M. *et al.* Soils and landforms from Fildes Peninsula and Ardley Island, Maritime Antarctica. **Geomorphology**, [*s. l.*], v. 225, n. C, p. 76–86, 2014.

MUNARI, Cristina *et al.* Microplastics in the sediments of Terra Nova Bay (Ross Sea, Antarctica). **Marine Pollution Bulletin**, [*s. l.*], v. 122, n. 1–2, p. 161–165, 2017.

ONINK, Victor *et al.* The Role of Ekman Currents, Geostrophy, and Stokes Drift in the Accumulation of Floating Microplastic. **Journal of Geophysical Research: Oceans**, [*s. l.*], v. 124, n. 3, p. 1474–1490, 2019.

PARK, Jeong Soo; AHN, In Young; LEE, Eun Ju. Influence of soil properties on the distribution of Deschampsia antarctica on King George Island, Maritime Antarctica. **Polar Biology**, [*s. l.*], v. 35, n. 11, p. 1703–1711, 2012.

PELAYO, Marta *et al.* Characterization and distribution of clay minerals in the soils of Fildes Peninsula and Ardley Island (King George Island, Maritime Antarctica). **Clay Minerals**, [*s. l.*], v. 57, n. 3–4, p. 264–284, 2022.

PENN, Chad J.; CAMBERATO, James J. A critical review on soil chemical processes that control how soil ph affects phosphorus availability to plants. **Agriculture (Switzerland)**, [*s. l.*], v. 9, n. 6, p. 1–18, 2019.

PERFETTI-BOLAÑO, Alessandra *et al.* Occurrence and Distribution of Microplastics in Soils and Intertidal Sediments at Fildes Bay, Maritime Antarctica. **Frontiers in Marine Science**, [*s. l.*], v. 8, n. February, 2022.

PIGNATTELLI, Sara; BROCCOLI, Andrea; RENZI, Monia. Physiological responses of garden cress (L. sativum) to different types of microplastics. **Science of the Total Environment**, [*s. l.*], v. 727, p. 138609, 2020.

PIRES, C. V. *et al.* Soil organic carbon and nitrogen pools drive soil C-CO2 emissions from selected soils in Maritime Antarctica. **Science of the Total Environment**, [*s. l.*], v. 596–597, p. 124–135, 2017.

QI, Yueling *et al.* Impact of plastic mulch film debris on soil physicochemical and hydrological properties. **Environmental Pollution**, [*s. l.*], v. 266, p. 115097, 2020.

QIU, Yifei *et al.* Soil microplastic characteristics and the effects on soil properties and biota: A systematic review and meta-analysis. **Environmental Pollution**, [*s. l.*], v. 313, n. June, p. 120183, 2022.

RILLIG, Matthias C. *et al.* Microplastic fibers affect dynamics and intensity of CO2 and N2O fluxes from soil differently. **Microplastics and Nanoplastics**, [*s. l.*], v. 1, n. 1, p. 1–11, 2021.

RILLIG, Matthias C. *et al.* Shaping up: Toward considering the shape and form of pollutants. **Environmental Science and Technology**, [*s. l.*], v. 53, n. 14, p. 7925–7926, 2019.

RILLIG, Matthias C.; KIM, Shin Woong; ZHU, Yong Guan. The soil plastisphere. **Nature Reviews Microbiology**, [*s. l.*], 2023.

RILLIG, Matthias C.; MULLER, Ludo A.H.; LEHMANN, Anika. Soil aggregates as massively concurrent evolutionary incubators. **ISME Journal**, [*s. l.*], v. 11, n. 9, p. 1943–1948, 2017.

RONG, Lili *et al.* LDPE microplastics affect soil microbial communities and nitrogen cycling. **Science of the Total Environment**, [*s. l.*], v. 773, p. 145640, 2021.

ROSA, Kátia K. da *et al.* Glacier fluctuations and a proglacial evolution in King George Bay (King George Island), Antarctica, since 1980 decade. **Anais da Academia Brasileira de Ciências**, [*s. l.*], v. 95, n. suppl 3, p. 1–15, 2023.

ROTA, Emilia *et al.* Macro- and Microplastics in the Antarctic Environment: Ongoing Assessment and Perspectives. **Environments - MDPI**, [*s. l.*], v. 9, n. 7, p. 1–17, 2022.

SCHEURER, Michael; BIGALKE, Moritz. Microplastics in Swiss Floodplain Soils. **Environmental Science and Technology**, [*s. l.*], v. 52, n. 6, p. 3591–3598, 2018.

SIMAS, Felipe N.B. *et al.* Ornithogenic cryosols from Maritime Antarctica: Phosphatization as a soil forming process. **Geoderma**, [*s. l.*], v. 138, n. 3–4, p. 191–203, 2007.

SUARIA, Giuseppe *et al.* Floating macro- and microplastics around the Southern Ocean: Results from the Antarctic Circumnavigation Expedition. **Environment International**, [*s. l.*], v. 136, n. January, p. 105494, 2020.

THOMAZINI, A. *et al.* CO2 and N2O emissions in a soil chronosequence at a glacier retreat zone in Maritime Antarctica. **Science of the Total Environment**, [*s. l.*], v. 521–522, p. 336–345, 2015.

THOMAZINI, André *et al.* The current response of soil thermal regime and carbon exchange of a paraglacial coastal land system in maritime Antarctica. **Land Degradation and Development**, [*s. l.*], v. 31, n. 5, p. 655–666, 2020.

TSCHERKO, D. *et al.* Biomass and enzyme activity of two soil transects at King George Island, maritime Antarctica. **Arctic, Antarctic, and Alpine Research**, [*s. l.*], v. 35, n. 1, p. 34–47, 2003.

VAN FRANEKER, Jan A.; BELL, Phil J. Plastic ingestion by petrels breeding in Antarctica. **Marine Pollution Bulletin**, [*s. l.*], v. 19, n. 12, p. 672–674, 1988.

VAN VLIET-LANOË, Brigitte. Frost Action. **Interpretation of Micromorphological Features of Soils and Regoliths**, [*s. l.*], p. 81–108, 2010.

VU, Elena; ELLEN SCHAUMANN, Gabriele; BUCHMANN, Christian. The contribution of microbial activity to soil–water interactions and soil microstructural stability of a silty loam soil under moisture dynamics. **Geoderma**, [*s. l.*], v. 417, n. March, p. 115822, 2022.

WAN, Lingfan *et al.* Global meta-analysis reveals differential effects of microplastics on soil ecosystem. **Science of the Total Environment**, [*s. l.*], v. 867, n. 18, p. 161403, 2023.

WANG, Wenfeng *et al.* Environmental fate and impacts of microplastics in soil ecosystems: Progress and perspective. **Science of the Total Environment**, [*s. l.*], v. 708, p. 134841, 2020.

WU, Zilan *et al.* Polycyclic aromatic hydrocarbons in Fildes Peninsula, maritime Antarctica: Effects of human disturbance. **Environmental Pollution**, [*s. l.*], v. 318, n. November 2022, p. 120768, 2023.

XU, Pengcheng *et al.* Sorption of polybrominated diphenyl ethers by microplastics. **Marine Pollution Bulletin**, [*s. l.*], v. 145, n. February, p. 260–269, 2019.

YANG, Zhenyu *et al.* Degradable microplastics induce more soil organic carbon loss via priming effects: a viewpoint. **Plant and Soil**, [*s. l.*], n. 0123456789, p. 10–13, 2023.

YANG, Ling *et al.* Microplastics in soil: A review on methods, occurrence, sources, and potential risk. **Science of the Total Environment**, [*s. l.*], v. 780, p. 146546, 2021.

YANG, Chao; LI, Jingjing; ZHANG, Yingjun. Soil aggregates indirectly influence litter carbon storage and release through soil pH in the highly alkaline soils of north China. **PeerJ**, [*s. l.*], v. 2019, n. 10, p. 1–17, 2019.

YANG, Chao; LIU, Nan; ZHANG, Yingjun. Soil aggregates regulate the impact of soil bacterial and fungal communities on soil respiration. **Geoderma**, [*s. l.*], v. 337, n. January 2018, p. 444–452, 2019a.

YEOMANS, J. C.; BREMNER, J. M. A rapid and precise method for routine determination of organic carbon in soil1. **Communications in Soil Science and Plant Analysis**, [*s. l.*], v. 19, n. 13, p. 1467–1476, 1988.

YU, Hong *et al.* Inhibitory effect of microplastics on soil extracellular enzymatic activities by changing soil properties and direct adsorption: An investigation at the aggregate-fraction level. **Environmental Pollution**, [*s. l.*], v. 267, p. 115544, 2020.

ZACHARIAS, Daniel C; SETZER, Alberto W. Características Mensais De Extremos De Pressão, Temperatura, Vento E Radiação Da Estação Antártica Com. Ferraz No Período 1992-2003. **XII SPA Instituto de Geociências da USP**, [*s. l.*], p. 104, 2004.

ZHANG, Shuwu *et al.* Microplastics influence the adsorption and desorption characteristics of Cd in an agricultural soil. **Journal of Hazardous Materials**, [*s. l.*], v. 388, n. October 2019, p. 121775, 2020.

ZHANG, Guohao *et al.* Priming effects induced by degradable microplastics in agricultural soils. **Soil Biology and Biochemistry**, [*s. l.*], v. 180, n. November 2022, p. 109006, 2023.

ZHANG, Xinfang *et al.* The soil carbon/nitrogen ratio and moisture affect microbial community structures in alkaline permafrost-affected soils with different vegetation types on the Tibetan plateau. **Research in Microbiology**, [*s. l.*], v. 165, n. 2, p. 128–139, 2014.

ZHANG, G. S.; LIU, Y. F. The distribution of microplastics in soil aggregate fractions in southwestern China. **Science of the Total Environment**, [*s. l.*], v. 642, p. 12–20, 2018.

ZHANG, G. S.; ZHANG, F. X.; LI, X. T. Effects of polyester microfibers on soil physical properties: Perception from a field and a pot experiment. **Science of the Total Environment**, [*s. l.*], v. 670, p. 1–7, 2019.

ZHAO, Tingting; LOZANO, Yudi M.; RILLIG, Matthias C. Microplastics Increase Soil pH and Decrease Microbial Activities as a Function of Microplastic Shape, Polymer Type, and Exposure Time. **Frontiers in Environmental Science**, [*s. l.*], v. 9, n. June, p. 1–14, 2021.

8 SUPPLEMENTARY MATERIAL FOR CHAPTER I

8.1 Supporting figures

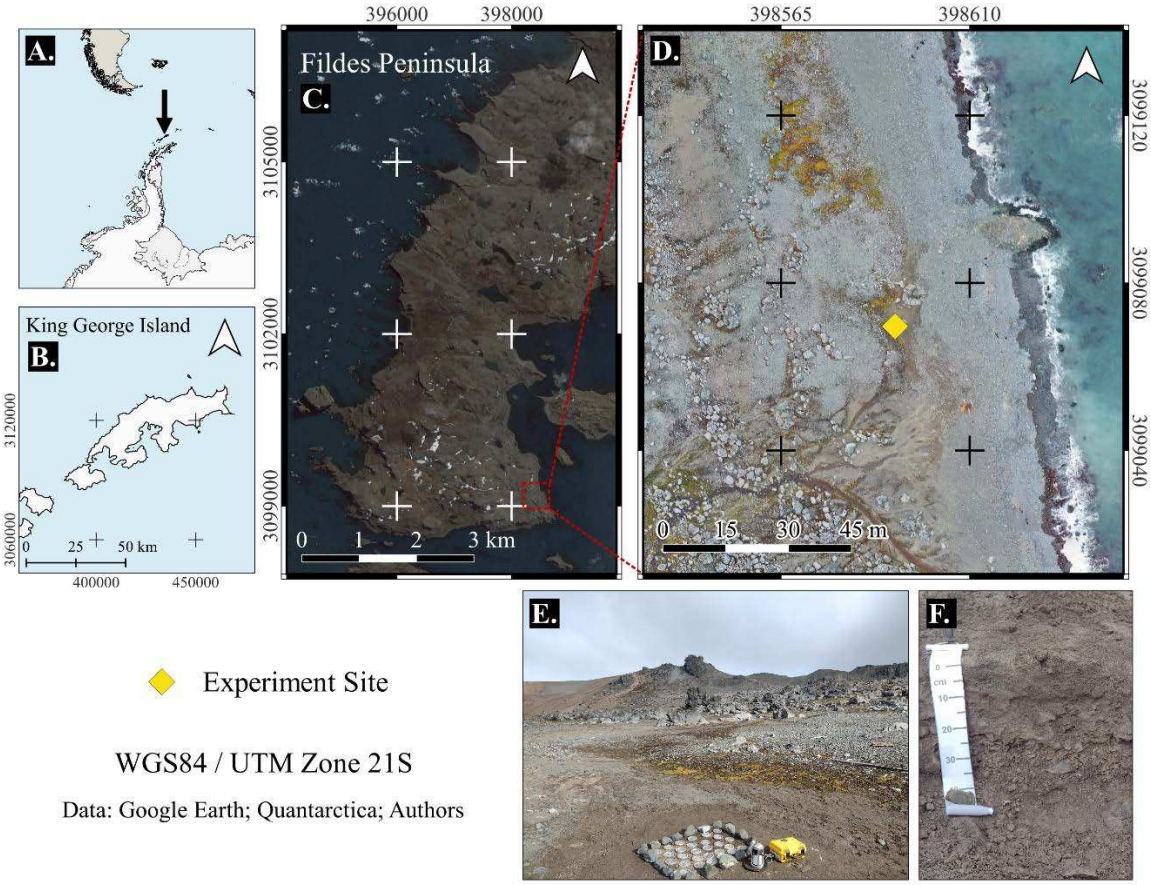

Figure S1. A. Regional settling of Maritime Antarctica; B. King George Island; C. Fildes Peninsula; D. Aerial view of the experimental site; E. Experimental site; F. Soil sampled for the experiment.

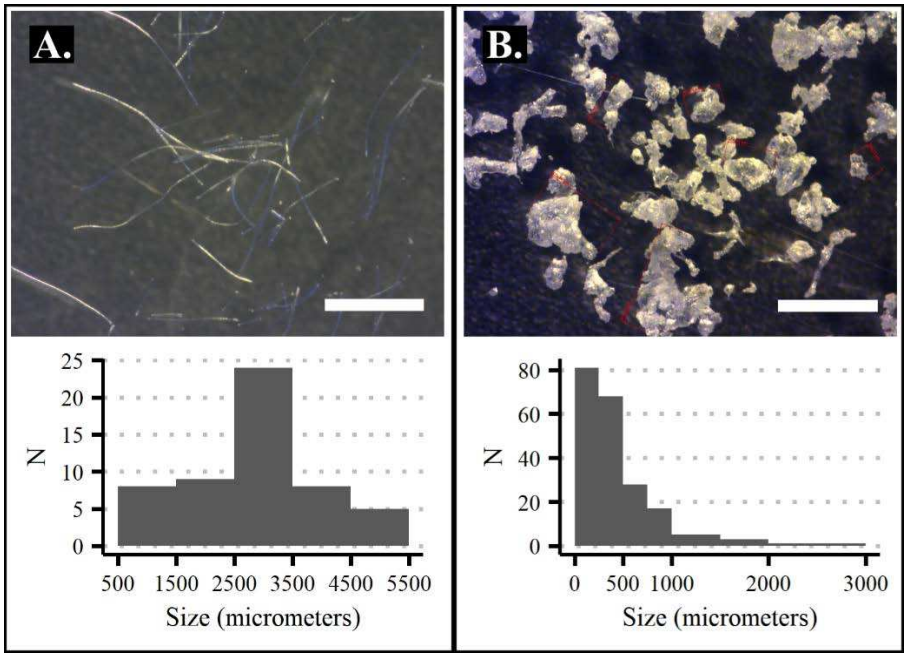

Figure S2. Two MP types tested in the current study and respective size distributions: A. PAN fibers; B. PE fragments. Scale bar represents 1.0 mm.

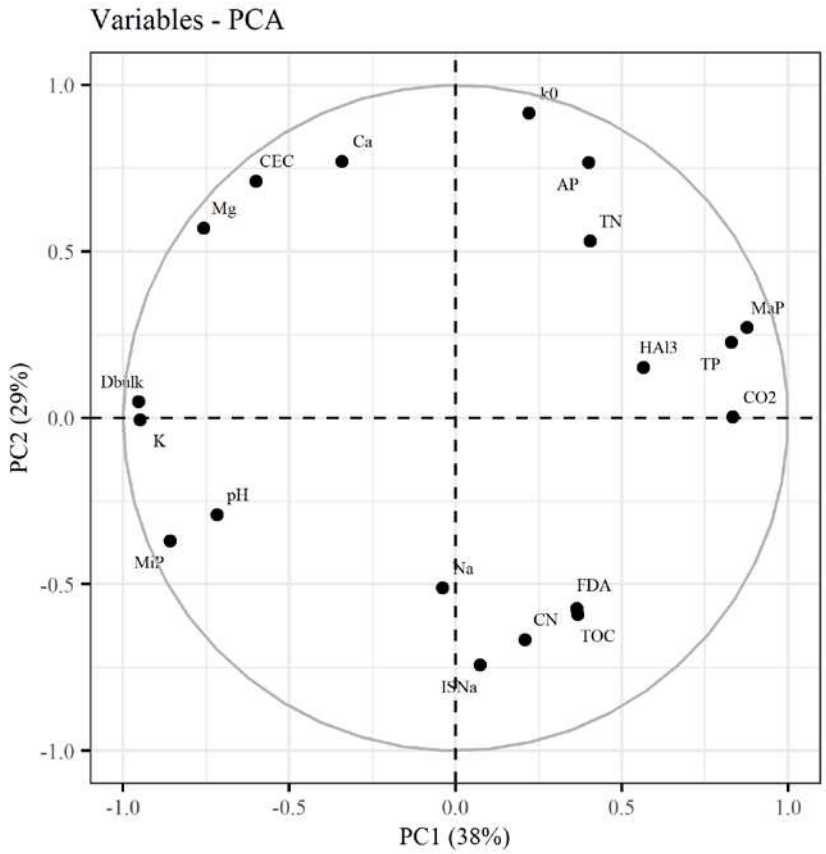

Figure S3. PCA variables correlation plot (PC1 x PC2) including all evaluated soil attributes. AP – available phosphorus; CEC – cation exchange capacity; Dbulk – soil bulk density; ISNa – sodium saturation; TOC – total organic carbon; TN – total nitrogen; k0 – hydraulic conductivity; CO2 – mean CO_2 fluxes; MaP – macroporosity; MiP – microporosity; TP – total porosity; FDA – microbial activity (FDA hydrolysis); HAl3 – potential acidity; CN – C:N ratio.

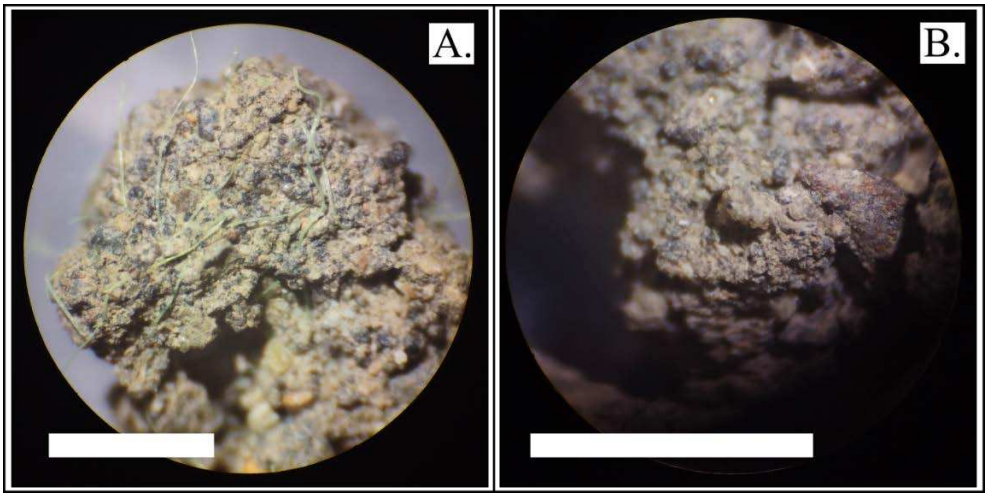

Figure S4. PAN fibers (A.) and PE fragments (B.) integrated into soil aggregates after the 22-day incubation period. The scale bar represents 1.0 mm.

8.2 Supporting tables

Table S1. Characterization of chemical parameters and texture of the soil used for the experiment. Mean values and standard deviation in parentheses (n = 3).

pH	**AP**	**Na^+**	**K^+**	**Ca^{2+}**	**Mg^{2+}**	**Al^{3+}**	**H^++Al^{3+}**	**CEC**
H_2O	**mg kg^{-1}**	**$cmol_c$ kg^{-1}**						
7.36	68.8	0.25	0.13	3.53	5.47	0.00	1.10	10.46
(0.03)	(6.00)	(0.00)	(0.01)	(0.12)	(0.26)	(0.00)	(0.00)	(0.34)
BS	**SS**	**TOC**	**TN**	**Prem**	**Coarse Sand**	**Fine Sand**	**Silt**	**Clay**
%		**g kg^{-1}**		**mg L^{-1}**	**kg kg^{-1}**			
89.47	2.35	1.93	1.64	38.1	0.4	0.23	0.16	0.22
(0.32)	(0.09)	(0.89)	(0.12)	(0.87)	(0.02)	(0.02)	(0.02)	(0.004)

/AP – available phosphorus; CEC – cation exchange capacity; BS – base saturation; SS – sodium saturation; TOC – total organic carbon; TN – total nitrogen; Prem – remaining phosphorus.

Table S2. Description of methods for soil physical and chemical parameters determinations according to Embrapa (2017).

Soil parameters	**Method description according to Embrapa (2017)**
Soil physical parameters	
Hydraulic conductivity in a saturated medium	Using the collected volumetric cylinders, the samples were saturated by capillarity and a piece of cheesecloth was inserted at the lower end of each cylinder and held in place by a rubber band, while at the top of the cylinder, another volumetric cylinder of the same diameter and 2 cm height was placed and fixed. Next, the set of cylinders was immersed in a vat containing water until the soil was saturated, and then transferred to the permeameter support positioned on screens, with a reservoir tube leveled to maintain a hydraulic load of 2 cm in height. Water was added carefully using a wash bottle, preventing air from entering the system, and the moment at which percolation began in each cylinder was observed and recorded. The percolated volume was measured after 10, 20, 30, 40, 50 and 60 minutes. Evaluations were made until the coefficient of variation of the last three samples was less than 20%. All percolated volumes were noted during the process. The hydraulic conductivity was then calculated from the equation: $k0 = (QL)\ (AHT)^{-1}$, where k0 is the hydraulic conductivity (cm min^{-1}); Q is the volume of water percolated (cm^{-3}); L is the height of the soil column (cm); H is the height of the soil column plus the water column (cm); A is the area of the cylinder (cm^2); and T is the time of percolation (min).
Soil microporosity	The volumetric cylinders containing the saturated samples were transferred to a tension table with -6 kPa of applied tension. After the equilibrium the samples were weighed and the soil microporosity was calculated from the equation: $MiP = m_{water}\ v^{-1}$, where MiP is the soil microporosity at -6 kPa ($cm^3\ cm^{-3}$; considering water density as 1 g cm^{-3}); m_{water} is the mass of water retained at a tension of -6 kPa (g); and v is the cylinder volume (cm^{-3}).
Soil bulk density	The dimensions of the cylinders containing the samples were measured and recorded in triplicate using a caliper and the volume of the cylinders were calculated. The samples were removed from the cylinders and transferred to a numbered container of known mass and dried in an oven at 105°C for a period of 48 hours. After drying, they were removed from the oven, left to cool in a desiccator and weighed. The soil bulk density was then calculated from the equation: $d_{bulk} = m_{sample}\ v^{-1}$, where d_{bulk} is the soil bulk density (g cm^{-3}); m_{sample} is the mass of dried soil (g); and v is the cylinder volume (cm^{-3}).
Soil particle density (used for the soil total porosity determination)	Twenty (20.0) grams of dried soil were weighed and transferred to a 50 mL volumetric flask with the aid of a funnel. Ethyl alcohol was added until the sample was completely covered, and the flask was shaken vigorously to eliminate any air bubbles that formed. The mixture was left to rest for half an hour. Subsequently, the operation continued slowly, until the volume of the balloon was filled, checking the absence of bubbles during the process. Finally, the volume of alcohol consumed was carefully noted. The soil particle density was then calculated from the equation: $d_{particle} = m_{sample}\ (v_{flask} - v_{alcohol})^{-1}$, where $d_{particle}$ is the soil particle density (g cm^{-3}); m_{sample} is the mass of soil added to the flask (g); v_{flask} is the volume of the volumetric flask (cm^{-3}); and $v_{alcohol}$ is the volume of alcohol used to fill the flask (cm^{-3}).

Soil total porosity	Total porosity was determined from the equation: $TP = 1 - d_{bulk}\ d_{particle}^{-1}$, where TP is the soil total porosity ($cm^3\ cm^{-3}$); d_{bulk} is the soil bulk density (g cm^{-3}); and $d_{particle}$ is the soil particle density (g cm^{-3}).
Soil macroporosity	Soil macroporosity was calculated from the equation: $MaP = TP - MiP$, where MaP is the soil macroporosity ($cm^{-3}\ cm^{-3}$); TP is the soil total porosity ($cm^3\ cm^{-3}$); and MiP is the soil microporosity ($cm^3\ cm^{-3}$).
Soil chemical parameters	
Soil pH	Ten (10.0) grams of soil were weighed and transferred to a 100 mL glass beaker and 25 mL of distilled water was added to the sample. The sample was shaken vigorously with a glass rod for approximately 60 seconds and left to rest for 1 hour to allow homogenization. After the rest period, the sample was slightly shaken again, and the pH electrodes were immersed in the homogenized suspension to take the pH reading.
Potential acidity ($H^+ + Al^{3+}$)	Five (5.0) grams of soil were weighed and placed in a 125 mL Erlenmeyer flask and 75 mL of calcium acetate solution (0.5 mol L^{-1}; pH 7.0) were added. The mixture was stirred for 10 minutes in a circular horizontal shaker and left to rest overnight after stirring. After the rest period, 25.0 mL of the supernatant solution were pipetted and transferred to another 125 mL Erlenmeyer flask. Then, the supernatant solution was titrated (phenolphthalein) with a NaOH solution (0.025 mol L^{-1}) until the development of a persistent pink color and the potential acidity ($H^+ + Al^{3+}$) was calculated based on the volume of NaOH solution used for titration.
Ca^{2+}, Mg^{2+} and Al^{3+}	Ten (10.0) grams of soil were weighed and transferred to a 125 mL Erlenmeyer flask and 100 mL of a KCl solution (1 mol L^{-1}) was added. The mixture was stirred for 5 minutes in a circular horizontal shaker and, after stirring, was left to rest overnight to allow sedimentation. After the rest period, 25.0 mL aliquots of the supernatant part of the extraction solution were pipetted to determine Ca^{2+}, Mg^{2+} and Al^{3+} contents through a atomic absorption spectrometer (Agilent 240FS).
Na^+, K^+ and available P	Ten (10.0) g of soil was weighed and transferred to a 125 mL Erlenmeyer flask and 100 mL of Mehlich-1 extracting solution (HCl 0.05 mol L^{-1} and H_2SO_4 0.0125 mol L^{-1}) was added. The mixture was stirred for 5 minutes in a horizontal circular shaker and left to settle overnight for sedimentation. After decantation, 25 mL of the extract was pipetted without filtering and transferred to a glass beaker. Five (5.0) mL of the extract was pipetted and placed in a 125 mL Erlenmeyer flask, where 10 mL of acidic ammonium molybdate solution and approximately 30 mg of powdered ascorbic acid were added as a reductant. The mixture was stirred for 1 to 2 minutes on a horizontal circular shaker. After stirring, the color was developed for 1 hour and then the optical density was read on the UV-Vis spectrophotometer (Femto 600S), using a red filter with a wavelength of 660 nm for P determination. In parallel, the remaining 20.0 mL of the extract were used to determine K^+ and Na^+ contents through a flame photometer (Micronal B462).

Table S3. Results of linear models [F values and p-values (in parenthesis) are shown] on soil physical parameters to MP doses (D), MP types (T) and their interaction (T × D; two-way ANOVA). The degrees of freedom (df) are $df_D = 1$, $df_T = 1$, $df_{T\times D} = 1$ $df_{residuals} = 8$. Bold values highlight significant p-values (< 0.05).

Soil physical parameters	MP dose (D)		MP type (T)		T × D	
	F value	p-value	F value	p-value	F value	p-value
Hydraulic Cond.	9.643	**0.015**	1.250	0.296	2.163	0.180
Bulk Density	5.714	**0.044**	0.148	0.710	6.034	**0.040**
Total Porosity	2.710	0.138	6.493	**0.034**	4.522	0.066
Microporosity	9.247	**0.016**	2.736	0.137	5.228	0.052
Macroporosity	5.994	**0.040**	6.351	**0.036**	6.150	**0.038**

Table S4. Results of linear models [F values and p-values (in parenthesis) are shown] on soil chemical parameters and microbial activity (FDA hydrolysis) to MP doses (D), MP types (T) and their interaction (T × D; two-way ANOVA). The degrees of freedom (df) are $df_D = 1$, $df_T = 1$, $df_{T\times D} = 1$ $df_{residuals} = 12$. Bold values highlight significant p-values (< 0.05).

Soil chemical parameters	MP dose (D)		MP type (T)		T × D	
	F value	p-value	F value	p-value	F value	p-value
Ca^{2+}	0.000	0.990	1.350	0.268	5.220	**0.041**
Mg^{2+}	0.476	0.504	0.605	0.452	0.436	0.522
Na^{+}	2.216	0.162	9.877	**0.008**	7.150	**0.020**
K^{+}	1.848	0.199	2.087	0.174	0.116	0.740
Sodium saturation	4.361	0.059	26.921	**< 0.001**	2.143	0.169
CEC	0.662	0.432	2.117	0.171	1.736	0.212
pH	125.393	**< 0.001**	0.533	0.479	3.793	0.075
P	1.232	0.289	1.979	0.185	6.607	**0.024**
Total organic carbon	1.664	0.221	0.025	0.878	2.781	0.121
Total nitrogen	50.713	**< 0.001**	63.766	**< 0.001**	21.796	**< 0.001**
C:N ratio	8.818	**0.012**	5.565	**0.036**	4.340	0.059
$H^{+} + Al^{3+}$	1.421	0.256	1.421	0.256	0.158	0.698
FDA hydrolysis	2.004	0.182	0.103	0.754	2.464	0.142

Table S5. Results of linear models [F values and p-values are shown] on soil physical parameters to PAN fibers and PE fragments treatments (one-way ANOVA). The degrees of freedom (df) are df_{fibers} = 3, $df_{fragments}$ = 3, $df_{residuals}$ = 8. Bold values highlight significant p-values (< 0.05).

Soil physical parameters	Fibers treatments		Fragments treatments	
	F value	p-value	F value	p-value
Hydraulic Conductivity	5.161	**0.028**	10.103	**0.004**
Bulk Density	12.322	**0.002**	4.765	**0.034**
Total Porosity	20.192	**< 0.001**	0.857	0.502
Microporosity	6.480	**0.016**	0.300	0.824
Macroporosity	15.447	**0.001**	0.859	0.500

Table S6. Results of linear models [F values and p-values are shown] on soil chemical parameters and microbial activity (FDA hydrolysis) to PAN fibers and PE fragments treatments (one-way ANOVA). The degrees of freedom (df) are df_{fibers} = 3, $df_{fragments}$ = 3, $df_{residuals}$ = 12. Bold values highlight significant p-values (< 0.05).

Soil chemical parameters	Fibers treatments		Fragments treatments	
	F value	p-value	F value	p-value
Ca^{2+}	16.226	**< 0.001**	15.630	**< 0.001**
Mg^{2+}	0.248	0.862	3.237	0.061
Na^{+}	3.807	**0.040**	8.367	**0.003**
K^{+}	0.780	0.528	0.552	0.657
Sodium saturation	10.018	**0.001**	9.251	**0.002**
CEC	5.367	**0.014**	9.881	**0.001**
pH	9.382	**0.002**	14.054	**< 0.001**
AP	10.610	**0.001**	2.362	0.123
Total organic carbon	3.051	0.070	48.199	**< 0.001**
Total nitrogen	15.473	**< 0.001**	1.687	0.223
C:N ratio	7.020	**0.006**	13.925	**< 0.001**
$H^{+} + Al^{3+}$	0.286	0.835	1.333	0.310
FDA hydrolysis	7.943	**0.003**	10.633	**0.001**

Table S7. Results of Kruskal Wallis test [chi-squared values and p-values (in parenthesis) are shown] on mean CO_2 fluxes and mean soil temperature to PAN fibers and PE fragments treatments. The degrees of freedom for the Kruskal Wallis tests are $df_{fibers} = 3$ and $df_{fragments} = 3$. Bold values highlight significant p-values (< 0.05).

Soil response parameters	Fibers treatments		Fragments treatments	
	Chi-squared	p-value	Chi-squared	p-value
Mean CO_2 fluxes	9.739	**0.021**	4.956	0.175
Mean soil temperature	0.707	0.872	0.167	0.983

Table S8. Summary of PCA results – importance and eigenvalues of the principal components, and variables coordinates.

	PC1	PC2	PC3	PC4	PC5	PC6
Importance of components						
Standard deviation	2.697	2.332	1.666	1.278	1.047	0.885
Proportion of variance	0.383	0.286	0.146	0.086	0.058	0.041
Cumulative proportion	0.383	0.669	0.815	0.901	0.959	1.000
Eigenvalues	7.275	5.438	2.774	1.634	1.096	0.783
Variables coordinates						
pH	-0.718	-0.291	-0.368	-0.055	-0.145	-0.491
Available Phosphorus	0.401	0.767	-0.114	0.077	-0.319	-0.361
K^+	-0.948	-0.006	0.022	0.282	-0.140	0.031
Na^+	-0.039	-0.511	-0.731	-0.181	-0.213	0.353
Ca^{2+}	-0.342	0.770	0.131	-0.491	-0.175	0.015
Mg^{2+}	-0.758	0.570	-0.278	-0.075	-0.121	0.055
CEC	-0.600	0.711	0.018	-0.330	-0.161	0.013
Sodium Saturation	0.074	-0.743	-0.522	-0.341	-0.052	0.226
Total Organic Carbon	0.367	-0.591	0.656	-0.171	-0.235	0.016
C:N ratio	0.209	-0.666	0.581	-0.377	-0.180	0.011
Total nitrogen	0.406	0.531	0.107	0.649	-0.252	0.239
$H^+ + Al^{3+}$	0.565	0.151	-0.486	0.042	0.641	-0.097
Hydraulic conductivity	0.221	0.915	0.050	0.029	0.061	0.326
Microporosity	-0.858	-0.370	0.168	0.189	0.217	-0.123
Bulk density	-0.953	0.048	0.042	-0.092	0.267	0.089
Total porosity	0.829	0.226	-0.378	-0.316	-0.047	-0.129
Macroporosity	0.877	0.270	-0.307	-0.223	-0.069	-0.099
FDA hydrolysis	0.365	-0.574	-0.413	0.501	-0.333	-0.074
Mean CO_2 fluxes	0.834	0.002	0.518	-0.013	0.181	-0.060

CHAPTER II

Interactions of microplastics with an Antarctic marine terrace soil revealed by descriptive thin sections analysis

ABSTRACT

This study investigated the short-term interactions between microplastics (MPs) and the soil matrix of a marine terrace soil from the Fildes Peninsula (King George Island, Maritime Antarctica) using a descriptive micromorphological approach. Two types of MPs – polyethylene (PE) fragments and polyacrylonitrile (PAN) fibers – were added to soil pots in varying concentrations (from 0.001% to 1.0% w w^{-1}), and the samples were incubated under environmental conditions for 22 days. After incubation, thin sections were obtained from the experimental units and analyzed descriptively with a petrographic microscope using soil micromorphological concepts. The descriptive interpretations were related to previously obtained analytical results. Microphotographs showed PE fragments integrated into the soil mineral matrix and obstructing pores, corroborating the decrease reported for hydraulic conductivity. PAN fibers are frequently near vesicular and planar pores, possibly acting as preferential fracture points. Microfeatures related to processes driven by freeze-thaw cycles, such as translocation features, ovoid-shaped peds, planar and vesicular pores, occurred in the samples. Clay capping features on MP particles suggest that they may interact with active pedogenic processes in Antarctic periglacial soils. Our results reinforce the potential for MPs to affect soil dynamics in periglacial environments of Antarctica and encourage the use of descriptive soil micromorphological techniques to visually assess interactions of MPs with the natural soil matrix.

Keywords: soil micromorphology, Maritime Antarctica, soil pollution, fibers, fragments.

1 INTRODUCTION

Microplastics (MPs; plastic particles < 5 mm) are heterogeneous contaminants ubiquitous in several environmental compartments of marine and terrestrial ecosystems around the planet (Chen *et al.*, 2023; Weber; Bigalke, 2022), occurring in different shapes, sizes and chemical compositions. MPs can be generated by different primary (intentional production) or secondary sources (fragmenting from larger plastic items), interact with natural transport mechanisms (Surendran *et al.*, 2023; Tatsii *et al.*, 2024), and are widespread from low to high latitudes (Chen *et al.*, 2023), although their presence is more representative close to anthropic activities (Büks; Kaupenjohann, 2020). In this sense, MPs can be considered a factor of global change (Bernhardt; Rosi; Gessner, 2017; Rillig; Leifheit; Lehmann, 2021), as they are necessarily linked to anthropogenic activities, and can interact with living organisms and natural processes on a global scale (Saud *et al.*, 2023). Furthermore, by representing one of the main technological advances in terms of synthetic materials created by mankind, MPs have been pointed as candidates for geological markers to reinforce the Anthropocene epoch proposition (Chen *et al.*, 2022; Rangel-Buitrago; Neal, 2023; Zalasiewicz *et al.*, 2016).

Despite its remoteness, the Antarctic continent is no exception to MP contamination, as their presence has been reported in various environmental matrices of marine (Kelly *et al.*, 2020; Reed *et al.*, 2018; Suaria *et al.*, 2020; Zhang, Min *et al.*, 2022) and terrestrial ecosystems (Aves *et al.*, 2022; Bergami *et al.*, 2020; González-Pleiter *et al.*, 2020; Perfetti-Bolaño *et al.*, 2022). MPs can reach Antarctic ecosystems from external sources through long-range transport (Isobe *et al.*, 2017; Lozoya *et al.*, 2022), but local anthropogenic activities, concentrated on the few ice-free areas of the continent (Brooks *et al.*, 2019), have been pointed as the main sources for terrestrial and coastal environments (Lacerda *et al.*, 2019; Perfetti-Bolaño *et al.*, 2022). Ice-free areas of the Maritime Antarctic region are dominated by periglacial environments, characterized by the prevalence of cryoturbated soils (Bockheim, 2014; Michel *et al.*, 2014b; Schaefer *et al.*, 2008; Simas *et al.*, 2008) and intense human activity (Brooks; Tejedo; O'Neill, 2019). Cryoturbation in soils involves sorting, heaving, stirring, and cracking soil material due to freezing-thawing cycles and temperature gradient between soil surface and permafrost, affecting soil chemical and physical properties through the movement of mineral and/or organic matter particles along the soil profile (Bockheim; Tarnocai, 1998).

Recently, extensive research has been carried out investigating the potential impacts of MP contamination on the soil structure and physical properties, revealing that MPs can interact with

the soil matrix differently depending on MP type (size, shape, polymeric composition) and concentration, but the soil type can also be decisive for the noticed effects. For example, MP fragments at increasing concentrations are likely to fill macropores in sandy soils, decreasing the hydraulic conductivity due to the intrinsic hydrophobicity of MP particles (Guo *et al.*, 2022; Wang, Zhichao *et al.*, 2023), while MP fibers tend to decrease aggregation, probably by promoting preferential fracture points (Lehmann *et al.*, 2021; Liang *et al.*, 2021). On the other hand, MP fragments or fibers can enhance the binding of soil particles and favor aggregation in stronger structured loamy soils (Guo *et al.*, 2022; Wang, Zhichao *et al.*, 2023; Zhang; Zhang; Li, 2019). Analytical results on physical properties, visual analysis of aggregates, and additional techniques – such as computed tomography scanning and tracer dying – have been used to understand and describe the interactions of MPs with natural soil particles and pores (Guo *et al.*, 2022; Kim *et al.*, 2021; Lehmann *et al.*, 2021; Wang, Zhichao *et al.*, 2023; Zhang; Zhang; Li, 2019). However, using microphotographs to enable a detailed micromorphological description of this interaction remains largely unexplored.

Thin section analysis is a widely consolidated technique for micromorphological description (Karkanas; Goldberg, 2023; van der Meer; van Mourik, 2019), allowing the evaluation of the arrangement of soil constituents (e.g. mineral grains, micromass, pore space, pedological features) in undeformed samples, and revealing details of the soil structure related to pedogenic processes (Bullock; Fedoroff; Jongerius, 1985; Stoops; Vepraskas; Jongmans, 2003; Van Vliet-Lanoë; Fox; Gubin, 2004). This technique has been successfully used in identifying human-induced disturbances in the soil, such as remnants features of land management practices or the presence of allochthonous anthropogenic materials (e.g. construction materials, charcoal, bones) (Karkanas; Goldberg, 2023). In a scenario of MP contamination, micromorphological analysis of thin sections can potentially improve the understanding of the interaction mechanisms of MP particles with natural soil particles and their structural arrangement in the soil.

Following the first screening on the potential impacts of MPs on a cold environment soil under field conditions (de Miranda *et al.*, 2024), this study aimed to describe and analyze the structural arrangement of two types of MPs (polyethylene fragments and polyacrylonitrile fibers) in an Antarctic marine terrace soil of the Fildes Peninsula (King George Island, Maritime Antarctica). The analysis of thin section micrographs elucidated the interaction between MPs and soil particles, potential weathering of MPs, and contributed to the understanding of MPs role on soil properties changes.

2 MATERIALS AND METHODS

2.1 Site and soil descriptions

The soil used in the experiment was sampled at a marine terrace environment in the Fildes Peninsula, King George Island (62º13'S 58º57'W), in February 2022. The Fildes peninsula is historically affected by anthropogenic pressure as it hosts six research stations from different countries built between 1968 and 1994, including the Teniente Rodolfo Marsh Martin airport – one of the main entrances for logistical support in the Maritime Antarctic region. In addition to the disturbance associated with infrastructure establishment (Brooks; Tejedo; O'Neill, 2019), anthropogenic impacts on ice-free soils include contamination by heavy metals (Lu *et al.*, 2012), hydrocarbons (Wu *et al.*, 2023), and MPs (Lozoya *et al.*, 2022; Perfetti-Bolaño *et al.*, 2022). The marine terrace environment was selected for the experiment because it can be prone to MP contamination both through the drainage of meltwater streams (González-Pleiter *et al.*, 2020) and through coastal maritime influence (Perfetti-Bolaño *et al.*, 2022).

Soils in this area are predominantly classified as Fluvisols (according to the WRB system), formed by several layers of sediments derived from weathering of basaltic/andesitic lavas, resulting from periglacial and isostatic uplift processes (Michel *et al.*, 2014b). The clay mineralogy predominantly comprises smectites, chlorites and micas (Pelayo *et al.*, 2022). In a regional context, the soil used in this study represents the potentially MP-affected coastal soils in terms of mineralogy, texture, and carbon content. The soil was sampled (~25 kg) in an area susceptible to flooding by meltwater channels, at a 0–15 cm depth, in the transition between a poorly structured sandy surface horizon and a clayey subsurface horizon, with a slightly stronger developed structure of plastic consistency and characteristic expressions of swell-shrinking clay mineralogy (e.g. slickensides). The soil was sieved (2 mm) in the field at ambient temperature prior to the MP addition, resulting in a sandy-clayey-loamy texture soil, with neutral pH (7.36) and low contents of total organic carbon (0.20%) and nitrogen (0.17%) (Table 1). Regional and local details of the experiment site can be found at (de Miranda *et al.*, 2024).

Table 1. Characterization of selected chemical parameters and texture of the soil used for the experiment. Mean values and standard deviation in parentheses (n = 3).

pH H_2O	**TOC** dag kg^{-1}	**TN**	**AP** mg kg^{-1}	**CEC** $cmol_c$ kg^{-1}	**CSand** kg kg^{-1}	**FSand**	**Silt**	**Clay**
7.36	0.20	0.17	68.8	10.46	0.40	0.23	0.16	0.22
(0.03)	(0.09)	(0.01)	(6.00)	(0.34)	(0.02)	(0.02)	(0.02)	(0.004)

/AP – available phosphorus; CEC – cation exchange capacity; TOC – total organic carbon; TN – total nitrogen; CSand – coarse sand; FSand – fine sand.

2.2 Microplastics spiking to the soil

Two MP types were selected to be spiked to the soil: polyethylene (PE) fragments (mean size = 407 µm ± 369 µm), acquired from Bianquímica (São Paulo, Brazil; product No. MLB1282396142); and polyacrylonitrile (PAN) fibers (mean size = 2818 µm ± 1193 µm), obtained by manually cutting 100% "Mollet" acrylic threads (Círculo S/A, São Paulo, Brazil; product No. 781). Polyethylene MPs have been extensively reported in various environmental compartments of the Antarctic coastal environment (Cincinelli *et al.*, 2017; Fragão *et al.*, 2021; Lozoya *et al.*, 2022), while MP fibers are the most common shape found in Antarctic ecosystems (González-Pleiter *et al.*, 2020; Rota *et al.*, 2022), which includes acrylic and PAN polymers (Aves *et al.*, 2022; Bessa *et al.*, 2019). Both MP types were microwaved for 3 min (500 W) to minimize the risk of microbial contamination (Machado et al., 2019) – which did not cause visible damage to the particles according to a stereomicroscope inspection – and stored in previously sterilized glass bottles until addition to the soil. The size distribution and visual example of the MPs used in the experiment can be found in Miranda et al. (2024).

The MPs were weighed (± 0.001 g) and added to the soil at 0.01, 0.1, and 1.0% wet weight concentration for PE fragments, and at 0.001, 0.01, and 0.1% wet weight concentration for PAN fibers, which allowed MP particles to be effectively blended with the soil matrix without causing significant differences in the mixture (soil + MPs) volume. These range of concentrations consider real conditions found in highly polluted samples (Fuller; Gautam, 2016; Scheurer; Bigalke, 2018; Wang *et al.*, 2020), and were calculated by wet weight since the experiment was set in the field without drying the soil (actual moisture of 27%).

2.3 Experimental setup

After mixing the MPs with the soil at the predetermined concentrations, 700 g of spiked wet soil were stored (without compaction) in conical polypropylene pots (h = 8 cm, upper diameter = 11 cm, lower diameter = 9.5 cm) with four replicates for each treatment plus the control treatment (without MPs addition), totaling 28 pots. Then, the pots were partially buried randomly at the sample site to simulate real field conditions. Field conditions experimentation was prioritized for daily temperature and moisture variations. All pots had the same number of holes (3 mm) in the bottom to allow water percolation and were incubated for 22 days. To

mitigate the potential for contaminating the Antarctic environment and deeper soil layers, each experimental unit was covered with a holed plastic lid, allowing gas exchange and the entry of precipitation water, while a permeable paper covered each unit's bottom. After the experiment, a layer of soil immediately in contact with the pots (~3 cm) was collected and transported to the laboratory for proper disposal.

2.4 Soil physical properties and thin section analysis

In the laboratory, undisturbed samples representative of the newly built structure developed throughout the experiment were collected from the pots using steel volumetric cylinders to perform the analysis of soil physical properties (hydraulic conductivity, bulk density, micro-, macro-, and total porosity) according to the (Embrapa, 2017) guidelines. The analytical results of the soil physical properties have already been published and are re-presented in the Supplementary Material to support the discussion on the thin sections, therefore the detailed description of the used methods and statistical treatment can be found in Miranda et al. (2024).

An entire pot (replicate) of each treatment, including the control, was used to prepare the thin sections according to (Fitzpatrick, 1984). Considering the clay mineralogy and characteristic features of swell-shrinking clays in the soil used for the experiment, the soil moisture was entirely replaced by liquid acetone (Murphy, 1985). The samples were then impregnated with a polyester resin, and subsequently sectioned, laminated and polished on glass microscope slides (50 mm x 76 mm) until they reached a thickness of ~30 µm. The thin sections were analyzed using a petrographic microscope (Eclipse E600 POL, Nikon), described according to (Bullock; Fedoroff; Jongerius, 1985; Stoops; Vepraskas; Jongmans, 2003), and the micrographs were obtained with a digital camera coupled to the microscope (Canon EOS E3).

3 RESULTS

The soil matrix is composed of heterogeneous coarse grains (from fine sand to coarse sand) subspherical, subangular with undulated surface roughness, in a closed porphyric or enaulic distribution over a brownish groundmass of fine particles (silt and clay) with undifferentiated b-fabric, exalting the sandy-clayey-loamy texture (Figure 1; Table 1; Tables S1 to S6, Supplementary Material). The coarse fraction is predominantly of volcanic origin (andesitic/basaltic lavas) and of diverse composition, with sub-rounded dark pyroclastic particles and the presence of angular polymineral lithic clasts at different stages of oxidation, which suggests a reworking dynamics considering the glaciofluvial nature and susceptibility of the soil used to set up the experiment to prior cryoturbation (Schaefer *et al.*, 2008). However, the homogenization of the soil to prepare the experimental units resulted in a coarse mineral fraction without defined orientation, with vughy porosity present in the micromass and between the coarse mineral grains (Figure 1).

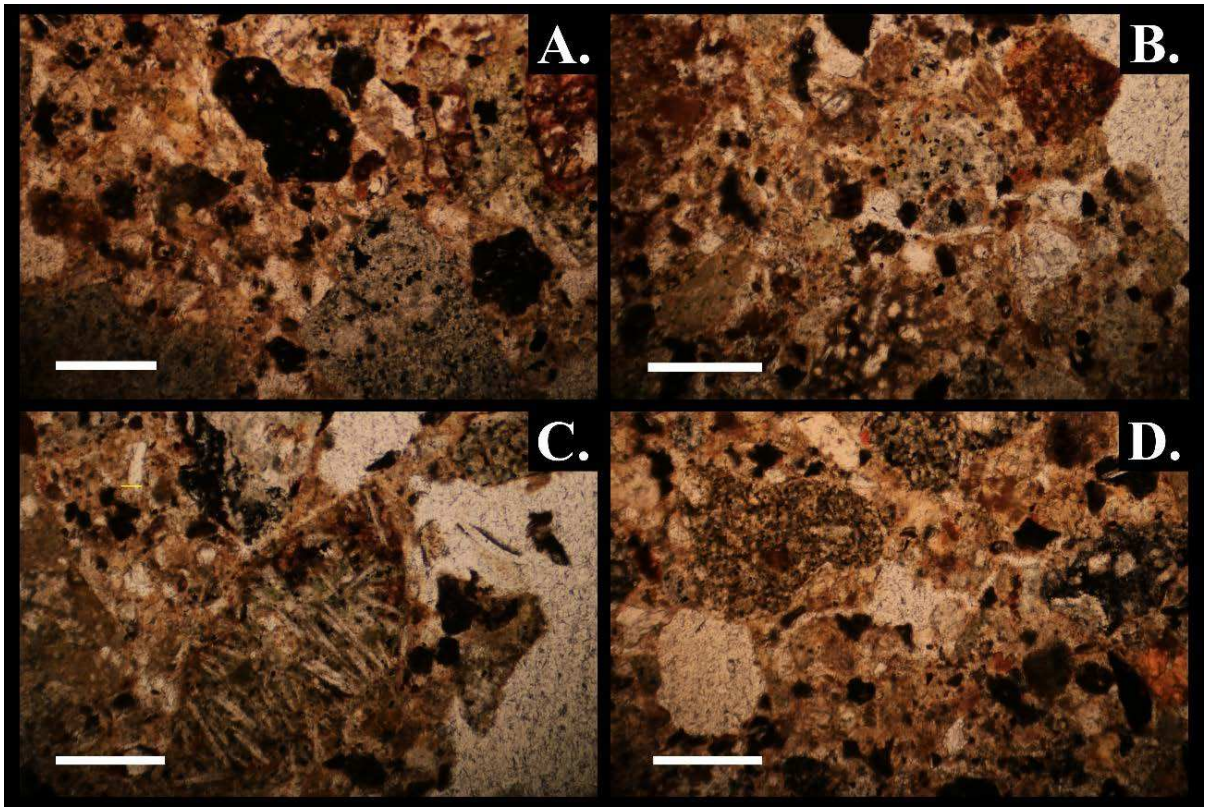

Figure 1. Representative micrographs of the groundmass and newly formed structure in the experimental units. All micrographs (A. to D.) were obtained from the control treatment. The scale bar represents 1 mm.

Despite the short incubation period, it was possible to identify the rare presence of individualized ovoidal-shaped peds, both in the control treatment (Figure 2.A) and in the MP treatments (Figures 2.B, 2.C and 2.D), suggesting an initial stage of aggregation processes possibly driven by the freeze-thaw cycles and snowmelt influence. These isolated units are composed of a clay/silt micromass domain with distributed fine sand grains, and generally occur at the groundmass interface with large macropores. The occurrence of vesicular and planar voids (Figures 1.D and 3), in some cases transforming into star-shaped voids (Figure 1.D), reinforces the indications of processes derived from freeze-thaw cycles during the short-term period of the experiment.

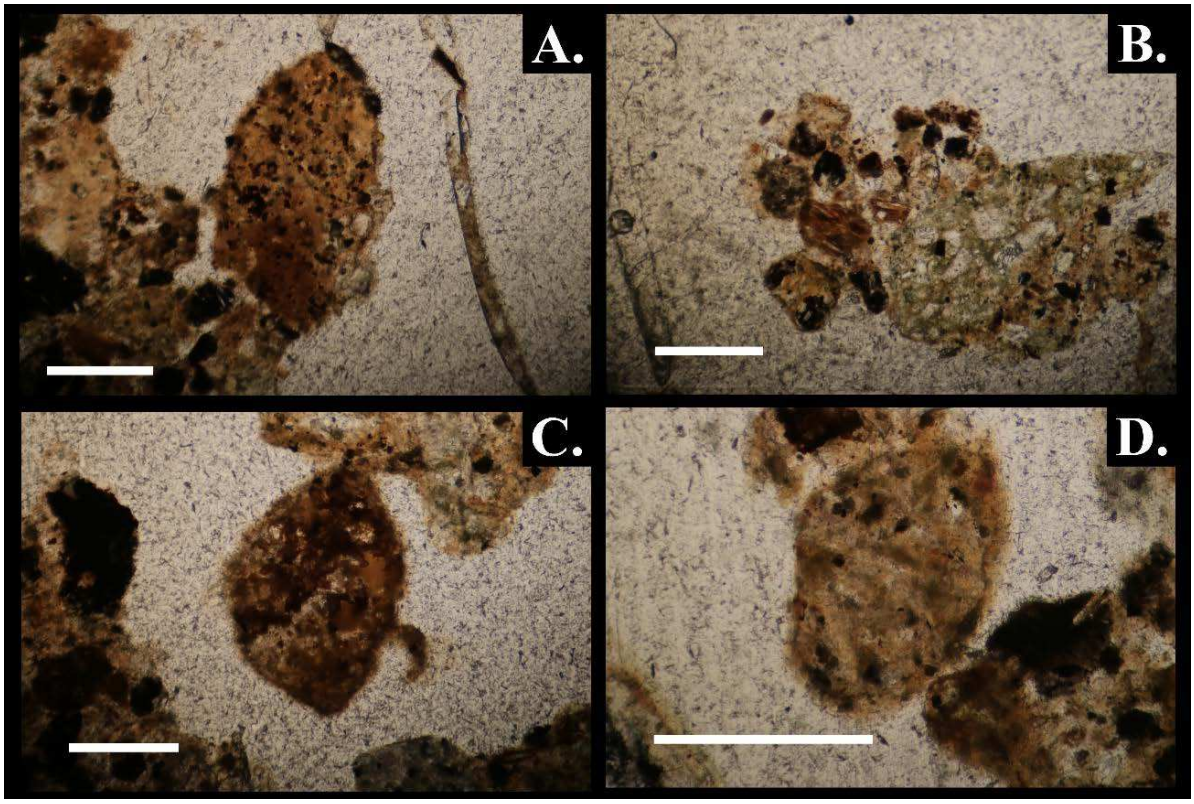

Figure 2. Micrographs highlighting the presence of individualized peds. A. Control; B. PE fragments at 0.01%; C. PE fragments at 1.0%; D. PAN fibers at 0.1%. The scale bar represents 1 mm.

The visualization of PAN fibers in the thin section was not so evident (Figure 4), as they always occurred capped by a dark micromass (Figure 4). However, they were able to cause more significant changes in the soil porous system (Figure 3), increasing the total and macroporosity at the highest dose (0.1%) and decreasing them at the lower doses (0.01% and 0.001%) (Figure S1, Supplementary Material). Corroboratively, the planar and vesicular pores were particularly evident and more frequent in PAN fibers treatments (Figure 3), generally presenting a mamillar

roughness and poor accommodation (Figures 3.D, 3.E and 3.F). It was possible to visually evidence the MP fibers acting as preferential shear stress areas for forming these pores (Figure 4.A). The thin sections obtained from PAN fibers treatments have the exclusive presence of large thick longitudinal structures (length ~5 mm; width ~0.5 mm) (Figures 4.C and 4.D), probably formed by gathering fibers with subsequent capping by the dark brown micromass. It is important to note that these particles were interpreted as MP fibers since they occur exclusively in treatments in which PAN fibers were added and considering the total absence of linear organic particles in this bare soil (see Supplementary Material for the complete collection of micrographs).

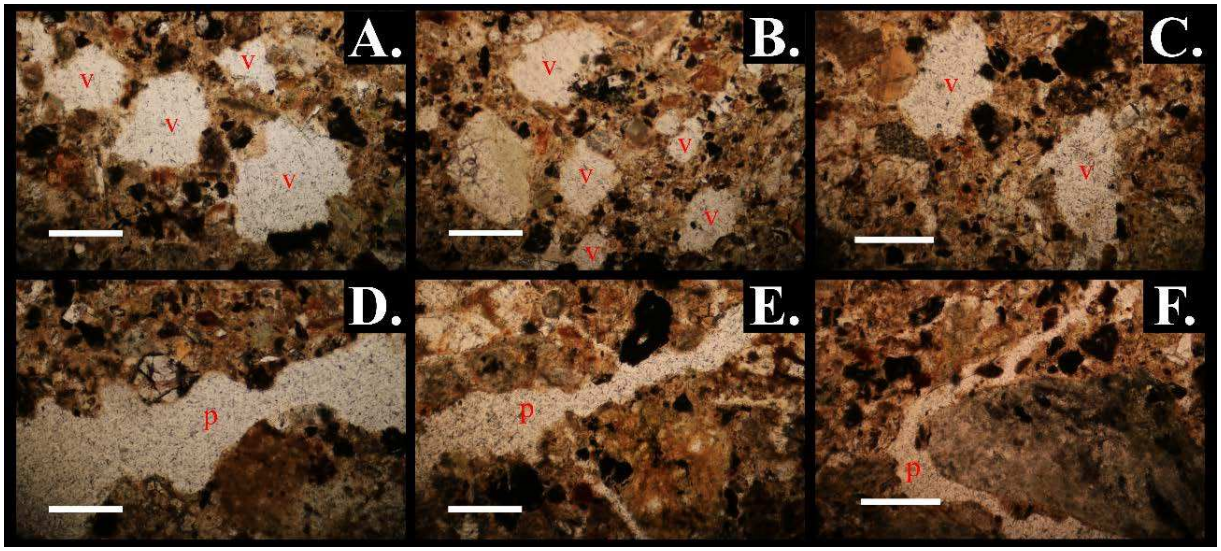

Figure 3. Vesicular (v) and planar (p) pores in PAN fiber treatments. All micrographs are in plane-polarized light. A, B, D, E. PAN fibers at 0.01%; C, F. PAN fibers at 0.1%. The scale bar represents 1 mm.

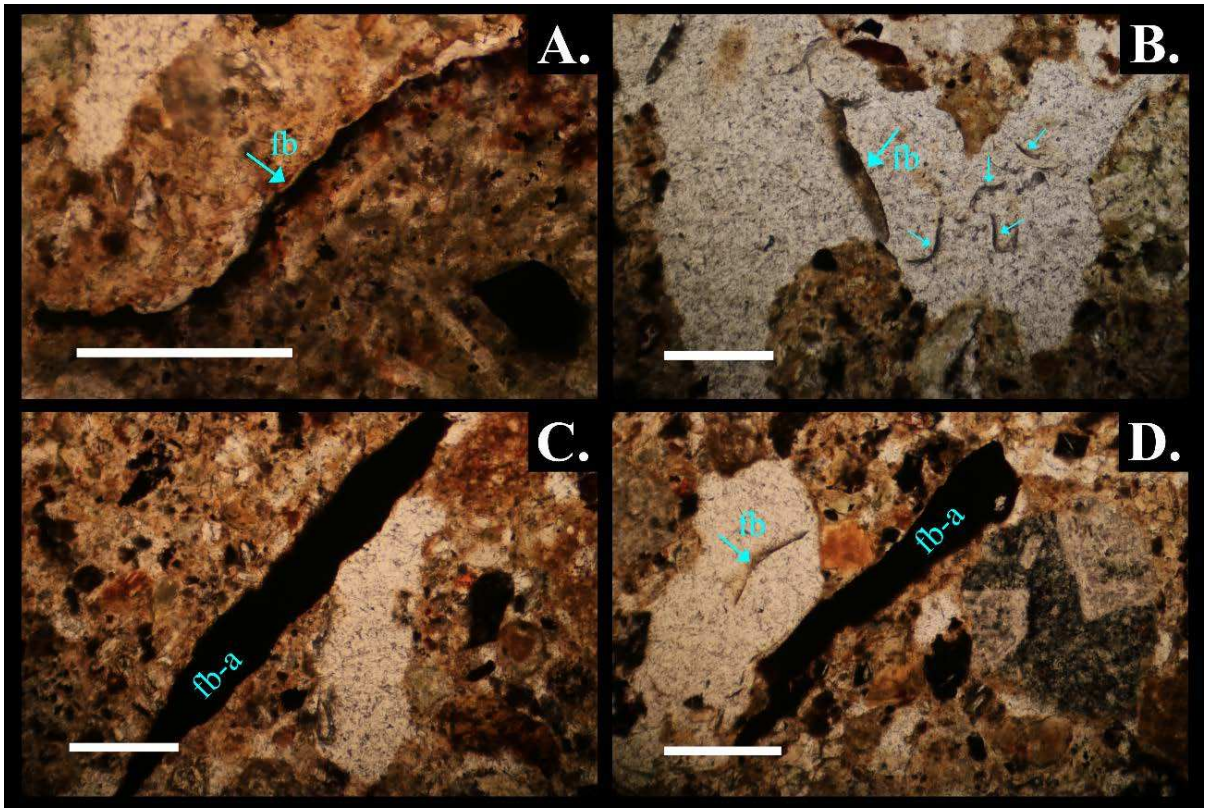

Figure 4. Micrographs highlighting the PAN fibers (fb) and the fibers "aggregates" (fb-a). A. and B. PAN fibers at 0.01%; C. PAN fibers at 0.001%; D. PAN fibers at 0.1%. The scale bar represents 1 mm.

PE fragments were likely effectively mixed with the soil matrix as they did not cause significant changes in soil porosity (Figure S1, Supplementary Material). It was possible to evidence them as part of the groundmass (Figure 5.A), on the pore walls (Figures 5.A and 5.D) and filling/obstructing pores (Figures 5.B and 5.D), which possibly address the decrease in hydraulic conductivity in PE fragments treatments (Figure S1, Supplementary Material). The PE fragments surfaces were partially or completely coated by the soil fine fraction (Figures 5.D, 6.B, 6.C and 6.D), although this coating presents a lighter color compared to what occurs on PAN fibers (Figure 4). Additionally, deformed PE fragments suggest fragmentation susceptibility and physical weathering by the tension exerted during soil freezing and ultra-desiccation (Figure 6.A).

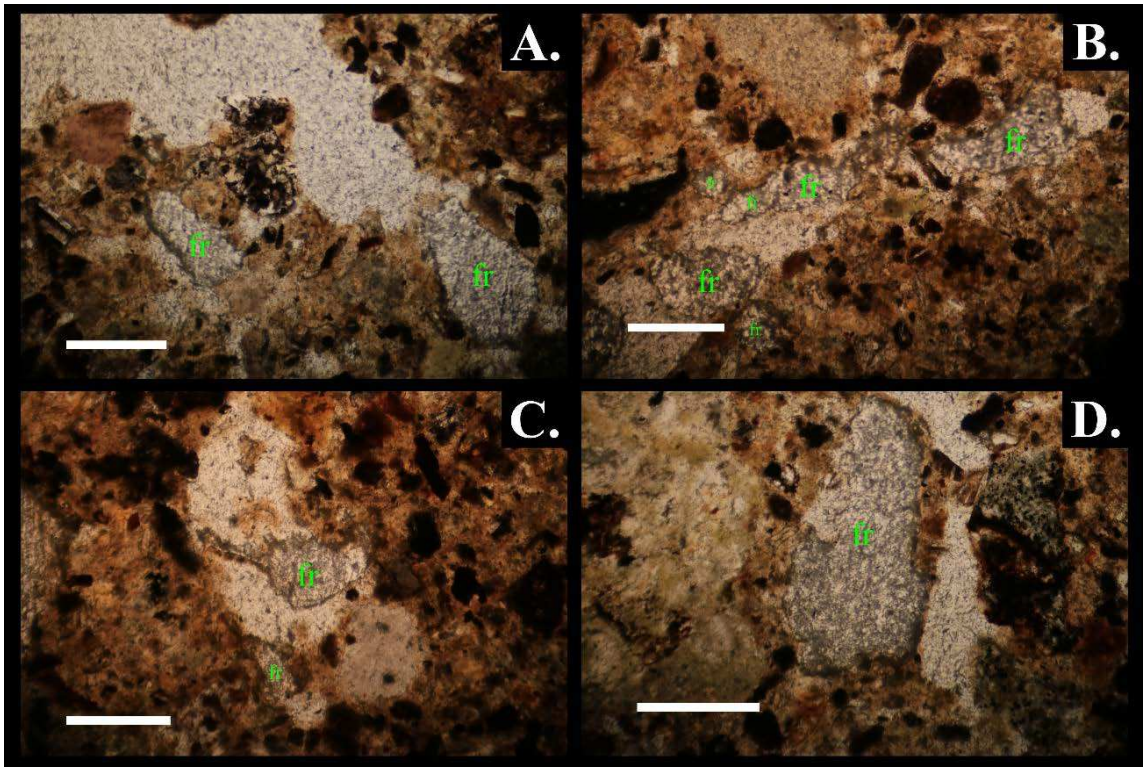

Figure 5. PE fragments (fr) mixed on the groundmass, filling pores, and occupying the pore walls. A, B, C, D. PE fragments at 1.0%. The scale bar represents 1 mm.

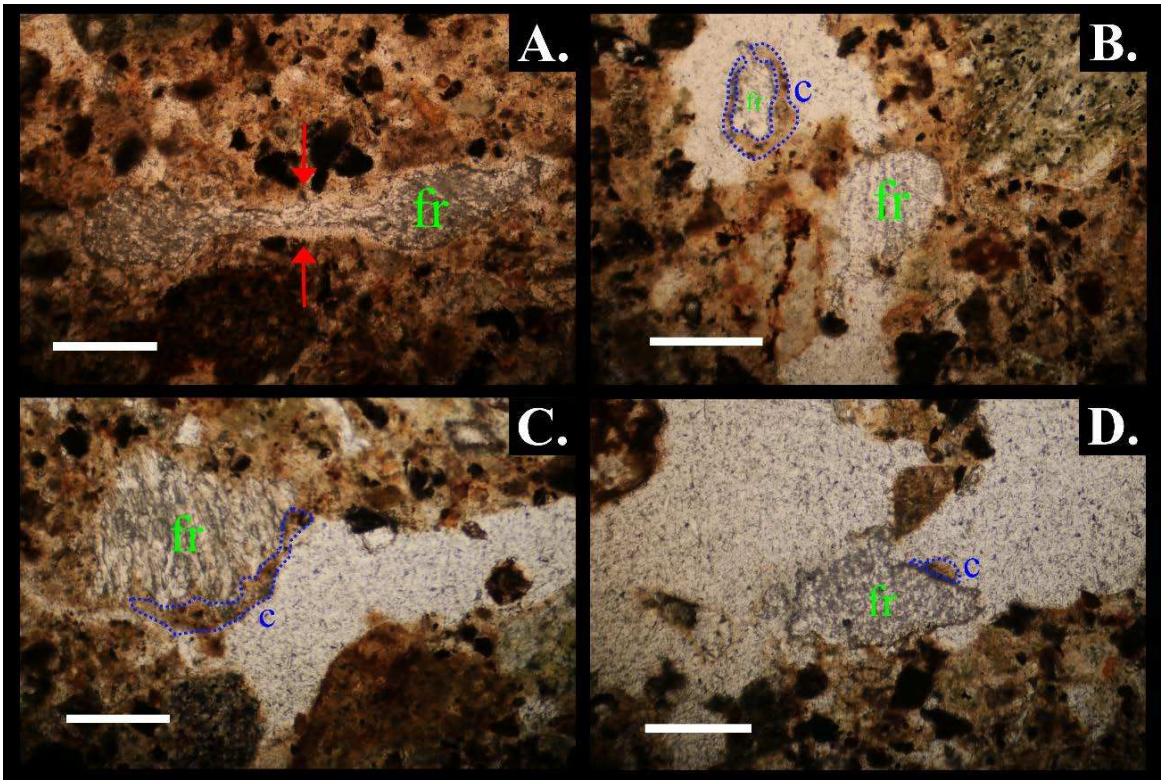

Figure 6. Deformed PE fragments (fr) and coated by the micromass (c). A, B, C. PE fragments at 1.0%; D. PE fragments at 0.01%. The scale bar represents 1 mm.

4 DISCUSSION

The thin sections analysis revealed details of the newly formed structural arrangement in the pots after a short-term incubation, which presented features and indications of processes associated with the frost action. Translocation features and formation of characteristic pores (vesicles, planar voids) can occur after 5 to 30 freeze-thaw cycles, and several cycles take place along the year in actively frozen environments, accelerating these processes (Van Vliet-Lanoë, 2010; Van Vliet-Lanoë; Fox; Gubin, 2004). The presence of water and temperature gradient are decisive factors for pedogenic processes linked to freeze-thaw cycles, which can occur both permafrost and non-permafrost areas, and are even more evident on the surface layers of saturated soils due to a rapid propagation of the freezing front (Van Vliet-Lanoë; Fox; Gubin, 2004). Field data from different areas of Maritime Antarctica show that the highest frequency of freeze-thaw days occurs at a depth of 0-10 cm in the summer period (Almeida *et al.*, 2017; Chaves *et al.*, 2017; Michel *et al.*, 2014a; Schaefer *et al.*, 2023). Therefore, the processes described here are very likely to occur in the area and season period in which the experiment was performed, even considering the short-term incubation of this study.

MP fibers supposedly hamper soil aggregation by introducing preferential fracture points in the aggregates and facilitating the aggregate breakdown (Lehmann *et al.*, 2021; Liang *et al.*, 2021; Lozano *et al.*, 2021). Conversely, the more frequent occurrence of planar voids in PAN fibers treatments suggest that they favor the characteristic platy microstructure and aggregation in soils subjected to frost action. Preferential fracture points favored by a differential heat conductivity may be responsible for creating frost desiccation cracks and inducing the platy microstructure (Van Vliet-Lanoë, 2010), as the specific heat capacity of the main clay minerals in Antarctic soils (e.g. smectites and chlorites) (Bockheim, 2014) are 5 to 10 times higher than that of PAN fibers (Gailhanou *et al.*, 2009, 2012; Gaur *et al.*, 1982). Consequently, liquid water from ice and snow melting can penetrate the soil cracks and the frost action further induces flocculation and attachment of clay particles to coarse grains surface, repacking soil clods (Van Huissteden, 2020; Van Vliet-Lanoë; Fox; Gubin, 2004).

The aggregation by reoccurring freeze-thaw cycles changes the soil porous space and favors a more efficient water supply and gas exchange, affecting microbial habitats and ultimately the nutrient cycling in these poorly developed soils (Meier *et al.*, 2019; Thomazini *et al.*, 2015). MPs occurrence in Antarctic terrestrial environments is likely more representative in coastal areas (Gurumoorthi; Luis, 2023; Perfetti-Bolaño *et al.*, 2022), which are experiencing

environmental adjustment due to glacial retreat (Thomazini *et al.*, 2020). These newly exposed areas undergo pedogenic processes and colonization by vegetation favoring labile C input and increase in CO_2 emissions (Thomazini *et al.*, 2015), which could potentially be intensified by high concentrations of MP fibers affecting soil aggregation processes and enhancing porosity (de Miranda *et al.*, 2024).

The capping features in both MP types suggest that the translocation and attachment of fine mineral particles also occur to the MPs surface, which were more representative (denoted by the darker color) in the PAN fibers than in the PE fragments, probably due to a larger specific surface (Yu *et al.*, 2023). Most MPs express a negative charge at slightly basic pH (Godoy *et al.*, 2019) – as in the soil used here, promoting specific binding of cations in solution and favoring a positive net surface charge able for attaching negatively charged clay minerals (Wang, Yi *et al.*, 2023). Divalent cations (Ca^{2+} and Mg^{2+}), which dominate the CEC of the studied soil, promote greater shielding of MPs surface negative charges than monovalent cations (Na^{+}), which may favor the clay attachment (Wang, Yi *et al.*, 2023). Heteroaggregation of MPs with clay minerals can enhance their mobility in a saturated soil condition (Li *et al.*, 2021), while the freeze-thaw cycle condition create preferential flow paths favoring the transport of plastic particles (Li *et al.*, 2023). Freeze-thaw cycles can also induce the homoaggregation of MPs, as observed here for PAN fibers treatments, and thus decrease their susceptibility to be transported (Alimi; Farner; Tufenkji, 2021). Heteroaggregation of MPs with clay minerals and homoaggregation between MP particles is chiefly governed by electrostatic attraction/repulsion forces (Wang, Yi *et al.*, 2023), hence affected by clay mineralogy, presence of organic matter, ionic strength and main cations present in the soil solution (Gao *et al.*, 2021; Li *et al.*, 2023; Wang, Yi *et al.*, 2023). Therefore, different Antarctic soils should be considered in future research to enhance our understanding on aggregation and mobility of MPs in this dynamic environment.

The decrease in hydraulic conductivity in soil with PE fragments is attributed to the hydrophobic nature of MP particles filling and creating pores mainly composed by MPs (Li *et al.*, 2023; Zhang, Xiaoting *et al.*, 2022), which could decrease the water flow promoted by the cryostatic pressure gradient (Shi *et al.*, 2024). However, unfrozen water penetrating into soil fissures with subsequent expansion and thermal stress upon freezing splits mineral coarse grains (Bockheim; Tarnocai, 1998; Van Huissteden, 2020), which was also likely suggested for MP particles by our results. The exposure to low temperatures enhances MPs brittleness (Chubarenko, 2022) and MP fragmentation derived from freeze-thaw conditions (Li *et al.*,

2024) can also contributes for migrating MPs, as smaller sized particles have a greater mobility (Gao *et al.*, 2021). Smaller MPs have a larger specific surface area and greater capacity for adsorbing other pollutants present in the Antarctic coastal environment (Gao *et al.*, 2018; Lu *et al.*, 2012), such as heavy metals and organic pollutants (Fu *et al.*, 2021; Zhang *et al.*, 2020). Thus, fragmenting MPs in periglacial soils could favor MPs impacting deeper soil layers.

Para- and periglacial environments of Antarctica are endowed with highly dynamics soils, constantly subjected to cryoturbation, reworking, erosion and sediment transfer (Francelino *et al.*, 2011; López-Martínez *et al.*, 2012; Thomazini *et al.*, 2020). In a sedimentary context, it is reasonable to consider that plastic materials go through processes analogous to a geological cycle (Rangel-Buitrago; Neal, 2023; Zalasiewicz *et al.*, 2016), from the extraction of raw material to production, disposal, transportation, degradation (fragmentation), accumulation and, possibly, lithification (Fernandino *et al.*, 2020; Rangel-Buitrago; Neal, 2023; Santos *et al.*, 2022). However, as markers of the Anthropocene, (micro)plastics are usually considered artifacts deposited in sedimentary stratigraphic columns (Chen *et al.*, 2022). Similarly, definitions for soils with anthropic or technogenic influence consider materials altered, transported, or added, and effectively mixed to the original soil matrix (generally upper layers) by human action (IUSS Working Group WRB, 2022; Soil Survey Staff, 2022). On the other hand, the observations made here suggest that MPs can interact and, possibly, mediate physical pedogenic processes – especially in soils significantly influenced by the thermal regime. It is also plausible to assume that in a long-term scenario the effects caused by MPs in the soil environment (e.g. recalcitrant carbon source, changes in pH, soil structure, etc.) (Liang *et al.*, 2021; Rillig; Leifheit; Lehmann, 2021; Zhao; Lozano; Rillig, 2021) may favor interactions with other pedogenic processes. In this case, MPs could potentially shape characteristic soils through anthropic influence, reinforcing the recognition of this contaminant as a hallmark of human capacity to affect the natural environments.

5 CONCLUSIONS

The micromorphological analysis revealed interactions of MPs with natural soil particles of a representative Antarctic periglacial soil. Our approach allowed to observe PE fragments replacing natural mineral particles and filling soil pore space, addressing the decrease in hydraulic conductivity reported by analytical results. PAN fibers possibly act as a structural disruptive agent by favoring preferential fracture points and were related to vesicular and planar porosity. Cryoturbic microfeatures (ovoid shaped peds, vesicular and planar voids, clay capping) were identified even at a short-term scale, including the clay capping of MP particles. The observations suggest that MPs can play a role in active pedogenic processes of Antarctic periglacial soils instead of simply occurring as artifacts and markers of human action, but the long-term ecological implications should be further investigated. We encourage the use of micromorphological analysis in future studies that aim to visually evaluate interactions and arrangements of MPs within the soil environment. The approach can be improved in future studies combined with use of tracers, to facilitate the identification of MPs in thin sections, and with elemental analyzes provided by instruments such as SEM-EDS, to evaluate the chemical behavior of MP particles when blended into the soil structure.

6 ACKNOWLEDGMENTS

The present work was carried with the support of the following Brazilian research agencies: National Council for Research and Development (Conselho Nacional Desenvolvimento Científico e Tecnológico – CNPq) and Coordination for the Improvement of Higher-Level Personnel (Coordenação de Aperfeiçoamento de Pessoal de Nível Superior – CAPES). This study was conducted within activities of project TERRANTAR/PERMACLIMA, financed by CNPq and the Brazilian Ministry of Science, Technology and Innovation – MCTI, under the scope of Brazilian Antarctic Program (PROANTAR). The authors thank the support of the Brazilian Ministries of Science, Technology and Innovation (MCTI), Environment (MMA) and Inter-Ministry Commission for Sea Resources (CIRM).

7 REFERENCES

ALIMI, Olubukola S.; FARNER, Jeffrey M.; TUFENKJI, Nathalie. Exposure of nanoplastics to freeze-thaw leads to aggregation and reduced transport in model groundwater environments. **Water Research**, [*s. l.*], v. 189, p. 116533, 2021.

ALMEIDA, Ivan C.C. *et al.* Long term active layer monitoring at a warm-based glacier front from maritime Antarctica. **Catena**, [*s. l.*], v. 149, p. 572–581, 2017.

AVES, Alex R. *et al.* First evidence of microplastics in Antarctic snow. **Cryosphere**, [*s. l.*], v. 16, n. 6, p. 2127–2145, 2022.

BERGAMI, Elisa *et al.* Plastics everywhere : first evidence of polystyrene fragments inside the common Antarctic collembolan Cryptopygus antarcticus. **Biology Letters**, [*s. l.*], v. 16, n. 6, 2020.

BERNHARDT, Emily S.; ROSI, Emma J.; GESSNER, Mark O. Synthetic chemicals as agents of global change. **Frontiers in Ecology and the Environment**, [*s. l.*], v. 15, n. 2, p. 84–90, 2017.

BESSA, Filipa *et al.* Microplastics in gentoo penguins from the Antarctic region. **Scientific Reports**, [*s. l.*], v. 9, n. 1, p. 1–7, 2019.

BOCKHEIM, J. G. Antarctic Soil Properties and Soilscapes. *In*: ANTARCTIC TERRESTRIAL MICROBIOLOGY. Berlin, Heidelberg: Springer Berlin Heidelberg, 2014. v. 9783642452, p. 293–315.

BOCKHEIM, J. G.; TARNOCAI, C. Recognition of cryoturbation for classifying permafrost-affected soils. **Geoderma**, [*s. l.*], v. 81, n. 3–4, p. 281–293, 1998.

BROOKS, Shaun T. *et al.* Our footprint on Antarctica competes with nature for rare ice-free land. **Nature Sustainability**, [*s. l.*], v. 2, n. 3, p. 185–190, 2019.

BROOKS, Shaun T.; TEJEDO, Pablo; O'NEILL, Tanya A. Insights on the environmental impacts associated with visible disturbance of ice-free ground in Antarctica. **Antarctic Science**, [*s. l.*], v. 31, n. 6, p. 304–314, 2019.

BÜKS, Frederick; KAUPENJOHANN, Martin. Global concentrations of microplastics in soils - A review. **Soil**, [*s. l.*], v. 6, n. 2, p. 649–662, 2020.

BULLOCK, P; FEDOROFF, N; JONGERIUS, A. **Handbook for Soil Thin Section Description**. Albrighton: Waine, 1985.

CHAVES, D. A. *et al.* Active layer and permafrost thermal regime in a patterned ground soil in Maritime Antarctica, and relationship with climate variability models. **Science of the Total Environment**, [*s. l.*], v. 584–585, p. 572–585, 2017.

CHEN, Hongyu *et al.* Are microplastics the 'technofossils' of the Anthropocene? **Anthropocene Coasts**, [*s. l.*], v. 5, n. 1, p. 1–11, 2022.

CHEN, Bingfeng *et al.* Global distribution of marine microplastics and potential for biodegradation. **Journal of Hazardous Materials**, [*s. l.*], v. 451, n. March, p. 131198, 2023.

CHUBARENKO, Irina. Physical processes behind interactions of microplastic particles with natural ice. **Environmental Research Communications**, [*s. l.*], v. 4, n. 1, 2022.

CINCINELLI, Alessandra *et al.* Microplastic in the surface waters of the Ross Sea (Antarctica): Occurrence, distribution and characterization by FTIR. **Chemosphere**, [*s. l.*], v. 175, p. 391–400, 2017.

DE MIRANDA, Caik Oliveira *et al.* Short-term impacts of polyethylene and polyacrylonitrile microplastics on soil physicochemical properties and microbial activity of a marine terrace environment in maritime Antarctica. **Environmental Pollution**, [*s. l.*], v. 347, n. December 2023, 2024.

EMBRAPA. **Manual de Métodos de Análise de Solo**. 3ªed. Brasília, DF: [*s. n.*], 2017.

FERNANDINO, Gerson *et al.* Anthropoquinas: First description of plastics and other man-made materials in recently formed coastal sedimentary rocks in the southern hemisphere. **Marine Pollution Bulletin**, [*s. l.*], v. 154, n. March, 2020.

FITZPATRICK, E. A. **Micromorphology of Soils**. Dordrecht: Springer Netherlands, 1984.

FRAGÃO, Joana *et al.* Microplastics and other anthropogenic particles in Antarctica: Using penguins as biological samplers. **Science of the Total Environment**, [*s. l.*], v. 788, p. 147698, 2021.

FRANCELINO, Marcio Rocha *et al.* Geomorphology and soils distribution under paraglacial conditions in an ice-free area of Admiralty Bay, King George Island, Antarctica. **Catena**, [*s. l.*], v. 85, n. 3, p. 194–204, 2011.

FU, Lina *et al.* Adsorption behavior of organic pollutants on microplastics. **Ecotoxicology and Environmental Safety**, [*s. l.*], v. 217, n. March, p. 112207, 2021.

FULLER, Stephen; GAUTAM, Anil. A Procedure for Measuring Microplastics using Pressurized Fluid Extraction. **Environmental Science and Technology**, [*s. l.*], v. 50, n. 11, p. 5774–5780, 2016.

GAILHANOU, H. *et al.* Thermodynamic properties of chlorite CCa-2. Heat capacities, heat contents and entropies. **Geochimica et Cosmochimica Acta**, [*s. l.*], v. 73, n. 16, p. 4738–4749, 2009.

GAILHANOU, H. *et al.* Thermodynamic properties of illite, smectite and beidellite by calorimetric methods: Enthalpies of formation, heat capacities, entropies and Gibbs free energies of formation. **Geochimica et Cosmochimica Acta**, [*s. l.*], v. 89, p. 279–301, 2012.

GAO, Xiaozhong *et al.* Occurrences, sources, and transport of hydrophobic organic contaminants in the waters of Fildes Peninsula, Antarctica. **Environmental Pollution**, [*s. l.*], v. 241, p. 950–958, 2018.

GAO, Jing *et al.* Vertical migration of microplastics in porous media: Multiple controlling factors under wet-dry cycling. **Journal of Hazardous Materials**, [*s. l.*], v. 419, n. May, p. 126413, 2021.

GAUR, Umesh *et al.* Heat Capacity and Other Thermodynamic Properties of Linear Macromolecules VI. Acrylic Polymers. **Journal of Physical and Chemical Reference Data**, [*s. l.*], v. 11, n. 4, p. 1065–1089, 1982.

GODOY, V. *et al.* The potential of microplastics as carriers of metals. **Environmental Pollution**, [*s. l.*], v. 255, 2019.

GONZÁLEZ-PLEITER, Miguel *et al.* First detection of microplastics in the freshwater of an Antarctic Specially Protected Area. **Marine Pollution Bulletin**, [*s. l.*], v. 161, n. October, p. 1–6, 2020.

GUO, Zi Qi *et al.* Soil texture is an important factor determining how microplastics affect soil hydraulic characteristics. **Environment International**, [*s. l.*], v. 165, n. May, p. 107293, 2022.

GURUMOORTHI, K.; LUIS, Alvarinho J. Recent trends on microplastics abundance and risk assessment in coastal Antarctica: Regional meta-analysis. **Environmental Pollution**, [*s. l.*], v. 324, n. January, p. 121385, 2023.

ISOBE, Atsuhiko *et al.* Microplastics in the Southern Ocean. **Marine Pollution Bulletin**, [*s. l.*], v. 114, n. 1, p. 623–626, 2017.

IUSS WORKING GROUP WRB. **World Reference Base for Soil Resources. International soil classification system for naming soils and creating legends for soil maps**. 4th. ed. Vienna, Austria: International Union of Soil Sciences (IUSS), 2022.

KARKANAS, Panagiotis; GOLDBERG, Paul. Soil Micromorphology. *In*: ENCYCLOPEDIA OF EARTH SCIENCES SERIES. [*S. l.: s. n.*], 2023. p. 1–13.

KELLY, A. *et al.* Microplastic contamination in east Antarctic sea ice. **Marine Pollution Bulletin**, [*s. l.*], v. 154, n. March, p. 111130, 2020.

KIM, Shin Woong *et al.* Indirect Effects of Microplastic-Contaminated Soils on Adjacent Soil Layers: Vertical Changes in Soil Physical Structure and Water Flow. **Frontiers in Environmental Science**, [*s. l.*], v. 9, n. May, p. 1–9, 2021.

LACERDA, Ana L.d.F. *et al.* Plastics in sea surface waters around the Antarctic Peninsula. **Scientific Reports**, [*s. l.*], v. 9, n. 1, p. 1–12, 2019.

LEHMANN, Anika *et al.* Microplastics have shape- and polymer-dependent effects on soil aggregation and organic matter loss – an experimental and meta-analytical approach. **Microplastics and Nanoplastics**, [*s. l.*], v. 1, n. 1, p. 1–14, 2021.

LI, Meng *et al.* Transport and deposition of microplastic particles in saturated porous media: Co-effects of clay particles and natural organic matter. **Environmental Pollution**, [*s. l.*], v. 287, n. June, p. 117585, 2021.

LI, Meng *et al.* Transport of plastic particles in natural porous media under freeze–thaw treatment: Effects of porous media property. **Journal of Hazardous Materials**, [*s. l.*], v. 442, n. August 2022, 2023.

LIANG, Yun *et al.* Effects of Microplastic Fibers on Soil Aggregation and Enzyme Activities Are Organic Matter Dependent. **Frontiers in Environmental Science**, [*s. l.*], v. 9, n. April, p. 1–11, 2021.

LÓPEZ-MARTÍNEZ, Jerónimo *et al.* Periglacial processes and landforms in the South Shetland Islands (northern Antarctic Peninsula region). **Geomorphology**, [*s. l.*], v. 155–156, p. 62–79, 2012.

LOZANO, Yudi M. *et al.* Microplastic Shape, Polymer Type, and Concentration Affect Soil Properties and Plant Biomass. **Frontiers in Plant Science**, [*s. l.*], v. 12, n. February, p. 1–14, 2021.

LOZOYA, Juan Pablo *et al.* Stranded Pellets in Fildes Peninsula (King George Island, Antarctica): New Evidence of Southern Ocean Connectivity. **SSRN Electronic Journal**, [*s. l.*], p. 119519, 2022.

LU, Zhibo *et al.* Baseline values for metals in soils on Fildes Peninsula, King George Island, Antarctica: The extent of anthropogenic pollution. **Environmental Monitoring and Assessment**, [*s. l.*], v. 184, n. 11, p. 7013–7021, 2012.

MEIER, Lars A. *et al.* Pedogenic and microbial interrelation in initial soils under semiarid climate on James Ross Island, Antarctic Peninsula region. **Biogeosciences**, [*s. l.*], v. 16, n. 12, p. 2481–2499, 2019.

MICHEL, Roberto F.M. *et al.* Active-layer thermal monitoring on the Fildes Peninsula, King George Island, maritime Antarctica. **Solid Earth**, [*s. l.*], v. 5, n. 2, p. 1361–1374, 2014a.

MICHEL, Roberto F.M. *et al.* Soils and landforms from Fildes Peninsula and Ardley Island, Maritime Antarctica. **Geomorphology**, [*s. l.*], v. 225, n. C, p. 76–86, 2014b.

MURPHY, C. P. Faster methods of liquid-phase acetone replacement of water from soils and sediments prior to resin impregnation. **Geoderma**, [*s. l.*], v. 35, n. 1, p. 39–45, 1985.

PELAYO, Marta *et al.* Characterization and distribution of clay minerals in the soils of Fildes Peninsula and Ardley Island (King George Island, Maritime Antarctica). **Clay Minerals**, [*s. l.*], v. 57, n. 3–4, p. 264–284, 2022.

PERFETTI-BOLAÑO, Alessandra *et al.* Occurrence and Distribution of Microplastics in Soils and Intertidal Sediments at Fildes Bay, Maritime Antarctica. **Frontiers in Marine Science**, [*s. l.*], v. 8, n. February, 2022.

RANGEL-BUITRAGO, Nelson; NEAL, William J. A geological perspective of plastic pollution. **Science of the Total Environment**, [*s. l.*], v. 893, n. June, p. 164867, 2023.

REED, Sarah *et al.* Microplastics in marine sediments near Rothera Research Station, Antarctica. **Marine Pollution Bulletin**, [*s. l.*], v. 133, 2018.

RILLIG, Matthias C.; LEIFHEIT, Eva; LEHMANN, Johannes. Microplastic effects on carbon cycling processes in soils. **PLoS Biology**, [*s. l.*], v. 19, n. 3, p. 1–9, 2021.

ROTA, Emilia *et al.* Macro- and Microplastics in the Antarctic Environment: Ongoing Assessment and Perspectives. **Environments - MDPI**, [*s. l.*], v. 9, n. 7, p. 1–17, 2022.

SANTOS, Fernanda Avelar *et al.* Plastic debris forms: Rock analogues emerging from marine pollution. **Marine Pollution Bulletin**, [*s. l.*], v. 182, n. August, 2022.

SAUD, Shah *et al.* New insights in to the environmental behavior and ecological toxicity of microplastics. **Journal of Hazardous Materials Advances**, [*s. l.*], v. 10, n. January, p. 100298, 2023.

SCHAEFER, Carlos Ernesto G.R. *et al.* Micromorphology and microchemistry of selected Cryosols from maritime Antarctica. **Geoderma**, [*s. l.*], v. 144, n. 1–2, p. 104–115, 2008.

SCHAEFER, Carlos Ernesto G.R. *et al.* Thermal monitoring of a Cryosol in a high marine terrace (Half Moon Island, Maritime Antarctica). **Anais da Academia Brasileira de Ciencias**, [*s. l.*], v. 95, p. 1–19, 2023.

SCHEURER, Michael; BIGALKE, Moritz. Microplastics in Swiss Floodplain Soils. **Environmental Science and Technology**, [*s. l.*], v. 52, n. 6, p. 3591–3598, 2018.

SHI, Yajun *et al.* Change of pore water near the freezing front during soil freezing: Migration and mechanisms. **Pedosphere**, [*s. l.*], v. 34, n. 4, p. 770–782, 2024.

SIMAS, Felipe N.B. *et al.* Genesis, properties and classification of Cryosols from Admiralty Bay, maritime Antarctica. **Geoderma**, [*s. l.*], v. 144, n. 1–2, p. 116–122, 2008.

SOIL SURVEY STAFF. **Keys to Soil Taxonomy, 13th ed**. Washington, DC: USDA-Natural Resources Conservation Service, 2022-. ISSN 10577149.

STOOPS, G; VEPRASKAS, M J; JONGMANS, A G. **Guidelines for Analysis and Description of Soil and Regolith Thin Sections**. [*S. l.*]: Soil Science Society of America, 2003.

SUARIA, Giuseppe *et al.* Floating macro- and microplastics around the Southern Ocean: Results from the Antarctic Circumnavigation Expedition. **Environment International**, [*s. l.*], v. 136, n. January, p. 105494, 2020.

SURENDRAN, U. *et al.* Microplastics in terrestrial ecosystem: Sources and migration in soil environment. **Chemosphere**, [*s. l.*], v. 318, n. January, p. 137946, 2023.

TATSII, Daria *et al.* Shape Matters: Long-Range Transport of Microplastic Fibers in the Atmosphere. **Environmental Science and Technology**, [*s. l.*], v. 58, n. 1, p. 671–682, 2024.

THOMAZINI, A. *et al.* CO2 and N2O emissions in a soil chronosequence at a glacier retreat zone in Maritime Antarctica. **Science of the Total Environment**, [*s. l.*], v. 521–522, p. 336–345, 2015.

THOMAZINI, André *et al.* The current response of soil thermal regime and carbon exchange of a paraglacial coastal land system in maritime Antarctica. **Land Degradation and Development**, [*s. l.*], v. 31, n. 5, p. 655–666, 2020.

VAN DER MEER, J. J.M.; VAN MOURIK, J. M. **Soil micromorphology**. [*S. l.*]: Elsevier, 2019. ISSN 15710866.v. 18

VAN HUISSTEDEN, J. **Thawing Permafrost**. Cham: Springer International Publishing, 2020.

VAN VLIET-LANOË, Brigitte. Frost Action. **Interpretation of Micromorphological Features of Soils and Regoliths**, [*s. l.*], p. 81–108, 2010.

VAN VLIET-LANOË, Brigitte; FOX, Catherine A.; GUBIN, Stanislaw V. Micromorphology of Cryosols. *In*: CRYOSOLS. Berlin, Heidelberg: Springer Berlin Heidelberg, 2004. p. 365–390.

WANG, Zhichao *et al.* Effects of microplastics on the water characteristic curve of soils with different textures. **Chemosphere**, [*s. l.*], v. 317, n. January, p. 137762, 2023.

WANG, Wenfeng *et al.* Environmental fate and impacts of microplastics in soil ecosystems: Progress and perspective. **Science of the Total Environment**, [*s. l.*], v. 708, p. 134841, 2020.

WANG, Yi *et al.* Influence of typical clay minerals on aggregation and settling of pristine and aged polyethylene microplastics. **Environmental Pollution**, [*s. l.*], v. 316, n. P2, p. 120649, 2023.

WEBER, Collin J.; BIGALKE, Moritz. Opening Space for Plastics—Why Spatial, Soil and Land Use Data Are Important to Understand Global Soil (Micro)Plastic Pollution. **Microplastics**, [*s. l.*], v. 1, n. 4, p. 610–625, 2022.

WU, Zilan *et al.* Polycyclic aromatic hydrocarbons in Fildes Peninsula, maritime Antarctica: Effects of human disturbance. **Environmental Pollution**, [*s. l.*], v. 318, n. November 2022, p. 120768, 2023.

YU, Yingxue *et al.* Minimal Impacts of Microplastics on Soil Physical Properties under Environmentally Relevant Concentrations. **Environmental Science and Technology**, [*s. l.*], v. 57, n. 13, p. 5296–5304, 2023.

ZALASIEWICZ, Jan *et al.* The geological cycle of plastics and their use as a stratigraphic indicator of the Anthropocene. **Anthropocene**, [*s. l.*], v. 13, p. 4–17, 2016.

ZHANG, Min *et al.* First Evidence of Microplastic Contamination in Antarctic Fish (Actinopterygii, Perciformes). **Water (Switzerland)**, [*s. l.*], v. 14, n. 19, 2022.

ZHANG, Shuwu *et al.* Microplastics influence the adsorption and desorption characteristics of Cd in an agricultural soil. **Journal of Hazardous Materials**, [*s. l.*], v. 388, n. October 2019, p. 121775, 2020.

ZHANG, Xiaoting *et al.* Size/shape-dependent migration of microplastics in agricultural soil under simulative and natural rainfall. **Science of the Total Environment**, [*s. l.*], v. 815, p. 152507, 2022.

ZHANG, G. S.; ZHANG, F. X.; LI, X. T. Effects of polyester microfibers on soil physical properties: Perception from a field and a pot experiment. **Science of the Total Environment**, [*s. l.*], v. 670, p. 1–7, 2019.

ZHAO, Tingting; LOZANO, Yudi M.; RILLIG, Matthias C. Microplastics Increase Soil pH and Decrease Microbial Activities as a Function of Microplastic Shape, Polymer Type, and Exposure Time. **Frontiers in Environmental Science**, [*s. l.*], v. 9, n. June, p. 1–14, 2021.

8 SUPPLEMENTARY MATERIAL FOR CHAPTER II

8.1 Supporting figures

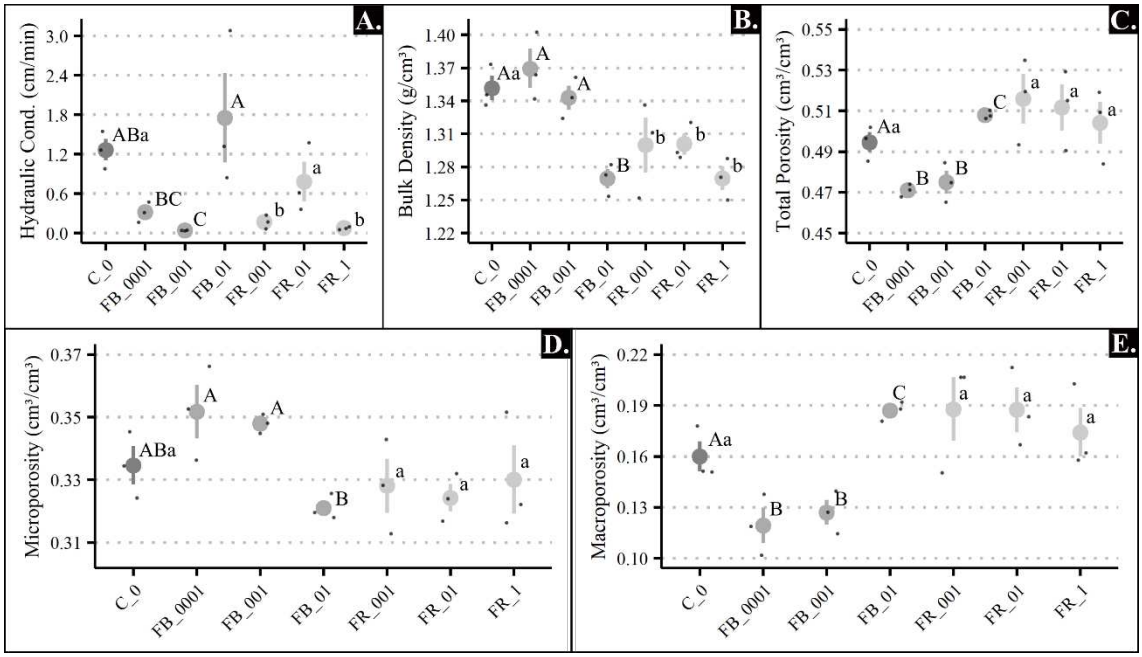

Figure S1. Effects of MP treatments on soil physical properties: A. saturated hydraulic conductivity; B. soil bulk density; C. soil total porosity; D. microporosity; E. macroporosity. Treatments are shape and color coded in grayscale, from darkest to lightest: control (C, circle); fibers (FB, triangle); and fragments (FR, square). Means with the same letters belong to the same group, by Fischer's LSD ($\alpha = 0.05$). Reproduced from de Miranda et al. (2024).

8.2 Supporting tables

Table S1. Collection of micrographs obtained from the treatment with PE fragments at 0.01%. All scale bars represent 1 mm.

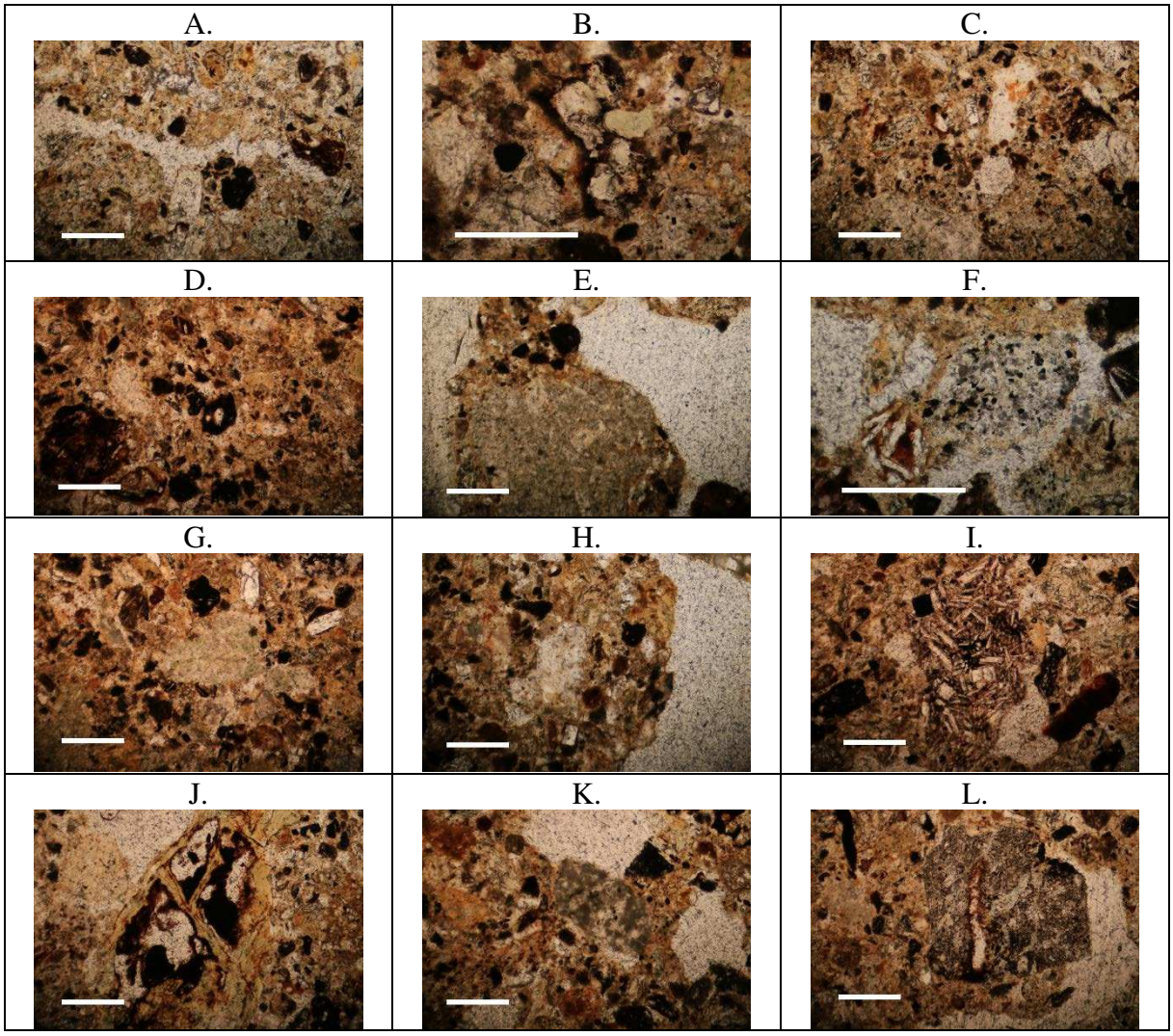

Table S2. Collection of micrographs obtained from the treatment with PE fragments at 0.1%. All scale bars represent 1 mm.

A. 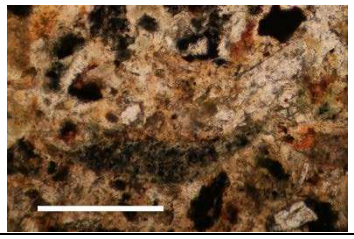	B. 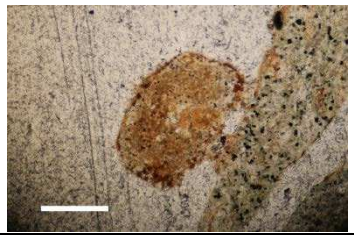	C. 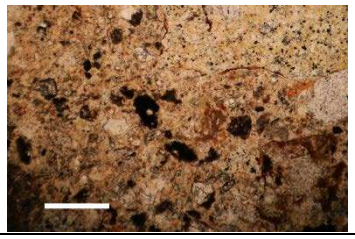
D. 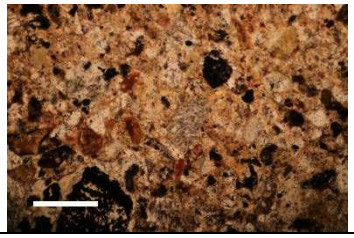	E. 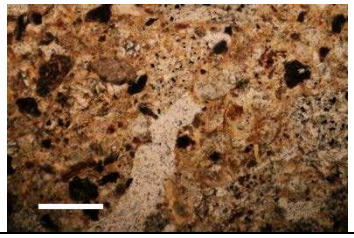	F. 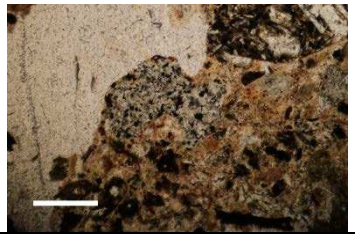
G. 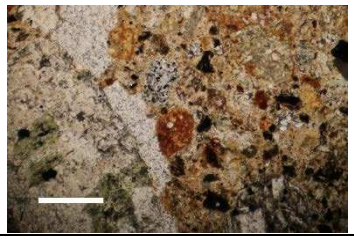	H. 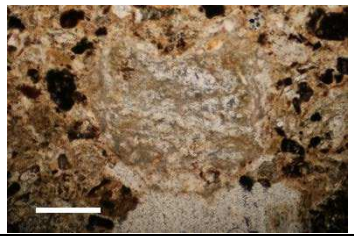	I. 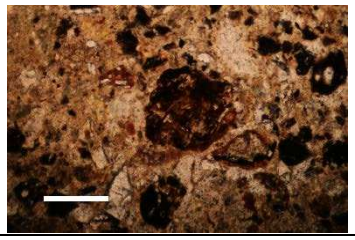

Table S3. Collection of micrographs obtained from the treatment with PE fragments at 1.0%. All scale bars represent 1 mm.

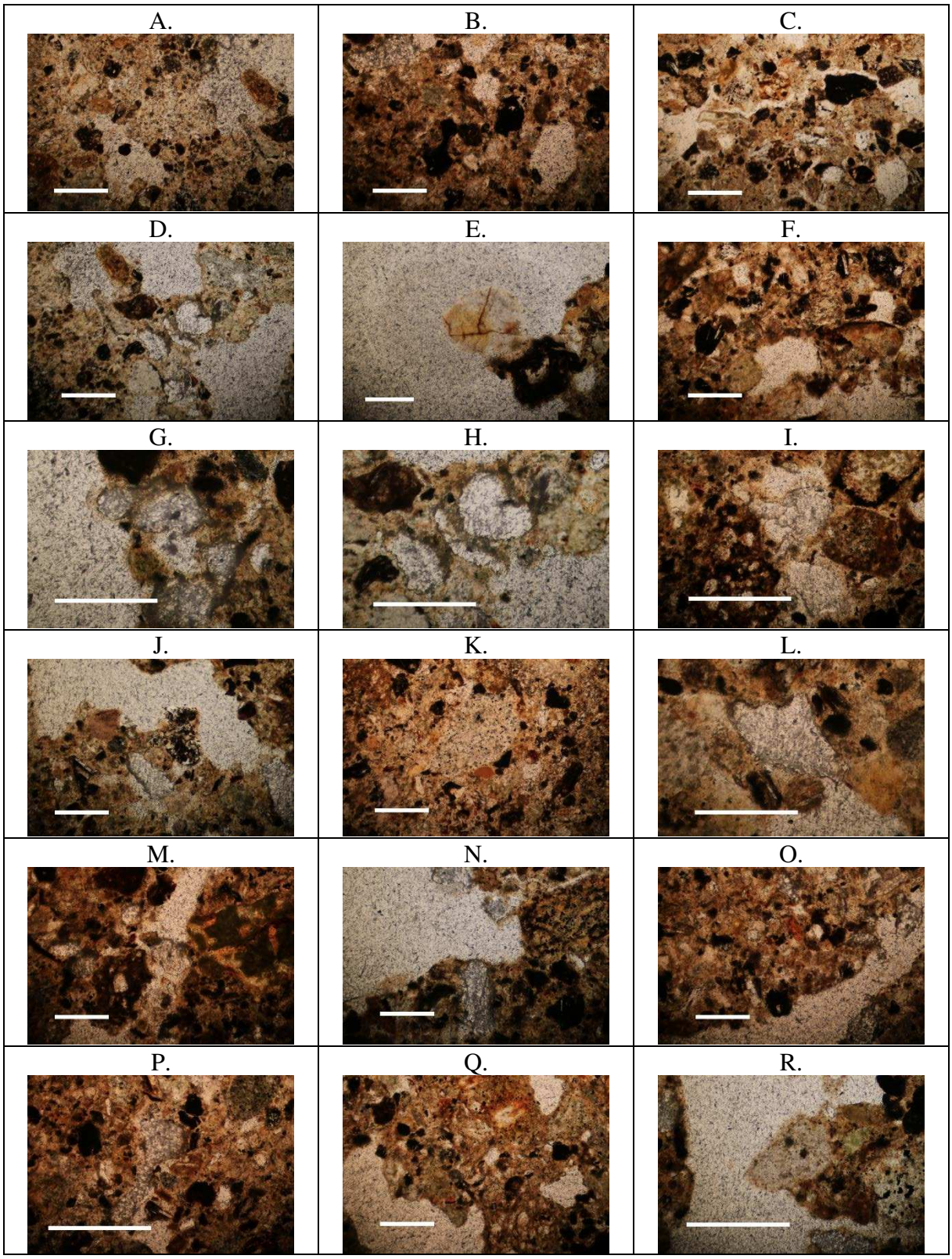

Table S4. Collection of micrographs obtained from the treatment with PAN fibers at 0.001%. All scale bars represent 1 mm.

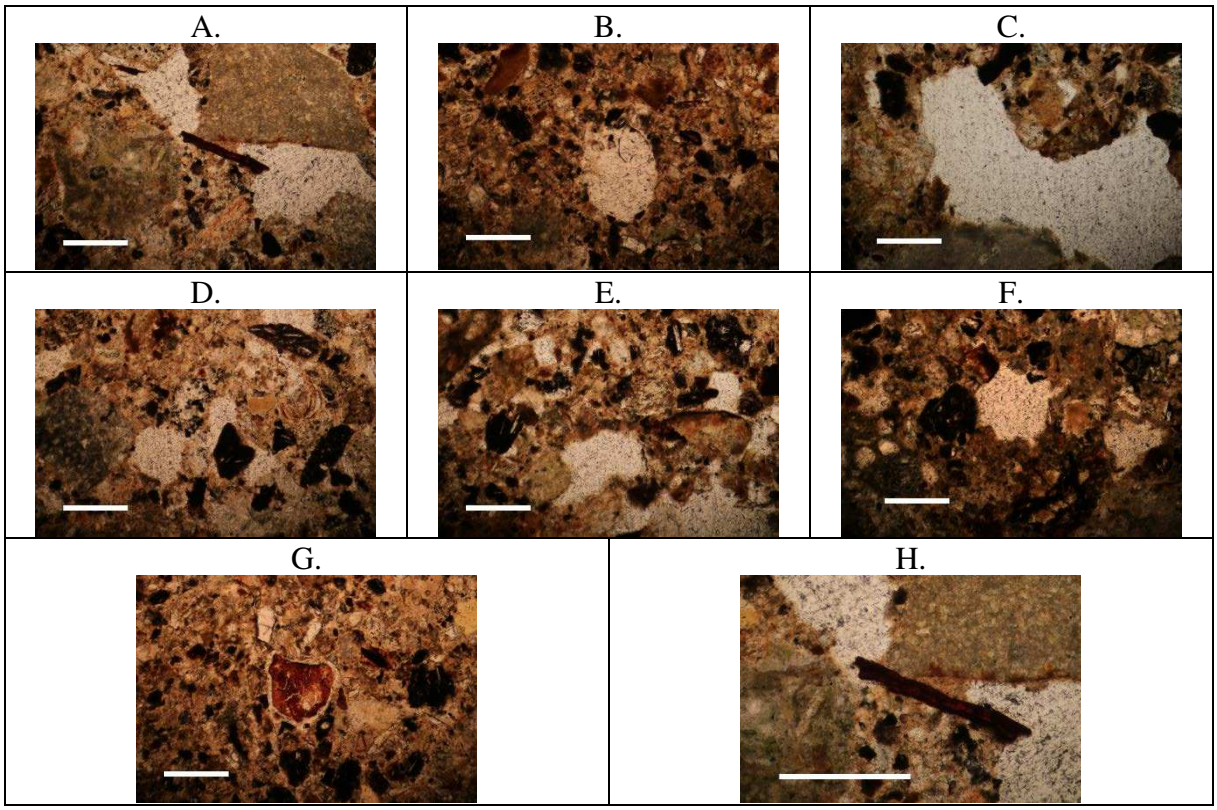

Table S5. Collection of micrographs obtained from the treatment with PAN fibers at 0.01%. All scale bars represent 1 mm.

A. 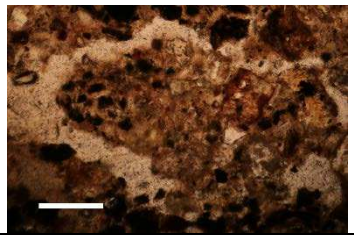	B. 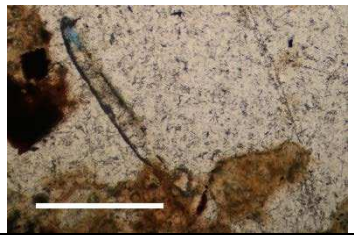	C. 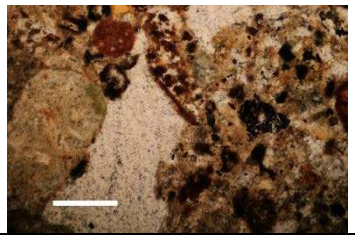
D. 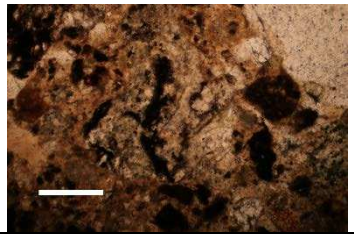	E. 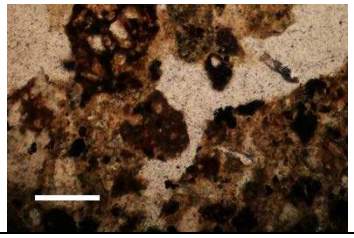	F. 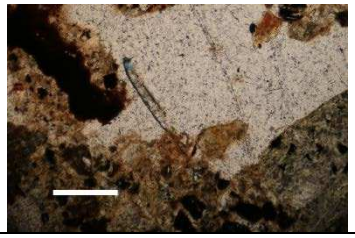
G 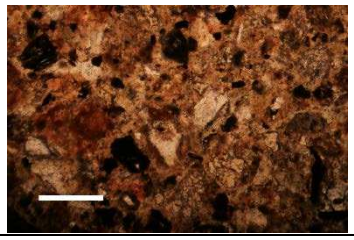	H. 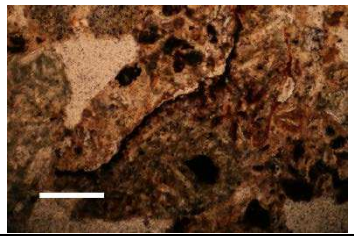	I. 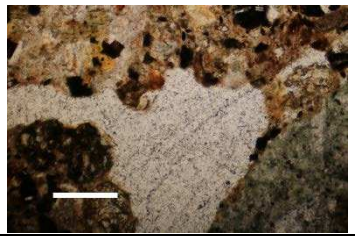
J. 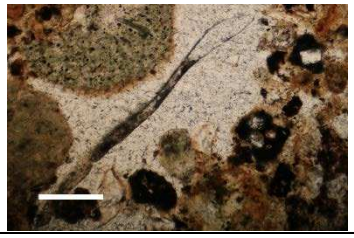	K. 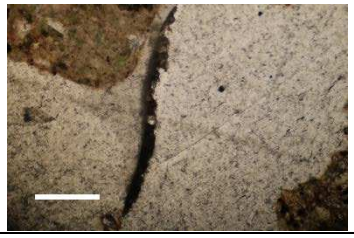	L. 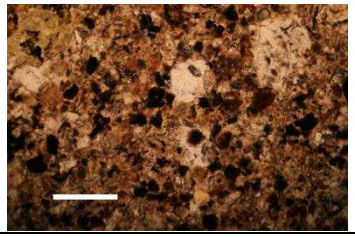

Table S6. Collection of micrographs obtained from the treatment with PAN fibers at 0.1%. All scale bars represent 1 mm.

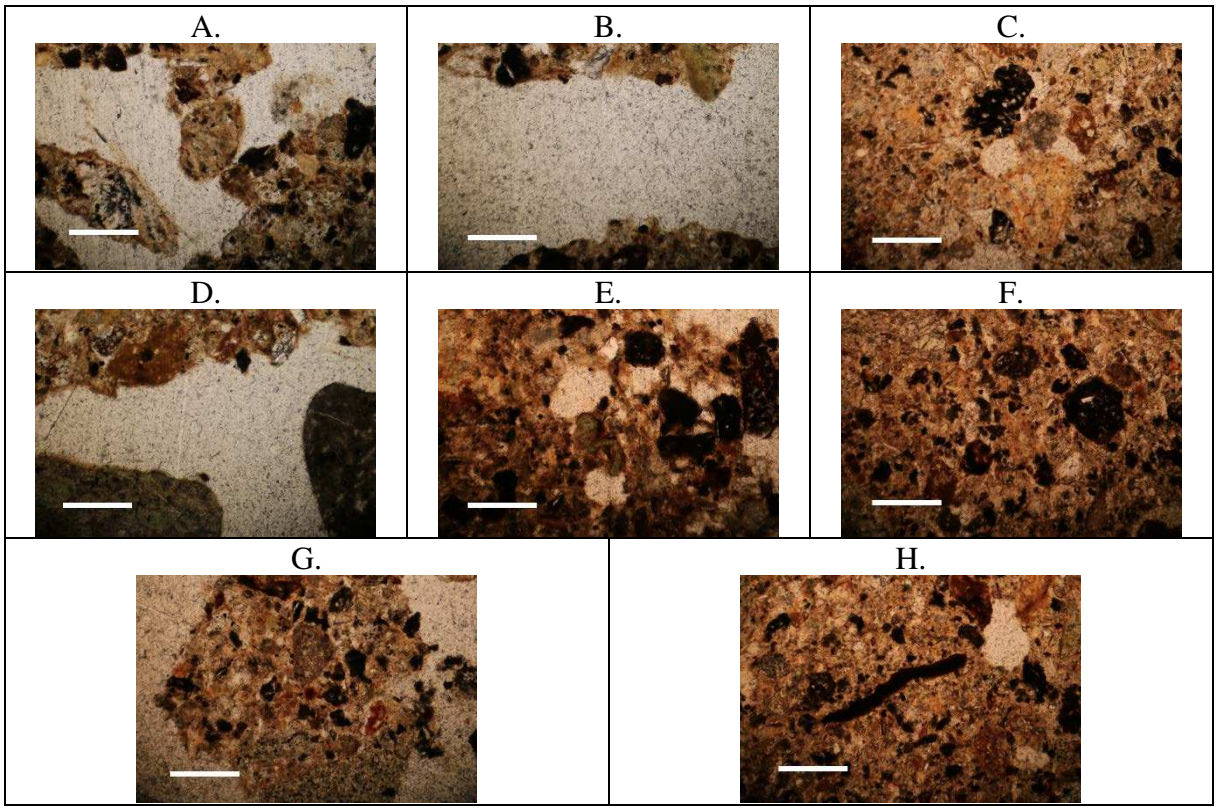

CHAPTER III

Microplastic vertical migration and physical properties in Antarctic soils under successive freezing-thawing cycles

ABSTRACT

Microplastics (MPs) are emerging contaminants in Antarctic periglacial environments, where pedogenic processes driven by freeze-thaw cycles (FTCs) and cryoturbation are active. We investigated the vertical migration of MP particles (polyethylene, polyethylene terephthalate, and polylactic acid) and impacts on physical properties in three Antarctic soils subjected to FTCs through a soil column experiment. Three layered soil columns (12.5 cm) were prepared with (0.01 % v v^{-1}) and without MP presence at the superficial layer (0 – 2.5 cm) and were incubated for 44 days subjected or not to FTCs conditions (10 successive FTCs). The abundance of MPs in the second (2.5 – 7.5 cm) and third (7.5 – 12.5 cm) layers relative to the surface layer, particle diameters and physical parameters were compared between treatments, layers and soil types. The results revealed MP vertical migration through the soil columns varying according to FTCs occurrence, soil types and polymer types. The more porous soil with a higher organic matter content (S3) showed higher relative abundance numbers in the lower layers of soil columns, while the more weathered and finer textured soil (S1) showed more representative effects of FTCs facilitating MP migration. Polyethylene particles showed greater mobility and there was a trend to find smaller MP particles with increasing soil depth. In general, soil columns subjected to FTCs showed significant thaw subsidence, increased porosity (driven by macroporosity) in the surface layer, and compaction of lower layers. The mixed effect of MPs and FTCs was observed in soil S1, with MPs potentially alleviating the increase in bulk density of lower soil layers, and soil S2, with MPs decreasing macroporosity in the surface layer. Our study suggests that soil type and MP characteristics are determining factors affecting their vertical migration and impacts on soil physical properties of periglacial Antarctic soils under FTCs.

Keywords: soil pollution, cryoturbation, soil columns experiment, particle movement.

1 INTRODUCTION

Microplastics (MPs) are plastic particles smaller than 5 mm, of different shapes and compositions, that can be formed by the fragmentation of larger plastic items (secondary MPs) or intentionally produced by the industry (primary MPs). As a major consequence of the inappropriate use and consumption of plastic materials by the society along the years, MPs are now emerging pollutants with a ubiquitous presence confirmed in several marine and terrestrial environmental compartments on the planet (Geyer; Jambeck; Law, 2017; Hale *et al.*, 2020; Koutnik *et al.*, 2021). The main sources of MPs to terrestrial environments and soils are related to agricultural practices and to the pressure of urbanization and industrialization (Campanale *et al.*, 2022; Horton *et al.*, 2017). The proximity of sources influences the abundance and extent of contamination, but the occurrence of MPs is not restricted to highly anthropized areas and can also reach remote environments (Büks; Kaupenjohann, 2020; Evangeliou *et al.*, 2020; Horton *et al.*, 2017).

Antarctica is a pristine environment, geographically isolated, and an important hub for scientific research, as provided by the Protocol on Environmental Protection to the Antarctic Treaty (CEP, 1991b). The growth of human pressure on the continent in recent years (Carey, 2020) has highlighted the concern about human impacts in ice-free areas. This sensitive environment represents less than 0.5% of the area, where local human activities are concentrated (Brooks *et al.*, 2019). The glacier retreat has exposed new ice-free areas, affecting soil temperature, water regime, and promoting the establishment of periglacial environments (Francelino *et al.*, 2011). The soil ecosystem is evidenced as the main mediator of terrestrial ecological processes in Antarctica, acting in the cycling of nutrients, chemical, hydrological and biological processes (Lopes *et al.*, 2021; Simas *et al.*, 2007; Thomazini *et al.*, 2020). Therefore, Antarctic soils have been widely used as a proxy for anthropic impacts both at a local scale, by soil contamination with toxic substances (Alekseev; Abakumov, 2020), or at a global scale, as a response to the impacts of climate change (Almeida *et al.*, 2017).

Even isolated and protected by international law, the Antarctic continent is not free from MP contamination. Evidence of plastic pollution in the Antarctic ecosystem dates back to the 1980s (van Franeker; Bell, 1988), and recent studies have reported the presence of MPs in several environmental compartments of marine (Kelly *et al.*, 2020; Lacerda *et al.*, 2019; Reed *et al.*, 2018; Sfriso *et al.*, 2020) but also of terrestrial environments (González-Pleiter *et al.*, 2020), including soils (Perfetti-Bolaño *et al.*, 2022). External sources through maritime and

atmospheric long-distance transport are considered important inputs of MPs to the Antarctic environment (González-Pleiter *et al.*, 2020; Isobe *et al.*, 2017; Lozoya *et al.*, 2022), it is evident that the most significant concentrations are found in areas close to local human colonies and stations (Lacerda *et al.*, 2019; Munari *et al.*, 2017). Localized and concentrated anthropogenic contamination are known threats to Antarctic periglacial environments (Fabri *et al.*, 2018; Guerra *et al.*, 2013; Miranda; Lima Neto; Schaefer, 2024), but little is known about the extent and potential impacts of MP contamination.

MPs might impact soil structure, resulting in soil physical changes. Once the MPs are incorporated into the soil, they interact preferentially with soil aggregates (Zhang; Liu, 2018), generally conferring negative effects on aggregation by creating preferential fracture points favored by their unusual shape and composition compared to the soil matrix (Lozano *et al.*, 2021; Machado *et al.*, 2019). MPs conditionate soil porosity and, especially MP fibers, tend to reduce microporosity by promoting aggregate breakdown and micropore occlusion, but increase macroporosity by isolating soil particles (Zhang; Zhang; Li, 2019). Soil water dynamics are consequently affected by changes in soil structure and the hydrophobic nature of MPs (Kim *et al.*, 2021; Machado *et al.*, 2019; Qi *et al.*, 2020). The soil physical conditioning promoted by MPs is often cited as a key factor in triggering responses within the soil microbiota, possibly leading to ecological consequences (Machado *et al.*, 2018; Rillig *et al.*, 2021). Nevertheless, the impacts of MP contamination on soil structure are dependent on soil types, texture, mineralogy, and organic matter content, affecting the adhesion and interaction of MPs with the soil matrix (Guo *et al.*, 2022; Ingraffia *et al.*, 2022).

Soils in peri- and paraglacial environments of Maritime Antarctica are generally poorly weathered, poorly structured and coarse (Bockheim, 2014). These soils are frequently subject to freeze-thaw cycles (FTCs) and cryoturbation is an important and active pedogenic process (Chaves *et al.*, 2017; do Vale Lopes *et al.*, 2022; Francelino *et al.*, 2011; Michel *et al.*, 2014). Subfreezing temperatures at the surface of moist and permeable soils promote the growth of ice needles favoring the migration of water to the freezing front (Hallet, 2013; Van Vliet-Lanoë, 2010). The recurrent slow growth and decay of ice lenses fueled by the water flow migrating towards the ice fringe caused by temperature gradients promote a differential heaving of particles through the soil profile (Hallet, 2013). The expansion of frozen water and the segregation of ice in soil promotes frost desiccation, opening shrinking fissures and preferential flow paths (Bai *et al.*, 2020; Van Vliet-Lanoë, 2010). Therefore, these conditions favor the up and downward migration of fine particles – especially coarse silts – filling macropores and

capping coarse particles (Bockheim; Tarnocai, 1998; Van Vliet-Lanoë, 2010). The influence of cryostatic pressures and gravity also promotes soil involution, in which organic matter particles tend to accumulate in tongues between the involution polygons of active ice-wedge growth conditions (Bockheim; Tarnocai, 1998). On the other hand, cryoclastic weathering favors physical disruption and thermal cracking of particles by the differential effects of expansion and contraction of water subjected to freezing and thawing (Schaefer *et al.*, 2008).

In a scenario of MP contamination, cryoturbation has the potential to vertically transport MP particles through the soil profile. Soil columns that underwent FTCs enhance flow transport of small MPs (0.02 µm) in solution by the formation of preferential paths and increased pore volume (Li *et al.*, 2023). Thawing promote the release of MPs (< 1.0 µm) retained in sand and soil columns, increasing their vertical transport upon flushing (Hsieh *et al.*, 2024). Furthermore, FTCs can increase the specific surface area and hydrophobicity of MPs (Li; Xu; Yu, 2024), in turn affecting susceptibility for their vertical migration (Gao *et al.*, 2021). However, the vertical migration of MPs promoted by FTCs processes without induced flow, already observed for other particulate contaminants such as metal oxides (Xu *et al.*, 2021), has still been little explored.

The mobility of MPs in porous media vary according to characteristics of the medium such as mineralogy, salinity, and organic matter content (Hsieh *et al.*, 2024; Ivanic *et al.*, 2023; Wang *et al.*, 2023; Yang *et al.*, 2022). Antarctic periglacial environments have a wide diversity of soils originating from different parent materials and influenced by distinct pedogenic processes besides to cryoturbation, including ornithogenesis, acid-sulfate weathering and salinization (Lopes *et al.*, 2019; Simas *et al.*, 2007; Souza *et al.*, 2014). Therefore, investigating the potential for MP migration in soils with distinct environmental contexts is crucial to better understand the extent of further impacts.

The main objective of this study was to evaluate the potential for vertical movement of MP particles [polyethylene (PE), polyethylene terephthalate (PET) and polylactic acid (PLA)] in three different Antarctic soils subject to successive FTCs through a soil columns experiment. We also aimed to assess the cumulative impacts on soil bulk density and porosity. Soil columns containing MPs in the surface layer were incubated under FTCs condition, and MP particle analysis and soil physical analysis were subsequently conducted. Three representative soils of different environmental contexts and physicochemical properties of the Antarctic environment were tested. We hypothesized that FTCs would promote vertical migration of MPs differently

according to different soil types, and we assessed the potential for a polymer selective migration for each soil type. The contamination background of the samples used in the experiment was also determined and discussed.

2 MATERIALS AND METHODS

2.1 Soil description

Three distinct soils, characteristic of the Maritime Antarctica and Antarctic Peninsula regions, were selected to perform the experiment and were sampled (~10 kg; 0–15 cm) between 2022 and 2023 at King George Island and James Ross Island (Figure 1). The soil samples were freeze-dried, sieved (2 mm), and stored at 4 ºC until repacking into soil columns. The chemical attributes and texture of the soil samples used in the experiment are presented in detail in Table S1, and their environmental context is given below:

Soil S1 – Acid sulfate soil: Sampled on the Keller Peninsula, King George Island (62º04'S 58º23'W; Figure 1), at an area composed by soils classified as "Turbi-thionic Cryosols" (according to WRB system) (Simas *et al.*, 2008). Soils in this area are formed from pyritized andesites and are generally well drained, have cryoturbic features, granular structure and yellowish color related to the presence of jarosite and natrojarosite (Simas *et al.*, 2008; Siqueira *et al.*, 2022). The soil presents a relatively advanced stage of chemical weathering favored by the acid pH, which promotes the formation of stable aggregates and high proportion of fine particles (silt + clay) (Simas *et al.*, 2008). The soil used in the experiment has a pH of 3.1, 0.1% of total organic carbon, and 38% of sand 36% of silt and 26% of clay (Table S1).

Soil S2 – Alkaline soil: Sampled at a marine terrace area on the Ulu Peninsula, James Ross Island (63º49'S 57º55'W; Figure 1), composed by "Turbic Cryosols" developed from Cretaceous-Eocene sedimentary substrates of fine-grained rocks (e.g. sandstones, siltstones and silt-mudstones) (Daher *et al.*, 2019). This soil has a sandy texture, due to the influence of the parent material, alkaline pH and high exchangeable bases contents (especially Na^+) (Table S1), due to the influence of marine aerosols and the semi-arid transitional climate (Daher *et al.*, 2019). The soil used in the experiment has a pH of 8.0, 0.2% of total organic carbon, and 64% of sand, 23% of silt and 13% of clay.

Soil S3 – Organic matter rich soil: Sampled at a marine terrace area on the Keller Peninsula (62º04'S 58º25'W; Figure 1), mainly composed by "Cambisols" and "Regosols" developed from basaltic/andesitic substrate (Francelino *et al.*, 2011). This soil occurs in a flat area prone to water accumulation, under a "moss carpet community" chiefly composed by *S. uncinata* (Thomazini *et al.*, 2016), presenting the highest levels of organic carbon and particulate organic matter among the soils used in this study, and relatively high levels of exchangeable bases

(Table S1). The soil used in the experiment has a pH of 6.6, 1.9% of total organic carbon, and 47% of sand, 29% of silt and 24% of clay.

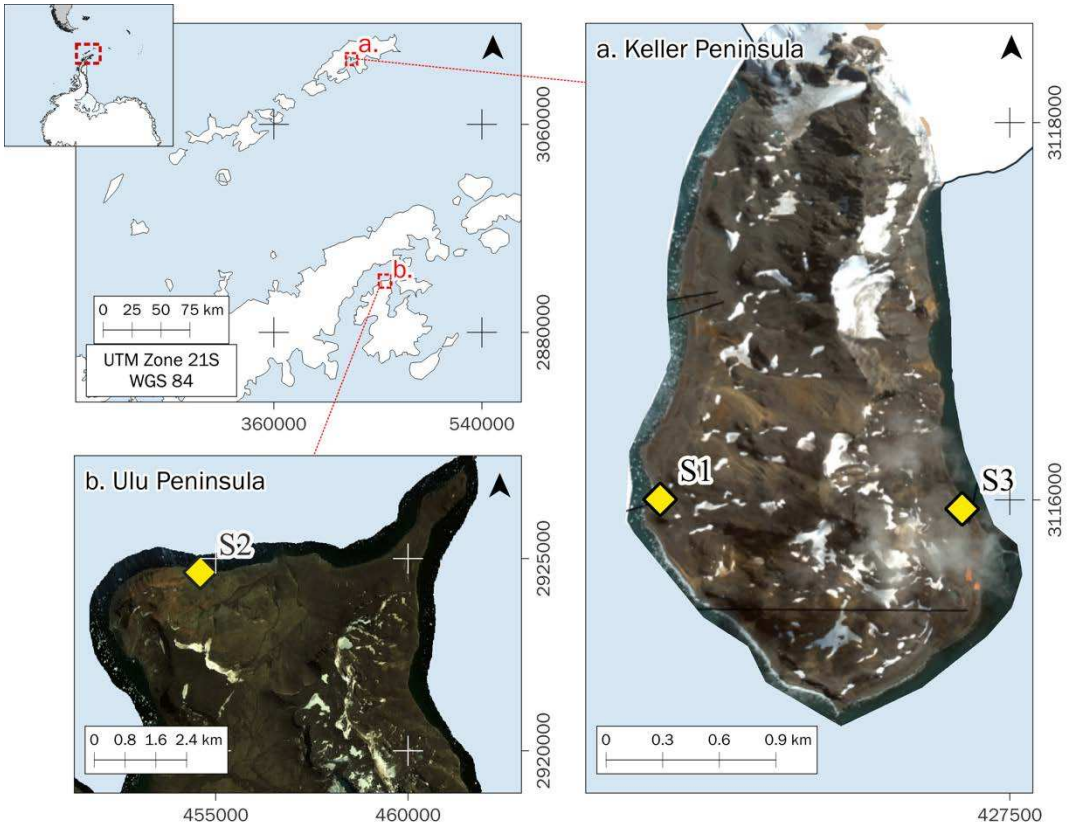

Figure 1. Location of soil sampling sites.

2.2 Experimental set up

2.2.1 Microplastics and soil columns preparation

To simulate the heterogeneous occurrence of different MP types as soil contaminants but allowing to evaluate the potential for migration of each type separately, a MP mix was prepared containing three MP fragment types in different relative volumetric concentrations: 50% polyethylene (PE), 40% polyethylene terephthalate (PET) and 10% polylactic acid (PLA). PE is widely used in single-use plastic packaging and one of the most common MP polymers found in coastal environments (Erni-Cassola *et al.*, 2019; Koutnik *et al.*, 2021), including Antarctica (Cincinelli *et al.*, 2017; Lozoya *et al.*, 2022; Suaria *et al.*, 2020). Since the polymer density affects the movement of MP particles in porous media subject to freeze-thaw cycles (Koutnik *et al.*, 2022), we selected PET as a representative of a high-density polymer (~1.38 g cm^{-3}), which is also present in the Antarctic ecosystem (Aves *et al.*, 2022; Jones-Williams *et al.*, 2020). PLA represents one of the main biodegradable polymer candidates to replace conventional plastic polymers in industrial, packaging and agricultural applications in the near future (Naser;

Deiab; Darras, 2021; Taib et al., 2023). The three MP types were dry sieved (75-212 µm) separately and then mixed in a 50 mL container by a rotational shaker (30 rpm; 10 minutes) in the predetermined proportion, resulting in 10.0 g of MP mix [mean diameters: 224.9 ± 82. (PE); 184.1 ± 65.34 µm (PET); 206.97 ± 72.57 µm (PLA)].

The three distinct soils were dry packed, in triplicate, without compaction in stainless steel columns of 5 cm diameter and 10 cm height (196.3 cm^3) divided into two layers of 5 cm. The soil columns were capillary saturated with distilled water from bottom to top for 48 hours and drained for 24 hours at pF ~0.7 matric potential to achieve a near saturated condition, representing melting in the summer (Batista *et al.*, 2022). A surface layer of 2.5 cm was prepared separately containing the MP mix added at 0.01% v v^{-1}, in addition to controls without MP addition. The concentration used here represents real conditions found in environmental samples from highly contaminated areas (Fuller; Gautam, 2016; Scheurer; Bigalke, 2018; Wang *et al.*, 2020), therefore simulating worse future conditions. Concentration on a volumetric basis was adopted to normalize the amount (n) of MP particles in each soil column, since each repacked soil type resulted in different bulk densities (Table S2). To prepare the surface layers, the MP mix was first added at pre-determined concentrations to ~500 g of each soil type in a 1 L glass container and homogenized by rotational shaker (30 rpm; 10 minutes), and subsequently dry packed and moistened as previously described for the bottom layers. Then, the surface MP containing layers (and controls) were stacked on top of the bottom layers with adhesive tape, finally comprising 12.5 cm soil columns (Figure S1).

2.2.2 Freeze-thaw cycles incubation

The soil columns were randomly placed in polystyrene insulation platforms (λ = 0.038 W mK^{-1}; Figure S1) covering their walls and bottom, which were subsequently placed in a horizontal freezer (458 liters; Model ZS4608T, Inventum). The insulation platform was used to ensure the heat exchange preferentially occurring through the soil surface – thus simulating environmental conditions. As different types of soil have different thermal behavior, preliminary tests were carried out to check which of the different soils had the highest and lowest resistivity to temperature changes, and two soil columns (soils S3 and S5, respectively) were used as monitoring controls to set the freezer activation and deactivation. A temperature sensor (T107, Campbell Scientific) was inserted into each monitoring control column, in addition to a third sensor monitoring the air temperature, and the temperature data was recorded by a datalogger (CR1000, Campbell Scientific) every 5 minutes. The consecutive freeze-thaw cycles were

induced by turning the freezer on until the average temperature of the monitoring control columns reached -5 ºC and then turning it off until the average temperature of the monitoring control columns reached +5 ºC. Ten consecutive freeze-thaw cycles were simulated over 44 days (Figure S2), while a control set of columns was kept incubated at a constant temperature of +5 ºC. The temperature range and number of cycles were selected considering real data on soil temperature at 10 cm depth, and the frequency of yearly freeze-thaw days from monitoring sites in the sampled regions (Almeida *et al.*, 2017; Correia *et al.*, 2024; Hrbáček *et al.*, 2016; Schaefer *et al.*, 2023). The experimental design evolved 36 soil columns: 3 soil types under 2 temperature conditions (FTCs/constant), with 2 MP conditions (presence/absence), and 3 replicates per treatment.

2.3 MPs analysis: background levels and experimental samples

MP abundance was quantified in the raw soil samples to assess the background levels before preparing the spiked soil columns for the experiment. Then, the MP abundance and diameters were assessed in all three layers of the repacked soil columns before and after the FTC (and NoFTC) incubation to assess potential vertical migration. The procedures for extracting microplastics from soil samples and their subsequent quantification, identification and characterization were described below.

2.3.1 MPs extraction from the soil samples

The MP extraction was carried out through the following procedure steps: density separation (i); organic matter pre-digestion (ii); organic matter digestion (iii); (second) density separation (iv).

i. Five grams (5.0 g) of dry soil, in triplicate, were added to 50 mL centrifuge tubes (with 30 mL of saturated NaBr solution ($\rho > 1.50$ g cm^{-3}). The mixture was sonicated for 10 minutes, shaken by a rotational shaker for 30 minutes at 100 rpm, and centrifuged for 30 minutes at 2500 g. Aided by a rubber disk, the supernatant was collected and vacuum filtered in a stainless-steel filter (Ø = 10 µm). The retained particles were washed with 10 mL of 1% HCl for 10 minutes to remove any potential calcium carbonate, and subsequently flushed 150 mL of distilled water to remove residual NaBr solution.
ii. The retained particles were transferred to a 50 mL centrifuge tube using 25 mL of natrium-thiourea solution (8% NaOH + 8% urea + 6.5% thiourea) and placed in a freezer for 40 minutes at -20 ºC to allow the buildup of mini-ice crystals. The samples were shaken for

30 minutes at 50 rpm to return to room temperature, vacuum filtered in a stainless-steel filter (Ø = 10 µm), and washed with 350 mL of distilled water to remove residual natrium-thiourea solution. The retained particles were transferred to a 50 mL centrifuge tube using distilled water and placed in a drying oven at 50 ºC until they dried.

iii. After drying, 15 mL of Fenton reagent [Fe(II)$SO_4 \cdot 7H_2O$ at 0.05 M; pH 2.5 – 3.0] and 15 mL of H_2O_2 were added to the samples in three steps to avoid violent reaction (adding 5 mL of each reagent in three steps with 30 minutes between them) while keeping the samples in an ice bath at 10 ºC. The reaction was carried out for at least 10 hours until no more foam was observed, and the samples were subsequently vacuum filtered in a stainless-steel filter (Ø = 10 µm).

iv. The retained particles were flushed into a 50 mL centrifuge tube using 30 mL of saturated NaBr solution and the samples went through sonication, shaking and centrifugation as described above. The supernatant was collected aided by a rubber disk and vacuum filtered in a polycarbonate filter (Ø = 8 µm; Whatman® Nuclepore™ Track-Etched Membrane). As the Fenton reaction promotes the formation of Fe (hydr)oxides, a few drops of H_2SO_4 (2.0 M) were added followed by immediate flushing with distilled water until their complete dissolution. The samples were then flushed with 150 mL of distilled water to remove residual NaBr, and the whole filter containing the retained particles was transferred to a 20 mL glass vial.

Approximately 2 mL of ethanol (96%) were added to the glass vial (enough to cover the filter containing retained particles) and the samples were sonicated for 5 minutes to allow the detachment of particles from the filter. Then the filter was collected with tweezers and flushed with ~1 mL of ethanol, remaining only the retained particles in an ethanol suspension contained in the glass vial.

Environmental samples and experimental (MP contained) samples underwent the same extraction procedure, but for the latter 1.0 g of soil was used instead of 5.0 g to avoid overlapping particles in the subsequent identification analysis.

2.3.2 Laser Direct Infrared (LDIR) spectroscopy analysis

The identification, quantification and characterization of microplastics were achieved through quantum cascade laser spectroscopy analysis on an Agilent 8700 Laser Direct Infrared (LDIR) Chemical Imaging System (Agilent Technologies). For the analysis, the glass vials were sonicated for 5 minutes, and the ethanol suspension containing the particles extracted from the

soil samples was transferred to a MirrIR low-e microscope slide (72 x 25 mm; Kevley Technologies) using a Pasteur pipette and left to air dry. To ensure the transfer of all particles contained in the glass vial, 1 mL of ethanol (96%) was added to the glass vial, and the transferring procedure was repeated at least 5 times. The whole slides were analyzed through the automated particle analysis of the Agilent Clarity software (version 1.5.58; Agilent Technologies), in which the infrared spectra acquisition (1800 to 975 cm^{-1}; 8 cm^{-1} accuracy) was performed, and particle diameters were obtained (50 – 5000 µm). Sensitivity was set to its maximum in the software. The acquired spectra were compared with the standard spectra database (Microplastic library 3.0) provided by Agilent, and spectra with a match quality > 0.90 were accepted.

Environmental and experimental samples underwent the same analysis procedure, but for the latter the library contained only the spectra of the spiked polymers (PE, PET and PLA; Figure S3), to decrease the analysis time by the instrument for each sample.

2.3.3 QA/QC for MPs analysis

The soil samples were collected using a metallic shovel and stored in paper bags with plastic bags (PE) as outer packages, until they were opened in the laboratory. All sample processing was carried out in a laboratory dedicated exclusively for this purpose, on clean work benches, using a cotton lab coat and nitrile gloves. All used chemicals (including the distilled water) were previously filtered in a stainless-steel filter (Ø = 10 µm). All tools and glassware were previously washed with filtered water before use. Negative and positive controls were employed for contamination control and method assurance. Negative controls (procedural blank samples) consisted of samples without a solid matrix that underwent all preparation and analysis procedures, and the particle count for each identified polymeric composition was used to correct the final values of the analyzed samples. Positive controls consisted of samples with a known number of added microplastic particles (PE, PET and PLA), and the final count was used to estimate the recovery rate. Detailed results and procedures of control samples can be found in Section 2 of Supplementary Material for Chapter III (Items 8.2.1 and 8.2.2).

2.4 Soil physical parameters: porosity and bulk density

The soil columns were subjected to analysis of soil physical parameters (bulk density, total porosity, microporosity and macroporosity) (Embrapa, 2017). The three layers were separated and saturated (pF 0) from bottom to top with distilled water in a sand box and weighed. The

soil microporosity was assessed by weighing the samples after they reached the equilibrium in the sand box at pF 1.8 (-6.0 kPa) of the applied tension and calculated following the Equation 1. The soil total porosity was determined by the direct method, following the Equation 2. The soil macroporosity was calculated as the difference between the TP and MiP, following the Equation 3. The soil bulk density was determined by the volumetric cylinder method with the following Equation 4.

Equation 1 $MiP = (m_{1.8} - m_{dry})\ v^{-1};$

Equation 2 $TP = (m_{sat} - m_{dry})\ v^{-1};$

Equation 3 $MaP = TP - MiP;$

Equation 4 $BD = m_{dry}\ v^{-1};$

where MiP is the soil microporosity ($cm^3\ cm^{-3}$), $m_{1.8}$ is the mass of soil and water retained at a tension of pF 1.8 (-6 kPa) (g), m_{dry} is the mass of dry soil (g), v is the cylinder volume (cm^{-3}), TP is the soil total porosity ($cm^3\ cm^{-3}$), m_{sat} is the mass of the saturated soil, MaP is the soil macroporosity ($cm^{-3}\ cm^{-3}$), and BD is the soil bulk density ($g\ cm^{-3}$).

The samples were then dried at 70 ºC (to avoid damaging the microplastics to be subsequently analyzed) until they reached constant mass, and the volumetric water content was calculated considering the density of distilled water as 1.00 $g\ cm^{-3}$.

2.5 Statistical analysis

To assess whether the treatments (MP presence and FTC condition) significantly affected the soil physical parameters regardless of the intrinsic variability addressed to the different soil types and layer depths, an analysis of variance (ANOVA) of mixed linear models was performed, considering the treatments as fixed effects and the soil type and layer depth as random effects. Then, to evaluate the effect of treatments on the different layers of each soil type, the data on soil physical parameters were modeled for each soil type separately using linear models including the layer as a fixed factor, with subsequent ANOVA. Tukey's HSD multiple comparison test was used as a post-hoc of the linear models for grouping means. Model residuals were verified for ANOVA assumptions of normality and homogeneity of variance.

Since the ANOVA assumptions were not met, statistical inferences on the MP data (abundance and diameter) were supported with non-parametric tests. To evaluate the potential for vertical

migration, the relative MP abundance (N ratio) in the second- and third-layers depth were compared. The N ratio was calculated by the ratio of particle number extracted from the second- and third-layers samples over the particle number extracted from the first layer sample of each replicate (i.e., if N ratio is equal to 1, the number of particles in the corresponding layer is equal to the number of particles in the first layer), following the equation 5:

Equation 5 $N\ ratio = n\ (n_{layer1})^{-1}$;

where N ratio is the relative MP abundance on the second/third layer of the soil columns (unitless), n is the MP abundance on the second/third layer of the soil columns (n), and n_{layer1} is the MP abundance on the first layer of the soil columns (n).

The diameter of MP particles extracted from the samples was compared. In this case, instead of using the mean value of the variables for each treatment, the complete data from all treatment replicates were pulled together to capture variability of the data set distribution. Kruskal-Wallis tests were performed on the total particle data comparing the FTC treatments and soil types, and for each soil, the FTC treatments and the different polymers were compared. The Dunn's test was used a post-hoc for grouping means.

The background MPs abundance was compared between the three soils sampled for the experiment through an ANOVA of linear model. All statistical analyses and graphs were achieved in R environment (R 4.2.2 with Rstudio 2021.09.0 interface). A 0.05 significance level was considered for all statistical tests. Mixed linear models were achieved with the lmer function from the "*lmerTest*" package, and linear models were achieved with the lm function from the R base package. Tukey's HSD tests were achieved with the HSD.test function, and Kruskal-Wallis tests were achieved with the kruskal function, both from the "*agricolae*" package. Packages "*dplyr*", "*Rmisc*", "*ggplot2*", and "*ggthemes*" were used for data manipulation and graphs.

3 RESULTS

3.1 Potential for MP vertical migration in Antarctic soils under successive FTCs condition

The relative abundance (N ratio) of MPs in the second (2.5 – 7.5 cm) and third (7.5 – 12.5 cm) layers of the soil columns presented significant differences between the different soil types and treatments (Table S3). However, the means of the FTC and NoFTC treatments for each soil type and layer were significantly different only for the third layer of the sulfated soil (S1) columns (Figure 3). The organic soil (S3) columns presented the highest overall N ratio values, with higher values in the second layer (up to 0.81 ± 0.52) compared to the third layer (up to 0.05 ± 0.07) for both FTC and NoFTC treatments. For the alkaline soil (S2), only the FTC treatment had a higher N ratio in the second layer (0.07 ± 0.08) compared to the third layer (0.00). The mean N ratio for soil S3 was the highest (0.50 ± 0.38) among the NoFTC treatments in the second layer. In the third layer, S1 and S3 soil columns that underwent FTCs had a significantly higher N ratio compared to S2 soil columns.

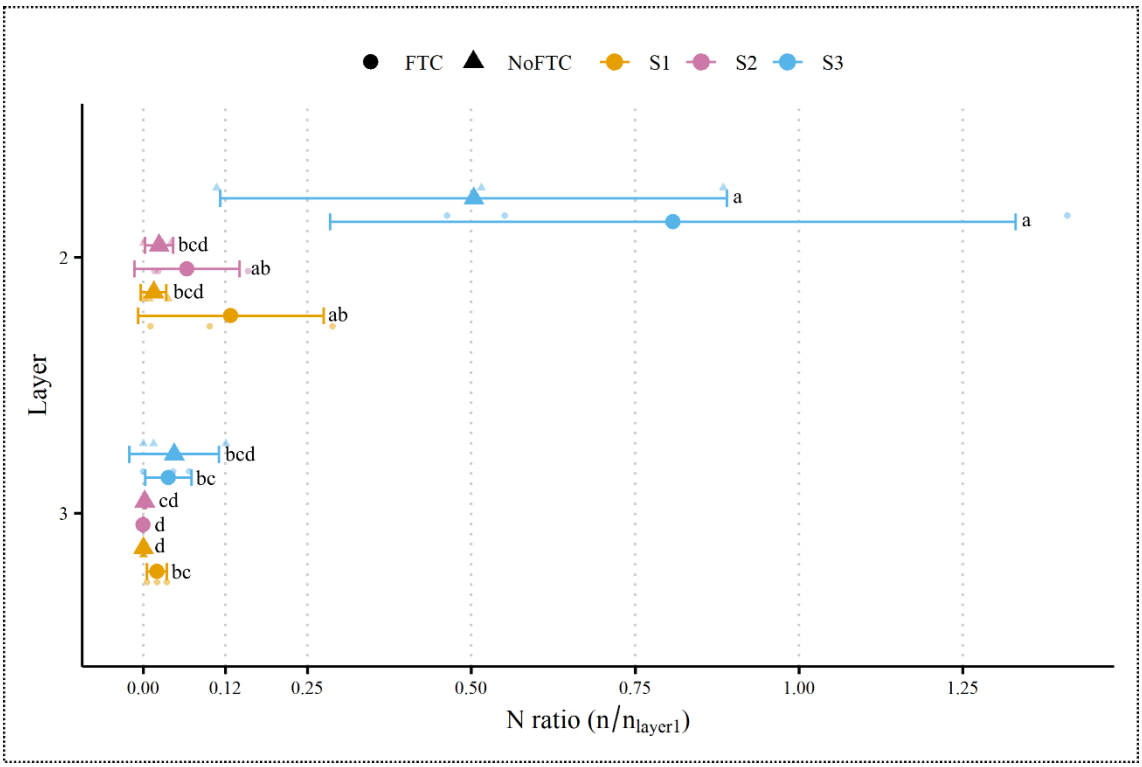

Figure 3. Mean relative abundance [N ratio (n/n_{layer1})] of the second (up) and third (down) layers of the three soil types for FTC and NoFTC treatments. Means with the same letters belong to the same group, by the Dunn's multiple comparison test (α = 0.05).

Separately, all soils presented significant differences in the N ratio for different polymer types and layers (Table S3). For soil S1, samples that underwent FTCs presented a higher N ratio for PET in the second layer (0.12 ± 0.15), and for PE in the third layer (0.05 ± 0.04), compared to the NoFTC treatment (0.00) (Figure 4.A). PE was the only polymer found in the second layer of S1 soil columns from the NoFTC treatment, and the only polymer that reached the third layer, when subjected to the FTC treatment. For S2 soil columns, the N ratio of PE (0.06 ± 0.06) and PET (0.08 ± 0.11) was higher in the second layer for the samples that underwent FTCs compared to the third layer (0.00) (Figure 4.B). Only low numbers of PET and PE particles in the NoFTC treatment reached the third layer, but the mean N ratio did not significantly differ from zero, while PLA particles were not present in the second and third layer of S2 soil columns. All three polymers had a higher mean N ratio in the second layer (up to 0.90 ± 0.72) compared to the third layer of S3 soil columns (up to 0.08 ± 0.07), in which PET and PLA polymers were not present.

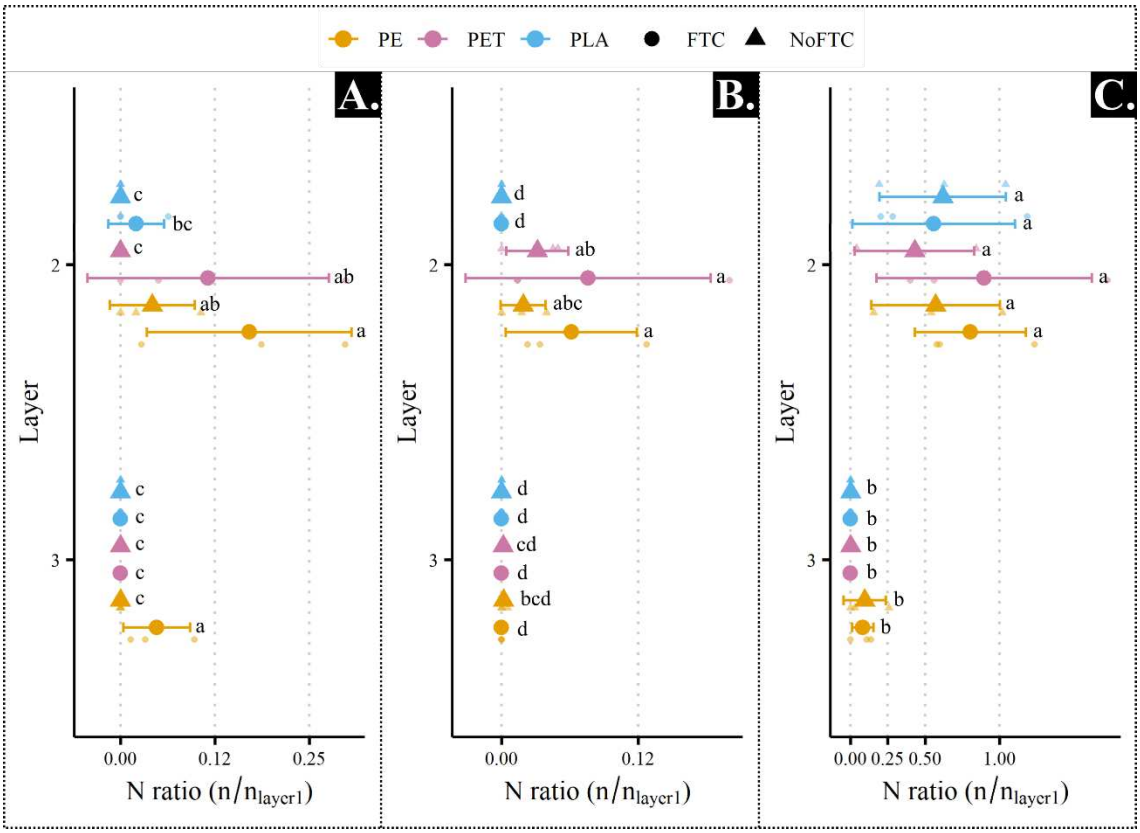

Figure 4. Mean relative abundance [N ratio (n/n_{layer1})] of the three polymers in the second and third layers for FTC and NoFTC treatments. A. Soil S1; B. Soil S2; C. Soil S3. Means with the same letters belong to the same group, by the Dunn's multiple comparison test (α = 0.05).

The diameter of MP particles identified in different layers of the three soil types showed significant differences (Table S4), although the mean values of FTC and NoFTC treatments for each soil and layer were not significantly different (Figure 5). The proportion of finer MP particles increased with increasing depth. Except for the first layer of S3 soil columns, MP particles extracted from all soils and layers were significantly finer than pristine particles. The S1 soil columns submitted to FTCs had the smallest diameter (178.6 ± 74.9 µm). The S3 soil columns had the coarsest particles of the first (up to 205.6 ± 90.9 µm, for the NoFTC treatment) and second layer (up to 187.5 ± 71.3 µm, for the FTC treatment). The third layer of S1 and S3 soil columns had MP particles with the smallest mean diameters (from 87.6 ± 51.9 µm to 105.6 ± 52.8 µm).

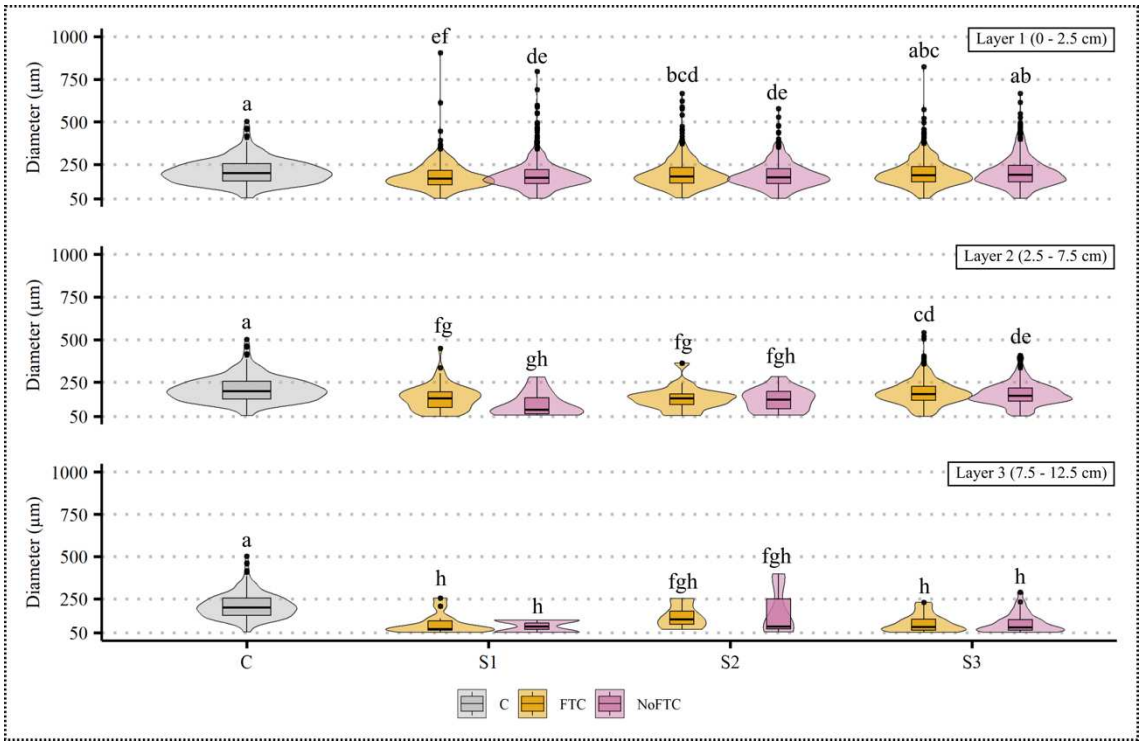

Figure 5. Mean diameter and size distribution (violin and boxplot) of MP particles on the three soil types and layers for FTC and NoFTC treatments. Mean diameter and size distribution of pristine particles (C) was also included in the comparison and are plotted on the three layers. Means with the same letters belong to the same group, by the Dunn's multiple comparison test ($\alpha = 0.05$).

All soil types analyzed separately showed significant differences in the diameter of different types of polymers in the three layers (Table S4). PE and PET particles from all layers of S1 soil columns had a smaller diameter compared to pristine particles, and there was no significant difference in the mean diameter among the three layers (Figure S4.A). For S2 soil columns, PE

and PLA particles had smaller diameter compared to pristine particles in both FTC and NoFTC treatments (Figure S4.B). PE particles from second and third layers were finer compared to the first layer on S2 soil columns, but the mean diameter of PET particles did not differ from the pristine particles regardless of layer or treatment. In the first layer of S3 soil columns, only PE (for the FTC treatment) and PLA particles had a smaller mean diameter compared to respective pristine particles (Figure S4.C), and there was a trend for PE particles of smaller mean diameter to occurring at greater layer depths. The mean diameter of PET particles from S3 soil columns also did not significantly differ from pristine particles.

3.2 Impacts of MPs and FTCs on porosity and bulk density of Antarctic soils

Regardless of the soil type and layer depth, MP presence significantly affected the soil bulk density, while the FTC treatment significantly affected soil bulk density, total porosity and macroporosity (Table S6). The interaction effect (MP presence x FTC treatment) was only significant for the soil total porosity. Analyzing the soil S1 separately, the FTC treatment, depth and MP presence significantly affected all the measured soil physical parameters, except for the soil microporosity for the latter two (Table S7). The interaction effects MP presence x FTC treatment and FTC treatment x depth were significant for all the measured soil physical parameters, but MP presence x depth was significant only for soil bulk density and total porosity.

The first layer of S1 soil columns had lower soil bulk density and a higher porosity (total and macro) compared to the two bottom layers, regardless of FTC treatment or MP presence (Figure 6). The soil total and macroporosity was higher in the first layer when subjected to the FTC treatment (up to 0.71 ± 0.03 $cm^3\ cm^{-3}$ and 0.24 ± 0.03 $cm^3\ cm^{-3}$, respectively) compared to the NoFTC samples (up to 0.60 ± 0.02 $cm^3\ cm^{-3}$ and 0.13 ± 0.01 $cm^3\ cm^{-3}$), regardless of the MP presence. In samples subjected to FTC, soil bulk density in the second and third layers was lower in soil columns containing MPs (1.26 ± 0.02 $g\ cm^{-3}$ and 1.31 ± 0.02 $g\ cm^{-3}$, respectively) compared to those without MPs (1.37 ± 0.01 $g\ cm^{-3}$ and 1.38 ± 0.02 $g\ cm^{-3}$, respectively), but not in the first layer.

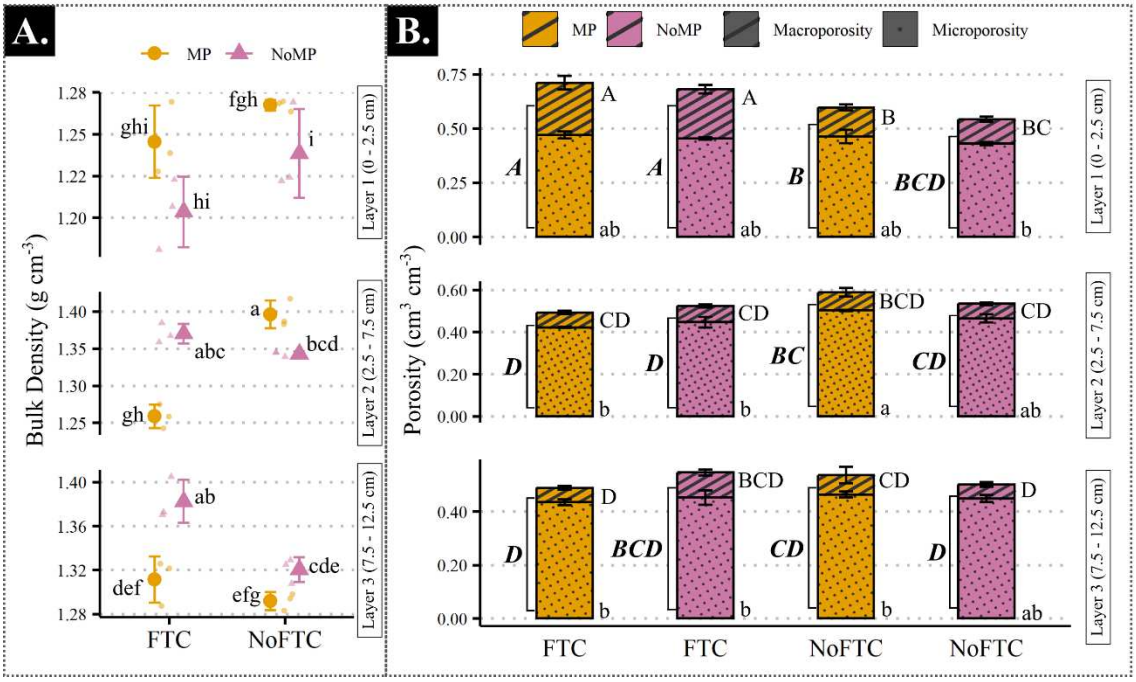

Figure 6. Results of soil physical parameters for the soil S1 after the incubation period. A. Bulk density (g cm^{-3}); B. Total, macro- and microporosity (cm^3 cm^{-3}). Capital-italic-bold letters refer to total porosity, capital letters refer to macroporosity, small letters refer to microporosity. Means with the same letters belong to the same group, by Tukey's HSD multiple comparison test ($\alpha = 0.05$).

For soil S2, all measured physical parameters were significantly affected by FTC treatment, but for MP presence and depth there was no significant effect for microporosity and bulk density, respectively (Table S8). All the interaction effects were significant for total and macroporosity, but none were significant for microporosity. In samples subjected to FTC treatment, the MP presence resulted in lower soil bulk density (1.33 ± 0.02 g cm^{-3}), total (0.53 ± 0.03 cm^3 cm^{-3}) and macroporosity (0.14 ± 0.01 cm^3 cm^{-3}) in the surface layer (Figure 7). Total and macroporosity were higher in the surface layer compared to the bottom layers of samples subjected to FTC treatment, regardless of MP presence.

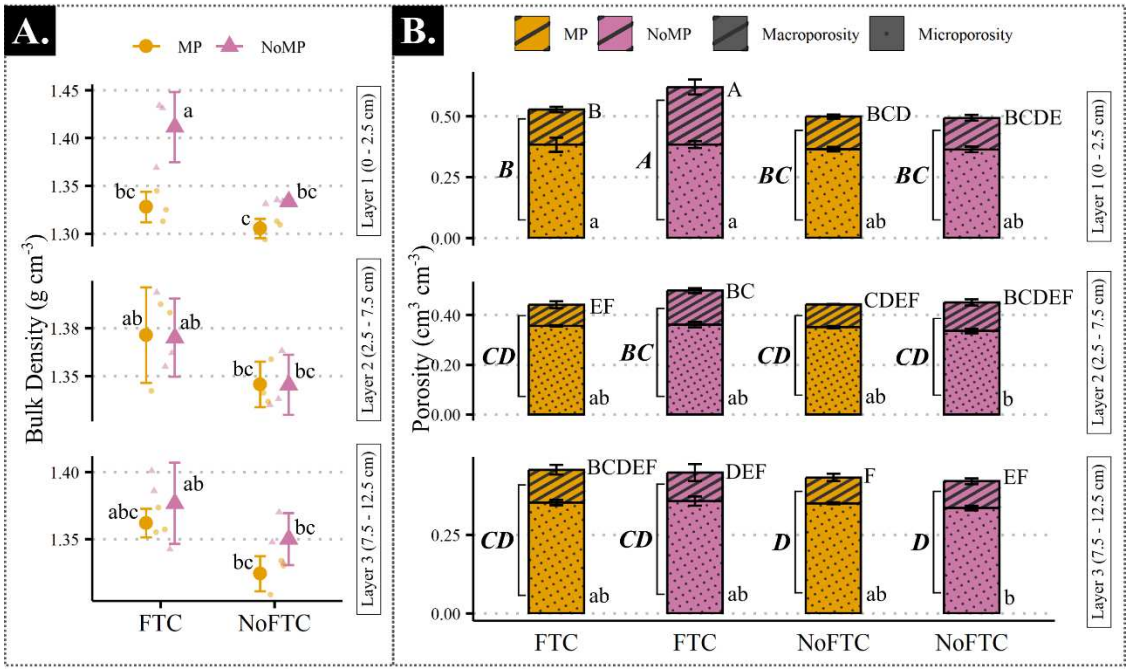

Figure 7. Results of soil physical parameters for the soil S2 after the incubation period. A. Bulk density (g cm^{-3}); B. Total, macro- and microporosity (cm^3 cm^{-3}). Capital-italic-bold letters refer to total porosity, capital letters refer to macroporosity, small letters refer to microporosity. Means with the same letters belong to the same group, by Tukey's HSD multiple comparison test ($\alpha = 0.05$).

MP presence only significantly affected the soil bulk density of S3, while FTC treatment and depth were significant for all physical parameters, except microporosity (Table S9). Due to the excessive subsidence observed in the first layer of FTC samples, the soil bulk density of the second layer (1.25 ± 0.03 g cm^{-3}) was significantly higher compared to the third layer (1.10 ± 0.03 g cm^{-3}) in the absence of MPs, but not when MPs were present (Figure 8.A). On the other hand, total and macroporosity were higher in the first layer of NoFTC treatments (up to 0.82 ± 0.02 cm^3 cm^{-3} and 0.35 ± 0.04 cm^3 cm^{-3}, respectively). In contrast, the second and third layers did not show significant differences in porosity with or without MPs or FTC (Figure 8.B).

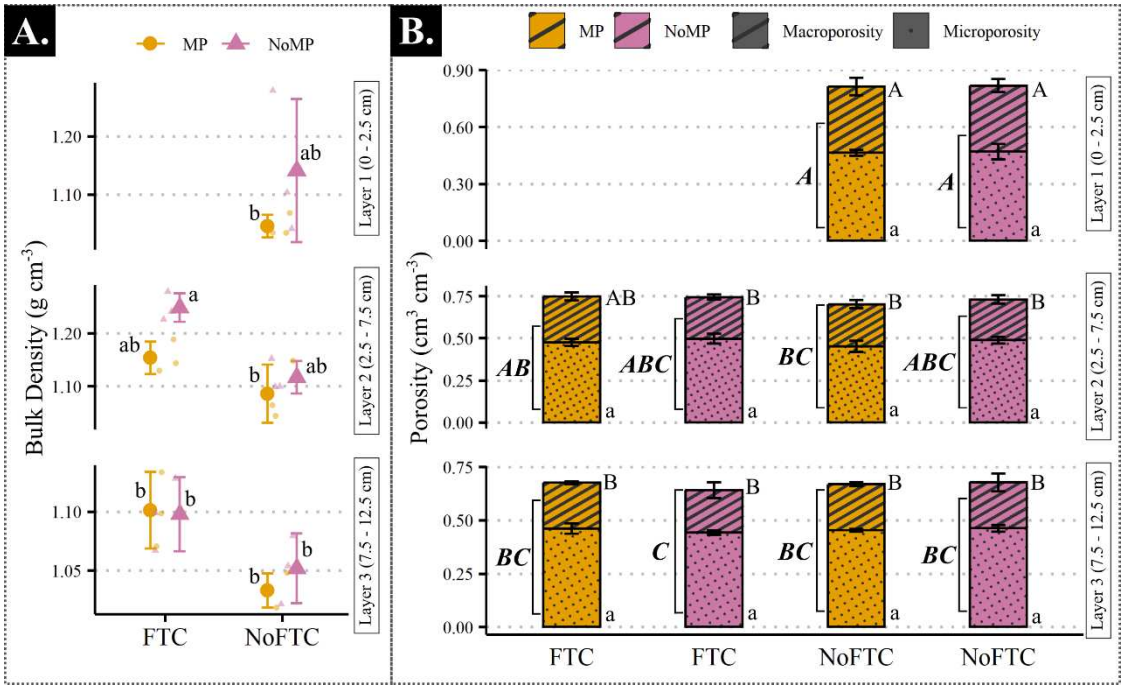

Figure 8. Results of soil physical parameters for the soil S3 after the incubation period. A. Bulk density (g cm^{-3}); B. Total, macro- and microporosity (cm^3 cm^{-3}). Capital-italic-bold letters refer to total porosity, capital letters refer to macroporosity, small letters refer to microporosity. Means with the same letters belong to the same group, by Tukey's HSD multiple comparison test ($\alpha = 0.05$).

The soil columns showed significant thaw subsidence after the 44-day incubation period for the FTC treatment and different soil types (p-value < 0.001) but were not affected by MP presence (p-value = 0.69). Soil S3 showed greater subsidence (up to 2.3 cm) when subjected to FTCs and was the only soil type in which subsidence occurred for NoFTC treatments (Table S5). The volume change promoted by subsidence was accounted to determine soil physical parameters. Although sampling for MP analysis was possible, the excessive subsidence in the first layer (0 – 2.5 cm) of the S3 soil columns made it unfeasible to separate intact layers for the analysis of soil physical parameters, therefore, their no results were not presented.

3.3 MP analysis: background levels

MPs were found at low levels in the three soil types before conducting the experiment, with a maximum mean concentration of 2.0 (± 0.7) items per gram of soil for soil S3, which does not significantly differ from the mean concentration for soil S1 or soil S2 [1.9 (± 0.6) and 1.3 (± 1.3) items per gram of soil, respectively] (Figure 3.A).

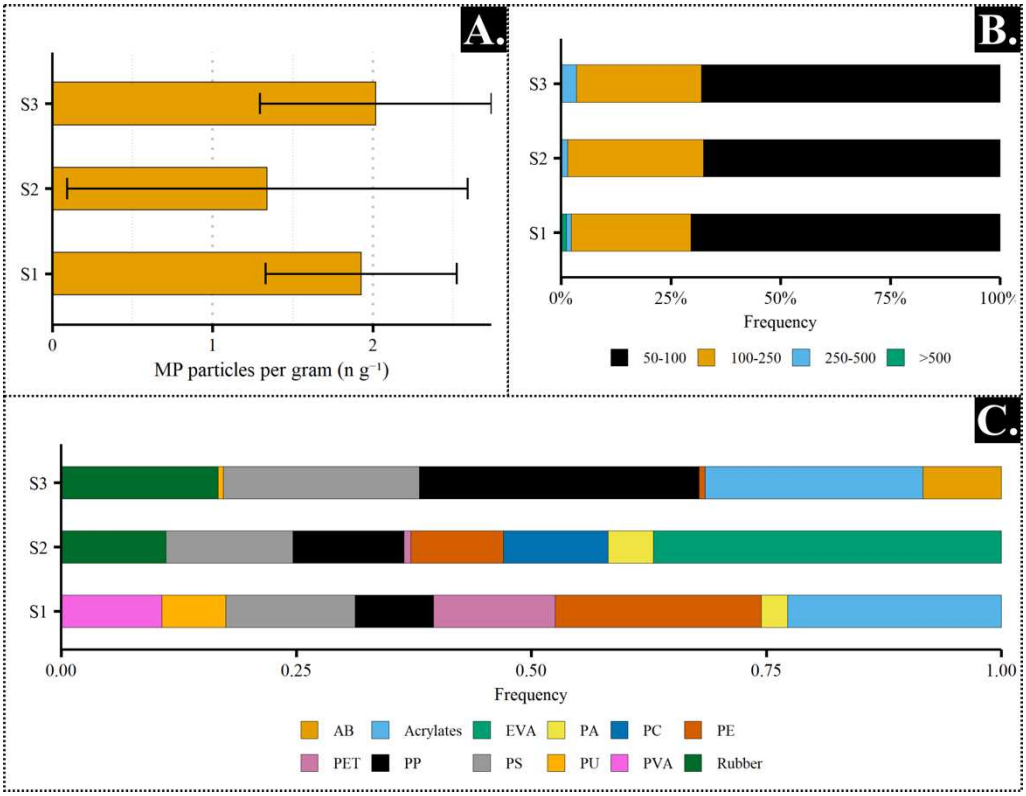

Figure 2. A. Mean background MP concentration (n g^{-1}) for the three soil samples used in the experiment; B. Size classes distribution (µm) of the MP particles identified with the LDIR for each soil type; C. Frequency of occurrence of polymers identified by the LDIR for each soil type.

The proportion of size classes was inverse to particle size. Particles of 50-100 µm were more than 67% while particles bigger than 250 µm were less than 4% for all soil samples (Figure 2.B). Twelve polymer types were identified by the LDIR [acrylate, acrylonitrile butadiene (AB), ethylene vinyl acetate (EVA), polyamide (PA), polycarbonate (PC), PE, PET, polypropylene (PP), polystyrene (PS), polyurethane (PU), polyvinyl acohol (PVA) and rubber. The most frequent polymers found in soil S1 were acrylates (23 ± 17%) and PE (22 ± 38%), while in soil S2 were EVA (37 ± 55%) and PS (14 ± 18%), and in soil S3 were PP (30 ± 52%), acrylates (23 ± 23%) and PS (21 ± 19%) (Figure 2.C). PS and PP were present in all soil samples, and represented half of the polymers found in soil S3.

4 DISCUSSION

4.1 Potential for MPs vertical migration in Antarctic soils under successive FTCs condition

MPs were found in the second and third layers of all soils after the incubation period, suggesting MP vertical migration, although only S1 and S3 soil columns submitted to FTCs presented N ratio significantly different from 0 in the third layer. A significant difference between the total relative abundance of the FTC and NoFTC treatments was only found for the third layer of the S1 soil columns. This suggests that FTCs were not responsible for the vertical migration of the MP mix in S2 and S3 soil columns. It also suggests that MP particle migration occurred in soil columns at constant temperature (4 °C), even without new water injection inducing flow. It was hypothesized the occurrence of gravity-driven flow favoring the water percolation from the lowest (first layer depth) to higher gravitational potentials (second- and third-layer depth, respectively), possibly carrying MPs. In this case, soil saturation is expected to increase in depth, which decreases and even stops gravitational flow (Shadab; Hesse, 2022), contributing to the lower relative abundance of most polymers in the third layer of all soils for NoFTC treatments. Furthermore, gravitational water flow and vertical migration of MP particles tend to be more intense in porous media with larger pores (Gao *et al.*, 2021; Shadab; Hesse, 2022), contributing, together with the greater subsidence, to a higher N ratio in S3 soil columns. On the other hand, finer porous media favor deposition and lower mobility of MP particles (Gao *et al.*, 2021; Li, Wang *et al.*, 2024; Ranjan *et al.*, 2023), corroborating the complete absence of all polymers in the second (except PE) and third layers of S1 soil columns for the NoFTC treatment.

Higher relative abundances of PE and PET were observed in the third and second layers, respectively, of S1 soil columns that underwent FTCs compared to the NoFTC treatment. During the soil freezing process, water tends to migrate towards the freezing front (upward) due to temperature and pressure gradients (Bai *et al.*, 2020; Shi *et al.*, 2024; Wang *et al.*, 2019). Free water dominates the flow in the early stages of freezing and adsorbed water (particle surface and micropores) in the later stages (Shi *et al.*, 2024). The water expansion with phase change induces frost heave, segregating soil particles and possibly creating preferential flow paths by increasing pore sizes (Bai *et al.*, 2020; Li *et al.*, 2023). Soil thawing can favor the detachment of previously deposited MP particles (Hsieh *et al.*, 2024) and induces free meltwater percolation downwards through preferential paths at a higher rate than the adsorbed

fraction (Shi *et al.*, 2022), possibly carrying MPs. This cyclic process would be significant to favor MP particles migration particularly for S1, as it is less likely to occur at constant temperature (NoFTC) due to the smaller grain size and, consequently, pore size (Gao *et al.*, 2021; Li, Wang *et al.*, 2024).

Furthermore, successive FTCs induce flocculation and attachment of clay particles into coarse grains (Van Huissteden, 2020; Van Vliet-Lanoë; Fox; Gubin, 2004). The process is also likely to occur to MPs giving their capacity for heteroaggregation by adsorption with clay minerals (Wang *et al.*, 2023), increasing their mobility (Li *et al.*, 2021). Additionally, pH is a determining factor regulating clay flocculation by affecting net particle charge of colloids (Chorom; Rengasamy; Murraya, 1994). Soils with high sodium saturation, such as S2, favor the dispersion of clay colloids at alkaline pH (Chorom; Rengasamy; Murraya, 1994). The excess of positive charges at low pH favors the neutralization of negative charges in the colloids, reducing the repulsion energy between clay particles (Chorom; Rengasamy; Murraya, 1994). Since MPs are also generally negatively charged (Godoy *et al.*, 2019; Wang *et al.*, 2023), the attachment of clays to MPs surface could also be favored. On the other hand, the low pH associated with the sulfated parent material of soil S1 is responsible for the advanced state of chemical weathering of this soil, resulting in a finer texture with a representative presence of clay minerals (Simas *et al.*, 2006, 2008). Therefore, the attachment of clay and cotransport of MPs with fine soil particles may also be responsible for enhancing the effects of FTCs on MP mobility in S1 soil columns (Hsieh *et al.*, 2024).

Even with the lowest density, PE particles were the only ones to present an N ratio different from zero in the third layer of the soil columns. These results are in line with that observed in previous studies, in which authors observed greater mobility of MP particles with a density close to that of water (PE) compared to those with higher density (PET) (Li, Wang *et al.*, 2024; Ranjan *et al.*, 2023). Gravity plays an important role in MP deposition at low flow rate (Li, Wang *et al.*, 2024) and may account for the limited migration of higher-density PET particles, while the lower number of PLA particles may have decreased the likelihood of their occurrence in lower layers. Surface hydrophobicity strongly correlates with MP mobility in porous media, as more hydrophobic polymers (PET compared to PE) has been shown to present restricted mobility (Gao *et al.*, 2021), corroborating our results. On the other hand, sorption of organic matter affects the surface properties of MPs, transitioning from a hydrophobic to a hydrophilic character, and resulting in a dominance of repulsive interactions (Ivanic *et al.*, 2023). That

promotes dispersion and increased mobility of MPs (Ivanic *et al.*, 2023), also supporting the higher overall MP abundance in lower layers of S3 soil columns.

FTCs cause aging damage and surface fractures to MP particles, increasing the specific surface area, and affecting hydrophobicity according to polymer type and particle size (Li; Xu; Yu, 2024). It was shown that the hydrophobicity of 50 μm PE particles subjected to FTCs decreased but that of 500 μm particles increased (Li; Xu; Yu, 2024), potentially increasing the mobility of smaller particles. Additionally, the retention of MPs during migration in porous media occurs mainly by physical straining, through the contact between particles (minerals and MPs) (Ranjan *et al.*, 2023). Thus, smaller MP particles have greater mobility and can reach deeper soil layers (Gao *et al.*, 2021; Ranjan *et al.*, 2023), reinforcing the trend for smaller particles occurring with increasing depth observed in this study. In turn, MP mobility also has been shown to be shape-dependent, and fibers and films already showed greater mobility than fragments related to a higher superficial area (Zhang *et al.*, 2022). Therefore, although we have shown different behaviors between polymers, the role of MP shape in MP vertical migration in FTC soils still needs to be investigated.

Despite the confirmed vertical migration of MPs after ten FTCs, the mean abundance did not exceed 13% in the second layer and 2% in the third layer relative to the first layer of FTCs S1 soil columns. However, authors suggest that thinning of the snowpack due to climate change will increase the frequency of FTCs (Henry, 2008; Klöffel *et al.*, 2024), which can further enhance MPs migration in soils such as S1. The increasing frequency of FTCs may also favor a negative priming effect and accumulation of organic matter in Maritime Antarctic soils, due to a selectivity of the microbiota in metabolizing freeze-preserved carbon (Matus *et al.*, 2023), potentially increasing MP mobility (Ivanic *et al.*, 2023). MP weathering driven by FTCs affects soil microbiota by altering the structure of microbial communities and inhibiting natural metabolic pathways (Li; Xu; Yu, 2024). MPs can also act as carriers of pollutants present in the Antarctic environment, such as heavy metals and organic pollutants (Cao *et al.*, 2021; Chang *et al.*, 2022; Gao *et al.*, 2018; Miranda; Lima Neto; Schaefer, 2024), and smaller particles have greater adsorption capacity due to surface properties (Fu *et al.*, 2021; Zhang *et al.*, 2020). Therefore, the selective migration of finer MP particles by FTCs can favor the transport of other pollutants and impact microbiota of deeper soil layers. In this context, an expected increase in the frequency of FTCs may bring long-term ecological impacts depending on multiple factors, which should be considered in further assessments.

4.2 Impacts of MPs and FTCs on physical parameters of Antarctic soils

The soil columns suffered significant subsidence when subjected to FTCs, a common process occurring in periglacial environments with seasonal soil freezing (French, 2007). Solid-state water in frozen soil occupies an excess volume relative to the pore space under unfrozen conditions, which causes structural rearrangement upon melting and drainage, resulting in thaw subsidence and compaction (Gruber, 2020; Leuther; Schlüter, 2021). This process is more pronounced in soils with vegetation cover, greater porosity and, consequently, higher water content when saturated (Chen *et al.*, 2020; Wang *et al.*, 2015), corroborating the higher subsidence observed in S3 soil columns. However, the structural rearrangement promoted by FTCs combines thaw subsidence and frost heave processes (Leuther; Schlüter, 2021), which can also increase porosity (Bai *et al.*, 2020; Li *et al.*, 2023), as observed in the first S1 and S2 soil columns. As a result, there is a decrease in porosity in compacted lower soil layers and an increase in porosity in upper layer, evident in soil columns that underwent FTC in this study, attributed to the formation of a platy structure (Leuther; Schlüter, 2021). Notably, the observed changes in total porosity were mainly governed by macroporosity (Joudieh *et al.*, 2024).

MPs are responsible for altering soil bulk density and porosity differently according to soil type and MP concentration (de Miranda *et al.*, 2024; Ingraffia *et al.*, 2022; Yu *et al.*, 2023). Generally, MP presence causes a decrease in soil bulk density due to the lower relative density in relation to soil mineral particles (Qiu *et al.*, 2022; Wang *et al.*, 2022). However, authors suggest that effects on soil structure may overlap the difference in relative density to change soil bulk density leading to contrasting results (Jing *et al.*, 2023; Machado *et al.*, 2019), as noticed for S1 soil columns increasing bulk density in the first MP contained layer of NoFTC treatments. S1 is the most weathered soil, with the highest aluminum saturation and greater flocculation capacity (Simas *et al.*, 2008). The presence of MPs hampers soil aggregation (Lozano *et al.*, 2021), and their low reactivity in the size range used in this study (Li; Liu, 2022; Xu *et al.*, 2019) could have deteriorated the formation of flocculated aggregates in the reconstructed soil columns, leading to particle accommodation and increased bulk density. Conversely, soil bulk density of the first layer of S2 columns submitted to FTCs was lower with MP presence, as expected (Qiu *et al.*, 2022; Wang *et al.*, 2022). In this case, the inherent soil lower structuring capacity due to coarser grains and high sodium saturation (Tang; She; Wang, 2021) may have hindered the effect of MPs on structure of the first layer of repacked S2 soil columns.

MP presence in S1 soil columns that underwent FTCs decreased bulk density of the second and third layers but not of the first layer, even though MPs were exclusively added to the first layer. Since the effects of MPs on soil physical properties are concentration dependent (Lozano *et al.*, 2021; Yu *et al.*, 2023), it is unlikely that the decrease in soil bulk density is directly due to MP presence in lower layers. Besides that, it has been shown that the presence of MP can affect soil water dynamics by reducing vertical flow into adjacent uncontaminated layers (Kim *et al.*, 2021). As previously stated, water migration is a determining factor for the occurrence of processes related to successive FTCs such as frost heave and thaw consolidation (Bai *et al.*, 2020; Joudieh *et al.*, 2024; Leuther; Schlüter, 2021). It is reasonable that a decrease in water migration between the upper layer and lower layers promoted by MPs has alleviated the compacting effect of successive FTCs in S1 soil columns.

MPs also can affect soil porosity and pore connectivity by occupying previous free pore space (de Miranda *et al.*, 2024; Wang, Zhichao *et al.*, 2024). Soils used in this study did not show significant differences between soil porosity of NoFTC soil columns with or without MPs, but MPs decreased total and macroporosity of the first layer of S2 soil columns when combined with FTCs. Soil S2 present the highest sodium saturation and lowest organic matter content among all soils tested. Hydrophobic electrostatic attraction between MP particles is favored in soils with low organic matter content (Ivanic *et al.*, 2023), while high salinity favors the homoaggregation of MPs (Wang *et al.*, 2023). The displacement of MP particles caused by the cyclic action of FTCs (Hsieh *et al.*, 2024) in a medium that favors homoaggregation must have contributed to the clogging of pores in S2 soil columns.

However, the effects of MPs on soil physical properties are also dependent on shape (Lozano *et al.*, 2021). For instance, MP fibers are known to cause more significant impacts, hampering aggregation but increasing soil macroporosity and aeration at high concentrations (de Miranda *et al.*, 2024; Zhang; Zhang; Li, 2019). The major changes in physical properties caused by MP fibers are often related to subsequent impacts on soil microbiota, such as increased microbial activity and greenhouse gas fluxes (de Miranda *et al.*, 2024; Machado *et al.*, 2018; Rillig *et al.*, 2021). Fibers were not tested in this experiment, so the effects of MP shape on FTC soils and their potential implications needs to be explored in future studies.

4.3 Background MP levels in three Antarctic soils

The three soil types presented low levels of MP background contamination that did not exceed 2.0 items g^{-1}; these results comparable to the few studies that assessed MP levels in Antarctic

soils to date (De-la-Torre *et al.*, 2024; Gurumoorthi; Luis, 2023). Soils samples from Thala Hills (East Antarctica) had a maximum concentration of 1.8 items g^{-1} (Kukharchyk; Kakareka; Rabychyn, 2024), while soils sampled close to research stations in Fildes Peninsula (King George Island) had a maximum concentration of 37 items per 50 mL of soil (~0.5 items g^{-1}, considering the specific weight of the soil as 1.5 g cm^{-3}) (Perfetti-Bolaño *et al.*, 2022). The higher proportion of fine MP particles in soils has been repeatedly reported in other studies (Cheng *et al.*, 2022; Kang *et al.*, 2024; Li, Longrui *et al.*, 2024), including in Antarctic soils (He *et al.*, 2024). Short-range atmospheric transport (local sources) followed by melt runoff has been suggested as a likely source of MPs in inland environments of Antarctica (Aves *et al.*, 2022; González-Pleiter *et al.*, 2020), and finer MPs are more susceptible to be transported and subsequently deposited (Fox *et al.*, 2024; Illuminati *et al.*, 2024). Therefore, the size distribution observed here could be expected, as sampling was not conducted in the immediate vicinity of research stations with visual signs of contamination (Perfetti-Bolaño *et al.*, 2022). On the other hand, these results suggest that the size distribution of MPs in the samples are more subject to potential vertical migration, following the observed selective migration of finer particles.

Especially for fine MP particles (< 500 μm), automatic MP analysis by spectroscopic techniques decreases the risk of missing false negatives as there is no prior selection of particles by visual inspection (Wang, Zaibin *et al.*, 2024). Using an automatic approach (LDIR) for MP identification, a maximum mean of 283.6 items g^{-1} was found at Cape Royds (Ross Island, Antarctica) (He *et al.*, 2024), two orders of magnitude larger than the numbers reported for this study. The Antarctic Peninsula region, where the soils of this study were sampled, has lower MP concentration levels for different environmental compartments (water, sediment, biota) than the Ross Island region (Gurumoorthi; Luis, 2023), but discrepancies between studies may also be linked to the identification procedure. Following a conservative approach to avoid false positives, the minimum match quality of this study was set to 90%, which is higher than the 65% used by He et al. (2024), and may contributed to the lower MP levels reported here. Even so, the background MP concentration in Antarctic soils is low compared to that reported by studies using the same technique (LDIR) in other regions of the world, including agricultural soils (Lwanga *et al.*, 2023), high mountain soils (Kang *et al.*, 2024) or coastal soils (Yu *et al.*, 2024).

All polymers identified in this study have already been reported as MP contaminants in different environmental compartments in Antarctica (Aves *et al.*, 2022; Gurumoorthi; Luis, 2023; Kelly

et al., 2020; Kim *et al.*, 2023), where PE, PP and polyester are the most common (De-la-Torre *et al.*, 2024). PP and PE are historically the most produced and used polymers in everyday life for packaging and disposables (Büks; Kaupenjohann, 2020; Geyer; Jambeck; Law, 2017), and are widespread as MP contaminants (Büks; Kaupenjohann, 2020). PS products, commonly used for food storage and fishing activities, are banned in the Antarctic Treaty area by the Madrid Protocol (CEP, 1991a), but PS MPs were at high proportions in all soils analyzed. Light density MPs (PS and PP/PE) are prone to marine transport (Erni-Cassola *et al.*, 2019), and their presence in all three soil types at high proportion may suggest the influence of marine input in the sampled areas (Lozoya *et al.*, 2022). Acrylate MPs, usually associated with textiles and waterproof clothing (González-Pleiter *et al.*, 2020; Janani *et al.*, 2023), represented a high proportion of polymers found in soil samples S1 and S3 (up to 23%), but were not detected in S2. This could be attributed to the proximity of local sources of contamination, as S1 and S3 were sampled on the Keller Peninsula, Admiralty Bay, which hosts three research stations (Brazil, Poland and Peru).

5 CONCLUSIONS

Our results showed that MPs migrated vertically along the soil columns, and the extent of MP transport were differently according to the soil type, polymer type and presence or absence of FTCs:

- Due to high porosity, organic matter and excessive subsidence, soil columns S3 (organic matter rich soil) presented greater susceptibility to MP migration, indicated by the highest numbers of relative MP abundance in lower layers.
- The FTCs particularly facilitate the migration of MP particles in finer and weathered soils, such as soil S1 (acid sulfate soil), compared to coarser soils, such as soil S2 (alkaline soil) and S3.
- PE particles showed higher mobility among the polymers tested (PET and PLA), and the preferential migration of finer MP particles was observed.
- FTCs promoted soil structural changes and thaw subsidence, generally increasing porosity in the surface layer and compacting lower layers.
- The interaction between MPs and FTCs was highlighted for soil S1, where MPs apparently alleviated the compacting effect of FTCs, and for soil S2, where MPs decreased macroporosity in the surface layer.

While MP properties (size and polymer) were shown to be relevant for potential vertical migration driven by FTCs, soil properties such as grain size, porosity, acidity, mineralogy and organic matter content seem to address the differences between soils. Our findings highlight the potential for ongoing pedogenic processes in Antarctic periglacial environments to favor MP vertical migration and affect soil physical properties of deeper layers. There is a rising concern with an expected increase in the FTCs frequency due to climate change, which could increase the magnitude of the effects observed in short-term scale. Therefore, further research is needed to investigate the specific mechanisms involved in MP migration driven by FTC in soils; assess/model MP migration rate in FTC soils under climate change scenarios in long-term scale; and investigate long-term ecological implications of MPs in Antarctic soils subjected to cryoturbation, as cumulative impacts on soil microbiota and greenhouse gas fluxes under climate change scenarios.

6 ACKNOWLEDGEMENTS

The present work was carried with the support of the following Brazilian research agencies: National Council for Research and Development (Conselho Nacional Desenvolvimento Científico e Tecnológico – CNPq) and Coordination for the Improvement of Higher-Level Personnel (Coordenação de Aperfeiçoamento de Pessoal de Nível Superior – CAPES). This study was conducted within activities of project TERRANTAR/PERMACLIMA, financed by CNPq and the Brazilian Ministry of Science, Technology and Innovation – MCTI, under the scope of Brazilian Antarctic Program (PROANTAR). The authors thank the support of the Brazilian Ministries of Science, Technology and Innovation (MCTI), Environment (MMA) and Inter-Ministry Commission for Sea Resources (CIRM). The authors thank the support of the Soil Physics and Land Management Group of the Wageningen University.

7 REFERENCES

ALEKSEEV, Ivan; ABAKUMOV, Evgeny. The content and distribution of trace elements and polycyclic aromatic hydrocarbons in soils of Maritime Antarctica. **Environmental Monitoring and Assessment**, [*s. l.*], v. 192, n. 11, 2020.

ALMEIDA, Ivan C.C. *et al.* Long term active layer monitoring at a warm-based glacier front from maritime Antarctica. **Catena**, [*s. l.*], v. 149, p. 572–581, 2017.

AVES, Alex R. *et al.* First evidence of microplastics in Antarctic snow. **Cryosphere**, [*s. l.*], v. 16, n. 6, p. 2127–2145, 2022.

BAI, Ruiqiang *et al.* Investigation on frost heave of saturated–unsaturated soils. **Acta Geotechnica**, [*s. l.*], v. 15, n. 11, p. 3295–3306, 2020.

BATISTA, Raí Ferreira *et al.* Freeze–thaw cycles affecting rheological properties of Antarctic soils. **Geoderma**, [*s. l.*], v. 428, n. February, 2022.

BOCKHEIM, J. G. Antarctic Soil Properties and Soilscapes. *In*: ANTARCTIC TERRESTRIAL MICROBIOLOGY. Berlin, Heidelberg: Springer Berlin Heidelberg, 2014. v. 9783642452, p. 293–315.

BOCKHEIM, J. G.; TARNOCAI, C. Recognition of cryoturbation for classifying permafrost-affected soils. **Geoderma**, [*s. l.*], v. 81, n. 3–4, p. 281–293, 1998.

BROOKS, Shaun T. *et al.* Our footprint on Antarctica competes with nature for rare ice-free land. **Nature Sustainability**, [*s. l.*], v. 2, n. 3, p. 185–190, 2019.

BÜKS, Frederick; KAUPENJOHANN, Martin. Global concentrations of microplastics in soils - A review. **Soil**, [*s. l.*], v. 6, n. 2, p. 649–662, 2020.

CAMPANALE, Claudia *et al.* Microplastics pollution in the terrestrial environments: Poorly known diffuse sources and implications for plants. **Science of the Total Environment**, [*s. l.*], v. 805, p. 150431, 2022.

CAO, Yanxiao *et al.* A critical review on the interactions of microplastics with heavy metals: Mechanism and their combined effect on organisms and humans. **Science of the Total Environment**, [*s. l.*], v. 788, p. 147620, 2021.

CAREY, Peter. Is it time for a paradigm shift in how Antarctic tourism is controlled?. **Polar Perspectives**, [*s. l.*], n. 1, 2020.

CEP, (Committee of Environmental Protection). **Annex III to the Protocol on Environmental Protection to the Antartic Treaty - Waste Disposal and Waste Management**. Antarctic Treaty: [*s. n.*], 1991a.

CEP, (Committee of Environmental Protection). **Protocol on Environmental Protection to the Antartic Treaty**. Antarctic Treaty: [*s. n.*], 1991b.

CHANG, Jianning *et al.* A critical review on interaction of microplastics with organic contaminants in soil and their ecological risks on soil organisms. **Chemosphere**, [*s. l.*], v. 306, n. April, p. 135573, 2022.

CHAVES, D. A. *et al.* Active layer and permafrost thermal regime in a patterned ground soil in Maritime Antarctica, and relationship with climate variability models. **Science of the Total Environment**, [*s. l.*], v. 584–585, p. 572–585, 2017.

CHEN, Jingyi *et al.* Active layer freeze-thaw and water storage dynamics in permafrost environments inferred from InSAR. **Remote Sensing of Environment**, [*s. l.*], v. 248, 2020.

CHENG, Yi Ling *et al.* Characterization of microplastics in sediment using stereomicroscopy and laser direct infrared (LDIR) spectroscopy. **Gondwana Research**, [*s. l.*], v. 108, p. 22–30, 2022.

CHOROM, M; RENGASAMY, P; MURRAYA, R S. **Clay Dispersion as Influenced by pH and Net Particle Charge of Sodic SoilsAust. J. Soil Res**. [*S. l.: s. n.*], 1994.

CINCINELLI, Alessandra *et al.* Microplastic in the surface waters of the Ross Sea (Antarctica): Occurrence, distribution and characterization by FTIR. **Chemosphere**, [*s. l.*], v. 175, p. 391–400, 2017.

CORREIA, Tamíres P. *et al.* Ground temperature trend and active layer dynamics in the Fildes Peninsula, King George Island - Marine Antarctica. **Anais da Academia Brasileira de Ciencias**, [*s. l.*], v. 96, p. e20230743, 2024.

DAHER, Mayara *et al.* Semi-arid soils from a topolithosequence at James Ross Island, Weddell Sea region, Antarctica: Chemistry, mineralogy, genesis and classification. **Geomorphology**, [*s. l.*], v. 327, p. 351–364, 2019.

DE MIRANDA, Caik Oliveira *et al.* Short-term impacts of polyethylene and polyacrylonitrile microplastics on soil physicochemical properties and microbial activity of a marine terrace environment in maritime Antarctica. **Environmental Pollution**, [*s. l.*], v. 347, n. December 2023, 2024.

DE-LA-TORRE, Gabriel Enrique *et al.* Assessing the current state of plastic pollution research in Antarctica: Knowledge gaps and recommendations. **Chemosphere**, [*s. l.*], v. 355, p. 141870, 2024.

DO VALE LOPES, Davi *et al.* Pedogeomorphology and weathering at Snow Island, Maritime Antarctica. **CATENA**, [*s. l.*], v. 217, n. July, p. 106515, 2022.

EMBRAPA. **Manual de Métodos de Análise de Solo**. 3ªed. Brasília, DF: [*s. n.*], 2017.

ERNI-CASSOLA, Gabriel *et al.* Distribution of plastic polymer types in the marine environment; A meta-analysis. **Journal of Hazardous Materials**, [*s. l.*], v. 369, n. February, p. 691–698, 2019.

EVANGELIOU, N. *et al.* Atmospheric transport is a major pathway of microplastics to remote regions. **Nature Communications**, [*s. l.*], v. 11, n. 1, 2020.

FABRI, Reginaldo *et al.* Trace elements in soil , lichens , and mosses from Fildes Peninsula , Antarctica : spatial distribution and possible origins. **Environmental Earth Sciences**, [*s. l.*], 2018.

FOX, Sydney *et al.* **Physical characteristics of microplastic particles and potential for global atmospheric transport: A meta-analysis**. [*S. l.*]: Elsevier Ltd, 2024.

FRANCELINO, Marcio Rocha *et al.* Geomorphology and soils distribution under paraglacial conditions in an ice-free area of Admiralty Bay, King George Island, Antarctica. **Catena**, [*s. l.*], v. 85, n. 3, p. 194–204, 2011.

FRENCH, Hugh M. **The periglacial environment, 4th ed**. [*S. l.: s. n.*], 2007.

FU, Lina *et al.* Adsorption behavior of organic pollutants on microplastics. **Ecotoxicology and Environmental Safety**, [*s. l.*], v. 217, n. March, p. 112207, 2021.

FULLER, Stephen; GAUTAM, Anil. A Procedure for Measuring Microplastics using Pressurized Fluid Extraction. **Environmental Science and Technology**, [*s. l.*], v. 50, n. 11, p. 5774–5780, 2016.

GAO, Xiaozhong *et al.* Occurrences, sources, and transport of hydrophobic organic contaminants in the waters of Fildes Peninsula, Antarctica. **Environmental Pollution**, [*s. l.*], v. 241, p. 950–958, 2018.

GAO, Jing *et al.* Vertical migration of microplastics in porous media: Multiple controlling factors under wet-dry cycling. **Journal of Hazardous Materials**, [*s. l.*], v. 419, n. May, p. 126413, 2021.

GEYER, Roland; JAMBECK, Jenna R.; LAW, Kara Lavender. Production, use, and fate of all plastics ever made. **Science Advances**, [*s. l.*], v. 3, n. 7, p. 19–24, 2017.

GODOY, V. *et al.* The potential of microplastics as carriers of metals. **Environmental Pollution**, [*s. l.*], v. 255, 2019.

GONZÁLEZ-PLEITER, Miguel *et al.* First detection of microplastics in the freshwater of an Antarctic Specially Protected Area. **Marine Pollution Bulletin**, [*s. l.*], v. 161, n. October, p. 1–6, 2020.

GRUBER, Stephan. Ground subsidence and heave over permafrost: Hourly time series reveal interannual, seasonal and shorter-term movement caused by freezing, thawing and water movement. **Cryosphere**, [*s. l.*], v. 14, n. 4, p. 1437–1447, 2020.

GUERRA, Marcelo Braga Bueno *et al.* Post-fire study of the Brazilian Scientific Antarctic Station: Toxic element contamination and potential mobility on the surrounding environment. **Microchemical Journal**, [*s. l.*], v. 110, p. 21–27, 2013.

GUO, Zi Qi *et al.* Soil texture is an important factor determining how microplastics affect soil hydraulic characteristics. **Environment International**, [*s. l.*], v. 165, n. May, p. 107293, 2022.

GURUMOORTHI, K.; LUIS, Alvarinho J. Recent trends on microplastics abundance and risk assessment in coastal Antarctica: Regional meta-analysis. **Environmental Pollution**, [*s. l.*], v. 324, n. January, p. 121385, 2023.

HALE, Robert C. *et al.* A Global Perspective on Microplastics. **Journal of Geophysical Research: Oceans**, [*s. l.*], v. 125, n. 1, p. 1–40, 2020.

HALLET, Bernard. Stone circles: Form and soil kinematics. **Philosophical Transactions of the Royal Society A: Mathematical, Physical and Engineering Sciences**, [*s. l.*], v. 371, n. 2004, 2013.

HE, Jianuo *et al.* Record of microplastic deposition revealed by ornithogenic soil and sediment profiles from Ross Island, Antarctica. **Environmental Research**, [*s. l.*], v. 262, 2024.

HENRY, Hugh A.L. Climate change and soil freezing dynamics: Historical trends and projected changes. **Climatic Change**, [*s. l.*], v. 87, n. 3–4, p. 421–434, 2008.

HORTON, Alice A. *et al.* Microplastics in freshwater and terrestrial environments: Evaluating the current understanding to identify the knowledge gaps and future research priorities. **Science of the Total Environment**, [*s. l.*], v. 586, p. 127–141, 2017.

HRBÁČEK, Filip *et al.* Active layer thickness variability on James Ross Island, eastern Antarctic Peninsula. **International Conference on Permafrost, Potsdam, Germany**, [*s. l.*], n. June, p. 1–2, 2016.

HSIEH, Lichun *et al.* Impact of freeze-thaw cycles on the remobilization behaviors of microplastics in natural soils. **Environmental Pollution**, [*s. l.*], v. 363, 2024.

ILLUMINATI, Silvia *et al.* Microplastics in bulk atmospheric deposition along the coastal region of Victoria Land, Antarctica. **Science of the Total Environment**, [*s. l.*], v. 949, 2024.

INGRAFFIA, Rosolino *et al.* Polyester microplastic fibers affect soil physical properties and erosion as a function of soil type. **Soil**, [*s. l.*], v. 8, n. 1, p. 421–435, 2022.

ISOBE, Atsuhiko *et al.* Microplastics in the Southern Ocean. **Marine Pollution Bulletin**, [*s. l.*], v. 114, n. 1, p. 623–626, 2017.

IVANIC, Federico M. *et al.* Soil organic matter facilitates the transport of microplastic by reducing surface hydrophobicity. **Colloids and Surfaces A: Physicochemical and Engineering Aspects**, [*s. l.*], v. 676, 2023.

JANANI, R. *et al.* **From acrylates to silicones: A review of common optical fibre coatings used for normal to harsh environments**. [*S. l.*]: Elsevier B.V., 2023.

JING, Xiaoyuan *et al.* How Do Microplastics Affect Physical Properties of Silt Loam Soil under Wetting–Drying Cycles?. **Agronomy**, [*s. l.*], v. 13, n. 3, 2023.

JONES-WILLIAMS, Kirstie *et al.* Close encounters - microplastic availability to pelagic amphipods in sub-antarctic and antarctic surface waters. **Environment International**, [*s. l.*], v. 140, n. April, 2020.

JOUDIEH, Zeina *et al.* Artificial Ground Freezing—On the Soil Deformations during Freeze–Thaw Cycles. **Geotechnics**, [*s. l.*], v. 4, n. 3, p. 718–741, 2024.

KANG, Qiangqiang *et al.* Characteristics of soil microplastics and ecological risks in the Qilian Mountains region, Northeast Tibetan Plateau. **Environmental Pollution**, [*s. l.*], v. 363, 2024.

KELLY, A. *et al.* Microplastic contamination in east Antarctic sea ice. **Marine Pollution Bulletin**, [*s. l.*], v. 154, n. March, p. 111130, 2020.

KIM, Shin Woong *et al.* Indirect Effects of Microplastic-Contaminated Soils on Adjacent Soil Layers: Vertical Changes in Soil Physical Structure and Water Flow. **Frontiers in Environmental Science**, [*s. l.*], v. 9, n. May, p. 1–9, 2021.

KIM, Youmin *et al.* Microplastics in gastrointestinal tracts of gentoo penguin (Pygoscelis papua) chicks on King George Island, Antarctica. **Scientific Reports**, [*s. l.*], v. 13, n. 1, p. 1–11, 2023.

KLÖFFEL, Tobias *et al.* Freeze-thaw effects on pore space and hydraulic properties of compacted soil and potential consequences with climate change. **Soil and Tillage Research**, [*s. l.*], v. 239, 2024.

KOUTNIK, Vera S. *et al.* Distribution of microplastics in soil and freshwater environments: Global analysis and framework for transport modeling. **Environmental Pollution**, [*s. l.*], v. 274, p. 116552, 2021.

KOUTNIK, Vera S. *et al.* Transport of microplastics in stormwater treatment systems under freeze-thaw cycles: Critical role of plastic density. **Water Research**, [*s. l.*], v. 222, n. July, p. 118950, 2022.

KUKHARCHYK, T I; KAKAREKA, S V; RABYCHYN, K O. Microplastics in Soils of the Thala Hills , East Antarctica. [*s. l.*], v. 57, n. 3, p. 502–512, 2024.

LACERDA, Ana L.d.F. *et al.* Plastics in sea surface waters around the Antarctic Peninsula. **Scientific Reports**, [*s. l.*], v. 9, n. 1, p. 1–12, 2019.

LEUTHER, Frederic; SCHLÜTER, Steffen. Impact of freeze-thaw cycles on soil structure and soil hydraulic properties. **Soil**, [*s. l.*], v. 7, n. 1, p. 179–191, 2021.

LI, Longrui *et al.* Characteristics of microplastics and their abundance impacts on microbial structure and function in agricultural soils of remote areas in west China. **Environmental Pollution**, [*s. l.*], v. 360, 2024.

LI, Wang *et al.* Effect of particle density on microplastics transport in artificial and natural porous media. **Science of the Total Environment**, [*s. l.*], v. 935, 2024.

LI, Meng *et al.* Transport and deposition of microplastic particles in saturated porous media: Co-effects of clay particles and natural organic matter. **Environmental Pollution**, [*s. l.*], v. 287, n. June, p. 117585, 2021.

LI, Meng *et al.* Transport of plastic particles in natural porous media under freeze–thaw treatment: Effects of porous media property. **Journal of Hazardous Materials**, [*s. l.*], v. 442, n. August 2022, 2023.

LI, Haixiao; LIU, Le. Short-term effects of polyethene and polypropylene microplastics on soil phosphorus and nitrogen availability. **Chemosphere**, [*s. l.*], v. 291, n. P2, p. 132984, 2022.

LI, Yanjun; XU, Guanghui; YU, Yong. Freeze-thaw aged polyethylene and polypropylene microplastics alter enzyme activity and microbial community composition in soil. **Journal of Hazardous Materials**, [*s. l.*], v. 470, 2024.

LOPES, Davi do Vale *et al.* Concretionary horizons, unusual pedogenetic processes and features of sulfate affected soils from Antarctica. **Geoderma**, [*s. l.*], v. 347, n. March, p. 13–24, 2019.

LOPES, Davi do Vale *et al.* Hydrogeochemistry and chemical weathering in a periglacial environment of Maritime Antarctica. **Catena**, [*s. l.*], v. 197, n. June 2020, p. 104959, 2021.

LOZANO, Yudi M. *et al.* Microplastic Shape, Polymer Type, and Concentration Affect Soil Properties and Plant Biomass. **Frontiers in Plant Science**, [*s. l.*], v. 12, n. February, p. 1–14, 2021.

LOZOYA, Juan Pablo *et al.* Stranded Pellets in Fildes Peninsula (King George Island, Antarctica): New Evidence of Southern Ocean Connectivity. **SSRN Electronic Journal**, [*s. l.*], p. 119519, 2022.

LWANGA, Esperanza Huerta *et al.* Microplastic appraisal of soil, water, ditch sediment and airborne dust: The case of agricultural systems. **Environmental Pollution**, [*s. l.*], v. 316, n. P1, p. 120513, 2023.

MACHADO, Anderson Abel de Souza *et al.* Impacts of Microplastics on the Soil Biophysical Environment. **Environmental Science and Technology**, [*s. l.*], v. 52, n. 17, p. 9656–9665, 2018.

MACHADO, Anderson Abel de Souza *et al.* Microplastics Can Change Soil Properties and Affect Plant Performance. **Environmental Science and Technology**, [*s. l.*], v. 53, n. 10, p. 6044–6052, 2019.

MATUS, Francisco *et al.* Freezing–thawing cycles affect organic matter decomposition in periglacial maritime Antarctic soils. **Biogeochemistry**, [*s. l.*], v. 163, n. 3, p. 311–325, 2023.

MICHEL, Roberto F.M. *et al.* Soils and landforms from Fildes Peninsula and Ardley Island, Maritime Antarctica. **Geomorphology**, [*s. l.*], v. 225, n. C, p. 76–86, 2014.

MIRANDA, Caik O.DE; LIMA NETO, Elias DE; SCHAEFER, Carlos Ernesto G.R. Anthropogenic effect on the pedochemical variability of potentially toxic elements at the vicinity of an Antarctic research station. **Anais da Academia Brasileira de Ciencias**, [*s. l.*], v. 96, p. e20230724, 2024.

MUNARI, Cristina *et al.* Microplastics in the sediments of Terra Nova Bay (Ross Sea, Antarctica). **Marine Pollution Bulletin**, [*s. l.*], v. 122, n. 1–2, p. 161–165, 2017.

NASER, Ahmed Z.; DEIAB, I.; DARRAS, Basil M. Poly(lactic acid) (PLA) and polyhydroxyalkanoates (PHAs), green alternatives to petroleum-based plastics: a review. **RSC Advances**, [*s. l.*], v. 11, n. 28, p. 17151–17196, 2021.

PERFETTI-BOLAÑO, Alessandra *et al.* Occurrence and Distribution of Microplastics in Soils and Intertidal Sediments at Fildes Bay, Maritime Antarctica. **Frontiers in Marine Science**, [*s. l.*], v. 8, n. February, 2022.

QI, Yueling *et al.* Effects of plastic mulch film residues on wheat rhizosphere and soil properties. **Journal of Hazardous Materials**, [*s. l.*], v. 387, n. November 2019, p. 121711, 2020.

QIU, Yifei *et al.* Soil microplastic characteristics and the effects on soil properties and biota: A systematic review and meta-analysis. **Environmental Pollution**, [*s. l.*], v. 313, n. June, p. 120183, 2022.

RANJAN, Ved Prakash *et al.* Preliminary investigation on effects of size, polymer type, and surface behaviour on the vertical mobility of microplastics in a porous media. **Science of the Total Environment**, [*s. l.*], v. 864, 2023.

REED, Sarah *et al.* Microplastics in marine sediments near Rothera Research Station, Antarctica. **Marine Pollution Bulletin**, [*s. l.*], v. 133, 2018.

RILLIG, Matthias C. *et al.* Microplastic fibers affect dynamics and intensity of CO2 and N2O fluxes from soil differently. **Microplastics and Nanoplastics**, [*s. l.*], v. 1, n. 1, p. 1–11, 2021.

SCHAEFER, Carlos Ernesto G.R. *et al.* Micromorphology and microchemistry of selected Cryosols from maritime Antarctica. **Geoderma**, [*s. l.*], v. 144, n. 1–2, p. 104–115, 2008.

SCHAEFER, Carlos Ernesto G.R. *et al.* Thermal monitoring of a Cryosol in a high marine terrace (Half Moon Island, Maritime Antarctica). **Anais da Academia Brasileira de Ciencias**, [*s. l.*], v. 95, p. 1–19, 2023.

SCHEURER, Michael; BIGALKE, Moritz. Microplastics in Swiss Floodplain Soils. **Environmental Science and Technology**, [*s. l.*], v. 52, n. 6, p. 3591–3598, 2018.

SFRISO, Andrea Augusto *et al.* Microplastic accumulation in benthic invertebrates in Terra Nova Bay (Ross Sea, Antarctica). **Environment International**, [*s. l.*], v. 137, n. February, p. 105587, 2020.

SHADAB, Mohammad Afzal; HESSE, Marc Andre. Analysis of Gravity-Driven Infiltration With the Development of a Saturated Region. **Water Resources Research**, [*s. l.*], v. 58, n. 11, 2022.

SHI, Yajun *et al.* Change of pore water near the freezing front during soil freezing: Migration and mechanisms. **Pedosphere**, [*s. l.*], v. 34, n. 4, p. 770–782, 2024.

SHI, Yajun *et al.* Investigating unfrozen water and its components during freeze–thaw action in loess using a novel NMR technique. **European Journal of Soil Science**, [*s. l.*], v. 73, n. 4, 2022.

SIMAS, Felipe N.B. *et al.* Clay-sized minerals in permafrost-affected soils (Cryosols) from King George Island, Antarctica. **Clays and Clay Minerals**, [*s. l.*], v. 54, n. 6, p. 721–736, 2006.

SIMAS, Felipe N.B. *et al.* Genesis, properties and classification of Cryosols from Admiralty Bay, maritime Antarctica. **Geoderma**, [*s. l.*], v. 144, n. 1–2, p. 116–122, 2008.

SIMAS, Felipe N.B. *et al.* Ornithogenic cryosols from Maritime Antarctica: Phosphatization as a soil forming process. **Geoderma**, [*s. l.*], v. 138, n. 3–4, p. 191–203, 2007.

SIQUEIRA, Rafael G. *et al.* Acid sulfate soils from Antarctica: Genesis and properties along a climatic gradient. **Anais da Academia Brasileira de Ciencias**, [*s. l.*], v. 94, p. 1–20, 2022.

SOUZA, Katia Karoline Delpupo *et al.* Soil formation in Seymour Island, Weddell Sea, Antarctica. **Geomorphology**, [*s. l.*], v. 225, n. C, p. 87–99, 2014.

SUARIA, Giuseppe *et al.* Floating macro- and microplastics around the Southern Ocean: Results from the Antarctic Circumnavigation Expedition. **Environment International**, [*s. l.*], v. 136, n. January, p. 105494, 2020.

TAIB, Nur Azzah Afifah Binti *et al.* **A review on poly lactic acid (PLA) as a biodegradable polymer**. [*S. l.*]: Springer Berlin Heidelberg, 2023-. ISSN 14362449.v. 80

TANG, Shengqiang; SHE, Dongli; WANG, Hongde. Effect of salinity on soil structure and soil hydraulic characteristics. **Canadian Journal of Soil Science**, [*s. l.*], v. 101, n. 1, p. 62–73, 2021.

THOMAZINI, A. *et al.* Geospatial variability of soil CO2-C exchange in the main terrestrial ecosystems of Keller Peninsula, Maritime Antarctica. **Science of the Total Environment**, [*s. l.*], v. 562, p. 802–811, 2016.

THOMAZINI, André *et al.* The current response of soil thermal regime and carbon exchange of a paraglacial coastal land system in maritime Antarctica. **Land Degradation and Development**, [*s. l.*], v. 31, n. 5, p. 655–666, 2020.

VAN FRANEKER, Jan A.; BELL, Phil J. Plastic ingestion by petrels breeding in Antarctica. **Marine Pollution Bulletin**, [*s. l.*], v. 19, n. 12, p. 672–674, 1988.

VAN HUISSTEDEN, J. **Thawing Permafrost**. Cham: Springer International Publishing, 2020.

VAN VLIET-LANOË, Brigitte. Frost Action. **Interpretation of Micromorphological Features of Soils and Regoliths**, [*s. l.*], p. 81–108, 2010.

VAN VLIET-LANOË, Brigitte; FOX, Catherine A.; GUBIN, Stanislaw V. Micromorphology of Cryosols. *In*: CRYOSOLS. Berlin, Heidelberg: Springer Berlin Heidelberg, 2004. p. 365–390.

WANG, Tian liang *et al.* An experimental study on the mechanical properties of silty soils under repeated freeze-thaw cycles. **Cold Regions Science and Technology**, [*s. l.*], v. 112, p. 51–65, 2015.

WANG, Zaibin *et al.* Comparative Evaluation of Analytical Techniques for Quantifying and Characterizing Polyethylene Microplastics in Farmland Soil Samples. **Agriculture (Switzerland)**, [*s. l.*], v. 14, n. 4, 2024.

WANG, Fayuan *et al.* Effects of microplastics on soil properties: Current knowledge and future perspectives. **Journal of Hazardous Materials**, [*s. l.*], v. 424, n. PC, p. 127531, 2022.

WANG, Zhichao *et al.* Effects of microplastics on the pore structure and connectivity with different soil textures: Based on CT scanning. **Environmental Technology and Innovation**, [*s. l.*], v. 36, 2024.

WANG, Wenfeng *et al.* Environmental fate and impacts of microplastics in soil ecosystems: Progress and perspective. **Science of the Total Environment**, [*s. l.*], v. 708, p. 134841, 2020.

WANG, Yi *et al.* Influence of typical clay minerals on aggregation and settling of pristine and aged polyethylene microplastics. **Environmental Pollution**, [*s. l.*], v. 316, n. P2, p. 120649, 2023.

WANG, Tian *et al.* The effects of freeze–thaw process on soil water migration in dam and slope farmland on the Loess Plateau, China. **Science of the Total Environment**, [*s. l.*], v. 666, p. 721–730, 2019.

XU, Guanghui *et al.* Freeze-thaw cycles promote vertical migration of metal oxide nanoparticles in soils. **Science of the Total Environment**, [*s. l.*], v. 795, p. 148894, 2021.

XU, Pengcheng *et al.* Sorption of polybrominated diphenyl ethers by microplastics. **Marine Pollution Bulletin**, [*s. l.*], v. 145, n. February, p. 260–269, 2019.

YANG, Xiaohan *et al.* Aggregation of microplastics and clay particles in the nearshore environment: Characteristics, influencing factors, and implications. **Water Research**, [*s. l.*], v. 224, n. August, p. 119077, 2022.

YU, Yingxue *et al.* Minimal Impacts of Microplastics on Soil Physical Properties under Environmentally Relevant Concentrations. **Environmental Science and Technology**, [*s. l.*], v. 57, n. 13, p. 5296–5304, 2023.

YU, Xue *et al.* Quantifying microplastics in sediments of Jinzhou Bay, China: Characterization and ecological risk with a focus on small sizes. **Science of the Total Environment**, [*s. l.*], v. 949, 2024.

ZHANG, Shuwu *et al.* Microplastics influence the adsorption and desorption characteristics of Cd in an agricultural soil. **Journal of Hazardous Materials**, [*s. l.*], v. 388, n. October 2019, p. 121775, 2020.

ZHANG, Xiaoting *et al.* Size/shape-dependent migration of microplastics in agricultural soil under simulative and natural rainfall. **Science of the Total Environment**, [*s. l.*], v. 815, p. 152507, 2022.

ZHANG, G. S.; LIU, Y. F. The distribution of microplastics in soil aggregate fractions in southwestern China. **Science of the Total Environment**, [*s. l.*], v. 642, p. 12–20, 2018.

ZHANG, G. S.; ZHANG, F. X.; LI, X. T. Effects of polyester microfibers on soil physical properties: Perception from a field and a pot experiment. **Science of the Total Environment**, [*s. l.*], v. 670, p. 1–7, 2019.

8 SUPPLEMENTARY MATERIAL FOR CHAPTER III

8.1 Section 1 – Supporting Figures and Tables

8.1.1 Supporting Figures

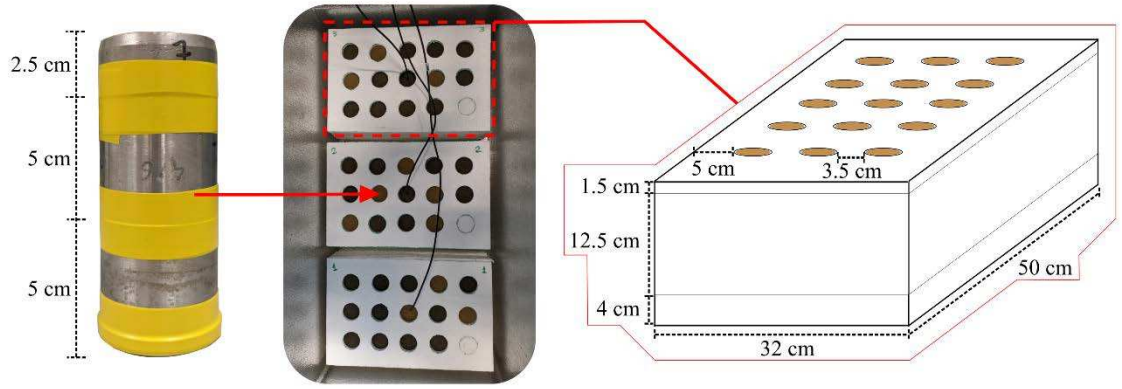

Figure S1. Illustrative scheme of the experimental setup including the soil columns and details of the insulation platforms used in the freeze-thaw cycles incubation.

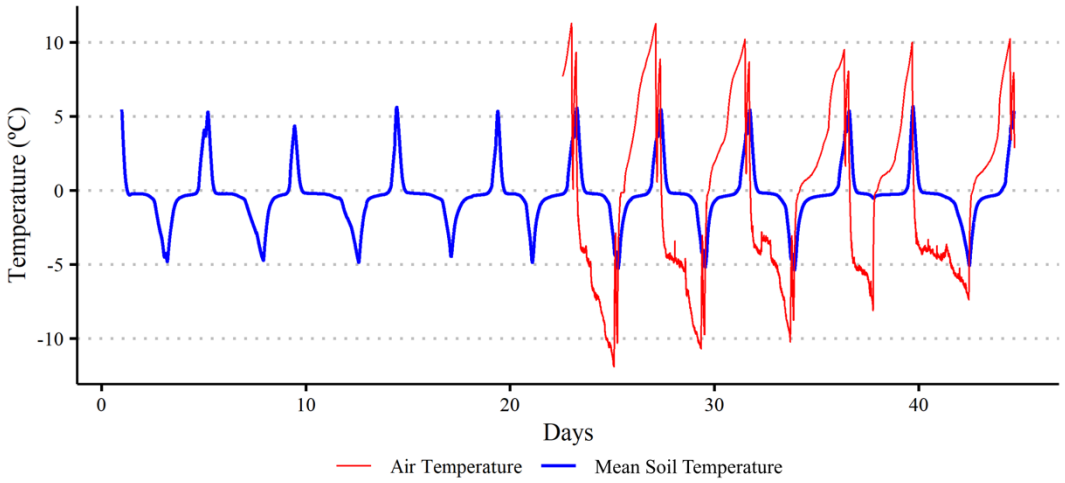

Figure S2. Mean soil temperature in the two monitoring columns (S3 and S5) and air temperature during the freeze-thaw cycles incubation period. Due to technical issues regarding the temperature sensor, the air temperature in the freezer was only recorded during half of the incubation period.

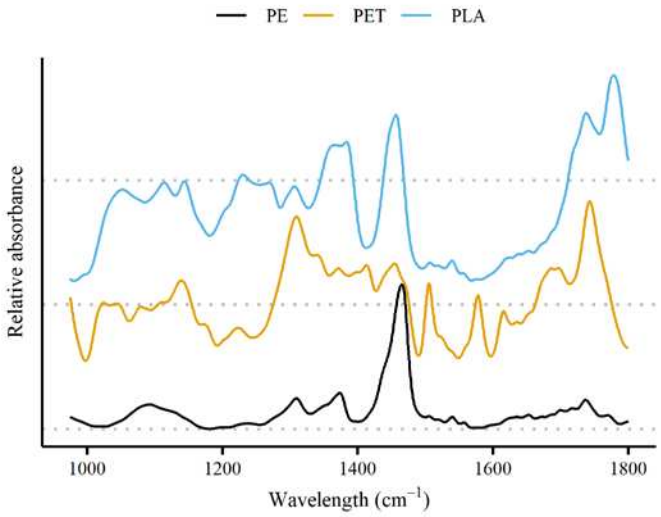

Figure S3. LDIR spectra of particles of the three different polymers used in the experiment [polyethylene (PE), polyethylene terephthalate (PET), polylactic acid (PLA)].

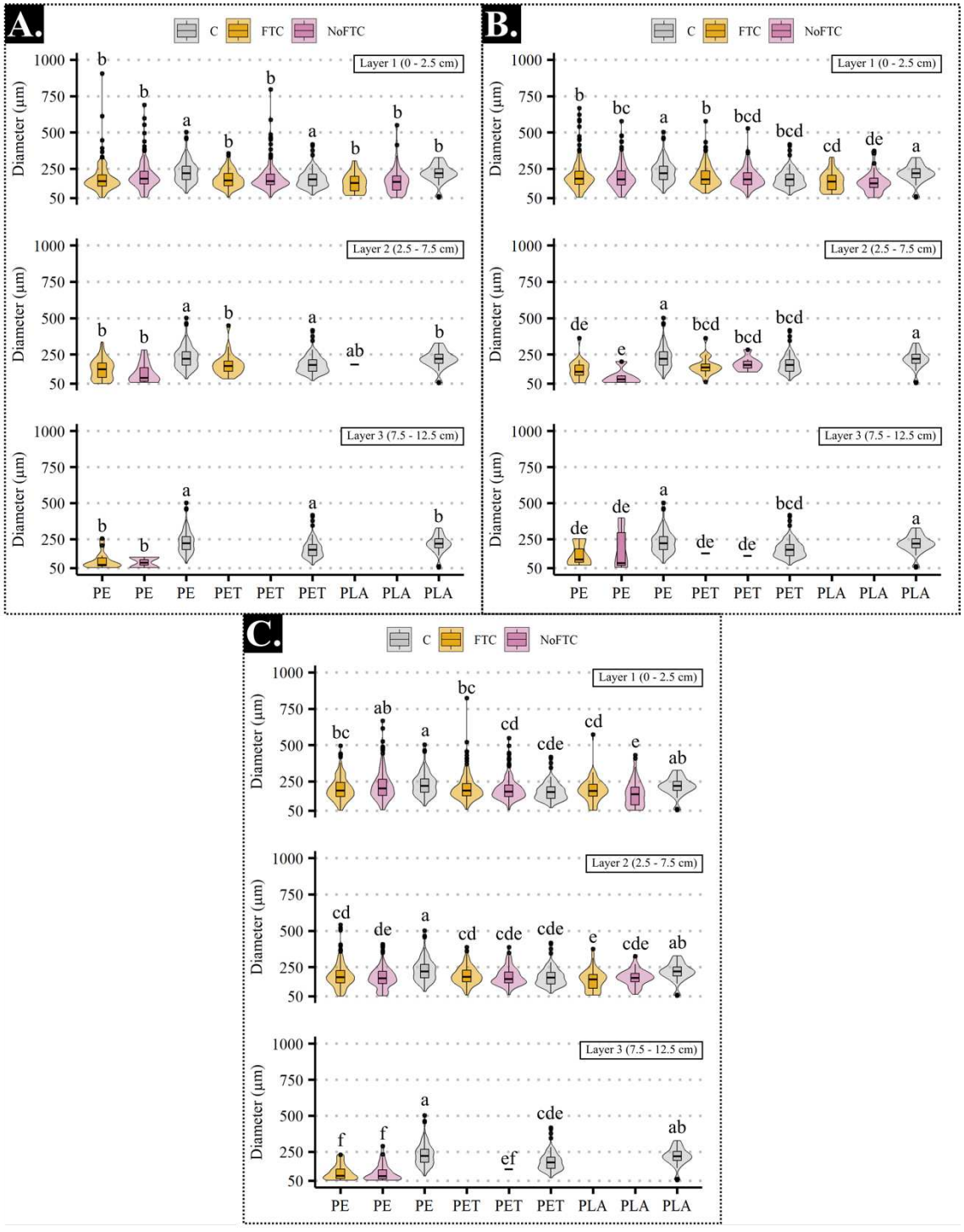

Figure S4. Mean diameter and size distribution (violin and boxplot) of the three polymer types in different soil columns layers depth for FTC and NoFTC treatments. A. Soil S1; B. Soil S2; C. Soil S3. Mean diameter and size distribution of pristine particles (C) was also included in the comparison and are plotted on the three layers. Means with the same letters belong to the same group, by the Dunn's multiple comparison test ($\alpha = 0.05$).

8.1.2 Supporting Tables

Table S1. Characterization of chemical parameters and texture of the three soils used for the experiment.

Sample	pH	K^+	Na^+	AP	Ca^{2+}	Mg^{2+}	Al^{3+}	H+Al	RemP
	-	mg/kg			cmolc/kg				mg/L
S1	3.1	32.0	23.7	22.8	1.1	0.5	33.8	43.6	1.3
S2	8.0	416.5	1335.1	40.5	35.8	6.6	0.5	0.7	18.6
S3	6.6	205.0	371.3	226.1	9.2	6.4	0.9	1.9	30.9

Sample	SB	CEC-H	CEC	BSat	AlSat	NaSat	TOC	TN	C:N
	cmolc/kg			%			g/kg		-
S1	1.8	35.6	45.4	3.9	95.1	0.2	1.3	0.11	11.6
S2	49.3	49.8	49.6	99.3	1.2	11.8	2.1	0.24	8.9
S3	17.7	18.5	19.6	90.3	4.7	8.3	18.9	0.90	21.0

Sample	S	Cu	Mn	Fe	Zn	Cr	Ni	Cd	Pb
	mg/kg								
S1	391.0	3.7	5.9	1817.8	0.1	0.5	1.1	0.4	1.9
S2	30.6	1.4	104.5	172.6	3.5	1.2	2.2	0.4	0.5
S3	17.9	18.6	262.8	287.8	5.1	0.4	1.1	0.4	3.5

Sample	CSand	FSand	Silt	Clay
	kg/kg			
S1	0.13	0.26	0.36	0.26
S2	0.32	0.32	0.23	0.13
S3	0.36	0.11	0.29	0.24

Table S2. Volumetric and mass-based polymer concentrations added to soil columns of the three soil types. Bulk density refers to the repacked soil columns.

Soil type	Bulk density	PE concentration		PET concentration		PLA concentration		MP mix concentration	
	$g\ cm^{-3}$	$v\ v^{-1}$	$w\ w^{-1}$	$v\ v^{-1}$	$w\ w^{-1}$	$v\ v^{-1}$	$w\ w^{-1}$	$v\ v^{-1}$	$w\ w^{-1}$
S1	1.26	0.005%	0.004%	0.004%	0.004%	0.001%	0.001%	0.010%	0.009%
S2	1.38	0.005%	0.003%	0.004%	0.004%	0.001%	0.001%	0.010%	0.008%
S3	0.86	0.005%	0.005%	0.004%	0.006%	0.001%	0.002%	0.010%	0.013%

Table S3. Results of the Kruskal-Wallis tests (chi-squared value and p-value are shown) on the N ratio values for layers 2 and 3 of the soil columns.

Soil	Chi-Squared Value	df	p-value
All soils	24.356	11	**0.011**
S1	24.737	11	**0.010**
S2	28.604	11	**0.003**
S3	24.720	11	**0.010**

Bold values highlight significant p-values (< 0.05).

Table S4. Results of the Kruskal-Wallis tests (chi-squared value and p-value are shown) on the diameter of particles extracted from the soil samples (layers 2 and 3).

Soil	Chi-Squared Value	df	p-value
All soils	196.878	18	**< 0.001**
S1	97.919	14	**< 0.001**
S2	66.125	16	**< 0.001**
S3	149.786	17	**< 0.001**

Bold values highlight significant p-values (< 0.05).

Table S5. Subsidence experienced by the soil columns after the 44-day incubation period.

Soil type	MP treatment	FTC treatment	Mean subsidence (SD) cm
S1	NoMP	FTC	0.8b (0.2)
S1	NoMP	NoFTC	0.0c (0.0)
S1	MP	FTC	0.9b (0.3)
S1	MP	NoFTC	0.0c (0.0)
S2	NoMP	FTC	0.5bc (0.4)
S2	NoMP	NoFTC	0.0c (0.0)
S2	MP	FTC	0.4bc (0.2)
S2	MP	NoFTC	0.0c (0.0)
S3	NoMP	FTC	2.3a (0.2)
S3	NoMP	NoFTC	0.6bc (0.1)
S3	MP	FTC	2.2a (0.4)
S3	MP	NoFTC	0.5bc (0.2)

Means with the same letters belong to the same group, by Tukey's HSD multiple comparison test ($\alpha = 0.05$).

Table S6. Results of the analysis of variance (ANOVA) of mixed linear models (F values and p-values are shown) on soil physical parameters considering the treatments as fixed effects and the soil type and layer (depth) as random effects.

Factors		**Soil physical parameters**			
		Bulk density	Total porosity	Macroporosity	Microporosity
MP presence (MP)	F value	8.675	0.227	0.607	0.075
	p-value	**0.004**	0.635	0.438	0.785
FTC treatment (FTC)	F value	6.244	8.344	10.873	0.160
	p-value	**0.014**	**0.005**	**0.001**	0.690
MP x FTC	F value	1.642	4.054	2.489	1.899
	p-value	0.203	**0.047**	0.118	0.172

Bold values highlight significant p-values (< 0.05).

Table S7. Results of the analysis of variance (ANOVA) of linear models (F values and p-values are shown) on soil physical parameters for the soil S1. Bold values highlight significant p-values (< 0.05).

Factors		**Soil Physical Parameters**			
		Bulk density	Total porosity	Macroporosity	Microporosity
MP presence (MP)	F value	6.677	4.426	0.569	3.063
	p-value	**0.016**	**0.046**	**< 0.001**	0.093
FTC treatment (FTC)	F value	6.306	12.018	46.764	7.216
	p-value	**0.019**	**0.002**	**< 0.001**	**0.013**
Depth	F value	129.723	112.753	157.674	0.894
	p-value	**< 0.001**	**< 0.001**	**< 0.001**	0.422
MP x FTC	F value	32.736	25.718	7.707	10.667
	p-value	**< 0.001**	**< 0.001**	**< 0.001**	**0.003**
MP x Depth	F value	20.765	5.189	1.980	1.783
	p-value	**< 0.001**	**0.013**	0.160	0.190
FTC x Depth	F value	25.728	62.567	40.51	11.029
	p-value	**< 0.001**	**< 0.001**	**< 0.001**	**< 0.001**
MP x FTC x Depth	F value	21.564	2.554	1.800	1.458
	p-value	**< 0.001**	0.099	0.187	0.253

Bold values highlight significant p-values (< 0.05).

Table S8. Results of the analysis of variance (ANOVA) of linear models (F values and p-values are shown) on soil physical parameters for the soil S2. Bold values highlight significant p-values (< 0.05).

Factors		**Soil Physical Parameters**			
		Bulk density	Total porosity	Macroporosity	Microporosity
MP presence (MP)	F value	14.452	10.188	23.937	0.818
	p-value	**< 0.001**	**0.004**	**< 0.001**	0.375
FTC treatment (FTC)	F value	29.473	37.788	25.844	14.06
	p-value	**< 0.001**	**< 0.001**	**< 0.001**	**< 0.001**
Depth	F value	1.44	71.949	65.46	14.84
	p-value	0.257	**< 0.001**	**< 0.001**	**< 0.001**
MP x FTC	F value	1.215	13.309	11.527	3.051
	p-value	0.281	**0.001**	**0.002**	0.093
MP x Depth	F value	6.248	5.766	8.672	0.184
	p-value	**0.006**	**0.009**	**0.001**	0.833
FTC x Depth	F value	1.259	6.672	9.222	0.217
	p-value	0.302	**0.005**	**0.001**	0.806
MP x FTC x Depth	F value	2.479	3.945	9.729	0.566
	p-value	0.105	**0.033**	**< 0.001**	0.575

Bold values highlight significant p-values (< 0.05).

Table S9. Results of the analysis of variance (ANOVA) of linear models (F values and p-values are shown) on soil physical parameters for soil S3.

Factors		**Soil Physical Parameters**			
		Bulk density	Total porosity	Macroporosity	Microporosity
MP presence (MP)	F value	6.951	0.003	0.951	1.633
	p-value	**0.016**	0.959	0.341	0.216
FTC treatment (FTC)	F value	15.11	5.717	11.058	0.161
	p-value	**< 0.001**	**0.027**	**0.003**	0.692
Depth	F value	8.391	31.773	39.187	2.986
	p-value	**0.002**	**< 0.001**	**< 0.001**	0.073
MP x FTC	F value	0.005	1.474	0.610	0.829
	p-value	0.942	0.239	0.444	0.374
MP x Depth	F value	1.965	0.418	0.087	1.836
	p-value	0.166	0.664	0.917	0.185
FTC x Depth	F value	1.147	2.314	0.884	1.409
	p-value	0.297	0.144	0.358	0.249
MP x FTC x Depth	F value	1.142	0.029	0.003	0.109
	p-value	0.298	0.866	0.957	0.745

Bold values highlight significant p-values (< 0.05).

8.2 Section 2 – MP analysis control samples

8.2.1 Negative control (blank samples) correction

The correction of the final MP content levels was based on results from blank samples that underwent the same analytical processing as the environmental/experimental samples. The correction was performed by multiplying the total raw particle counting extracted from each sample replicate by a mean correction factor (CF) for each polymer type, and subsequently subtracting the resulted value from the particle counting of the respective polymer type. The mean CF was pulled from the ratio of each polymer type counting over the total number of particles analyzed in the LDIR slide (regardless of the spectral match quality) of each blank sample. The procedure can be summarized with the following equations:

Equation S1: $CF_{polymer;B\_i} = (N_{polymer;\ B\_i})\ (N_{total\ per\ slide;\ B\_i})^{-1}$;

Equation S2: $N_{polymer;corrected} = N_{polymer;raw} - (CF_{polymer} \times N_{total\ per\ slide})$;

where $CF_{polymer;B\_i}$ is the correction factor estimated for a specific polymer type from a blank sample replicate (B_i), $N_{polymer;\ B\_i}$ is the particle counting of a specific polymer type from a blank sample replicate (B_i), $N_{total\ per\ slide;\ B\_i}$ is the total number of particles analyzed in the slide from a blank sample replicate, and i is the blank sample replicate; $N_{polymer;corrected}$ is the corrected particle counting for a specific polymer type from an experimental sample replicate, $N_{polymer;raw}$ is the raw particle counting for a specific polymer type from an experimental sample replicate, $CF_{polymer}$ is the mean correction factor for a specific polymer, and $N_{total\ per\ slide}$ is the total number of particles analyzed in the slide from an experimental sample replicate.

The mean levels achieved for each experimental sample (Table S15) were thus obtained after correcting the raw data. The procedure was performed separately for environmental samples and experimental samples considering the time frame for sample processing and the spectral library used in each case.

Environmental samples

Table S10. Abundance of MP particles identified in the blank samples and their respective correction factors.

Polymer Identification	**B_1**		**B_2**		**B_3**		**Mean (SD)**	
	n	**CF**	**n**	**CF**	**n**	**CF**	**n**	**CF**
Polypropylene (PP)	14	0.070	13	0.099	9	0.024	12.0 (2.6)	0.064
Ethylene Vinyl Acetate (EVA)	3	0.015	3	0.023	3	0.080	3.0 (0.0)	0.015
Polyethylene (PE)	2	0.010	4	0.031	1	0.003	2.3 (1.5)	0.014
Polyurethane (PU)	0	0	0	0	6	0.016	2.0 (3.5)	0.005
Polyethylene Terephthalate (PET)	0	0	1	0.008	0	0	0.3 (0.6)	0.003
Total	19		20		19		19.3 (0.6)	
Total particles per slide	199		131		381			

Table S11. Raw counting of MP particles in replicates of environmental samples.

Polymer Identification	**S1_1**	**S1_2**	**S1_3**	**S2_1**	**S2_2**	**S2_3**	**S3_1**	**S3_2**	**S3_3**
	n			**n**			**n**		
Acrylate	1	0	7	0	0	0	1	1	4
Acrylonitrile Butadiene	0	0	0	0	0	0	0	0	2
Ethylene Vinyl Acetate (EVA)	1	0	1	1	17	10	1	3	4
Polyamide (PA)	0	0	1	0	0	2	0	0	0
Polycarbonate (PC)	0	0	0	1	0	0	0	0	0
Polyethylene (PE)	10	4	3	5	2	12	12	8	1
Polyethylene Terephthalate (PET)	0	3	2	0	1	2	0	1	1
Polypropylene (PP)	16	22	8	12	27	41	21	48	21
Polystyrene (PS)	0	1	3	1	0	1	3	0	2
Polyurethane (PU)	0	3	0	0	0	0	3	3	0
Polyvinyl alcohol	0	2	0	0	0	0	0	0	0
Rubber	0	0	0	1	0	0	4	0	0

Table S12. Mean levels of MP particles abundance for environmental samples after correcting the raw counting with the correction factor calculated with the blank samples.

Polymer Identification	**S1**		**S2**		**S3**	
	Mean (SD)	**Ratio (SD)**	**Mean (SD)**	**Ratio (SD)**	**Mean (SD)**	**Ratio (SD)**
	n	**%**	**n**	**%**	**n**	**%**
Acrylate	2.7 (3.8)	22.7 (31.7)	0 (0)	0 (0)	2 (1.7)	23.2 (23.4)
Acrylonitrile Butadiene	0 (0)	0 (0)	0 (0)	0 (0)	0.7 (1.2)	8.3 (14.4)
Ethylene Vinyl Acetate (EVA)	0 (0)	0 (0)	1.3 (1.2)	37 (54.8)	0 (0)	0 (0)
Polyamide (PA)	0.3 (0.6)	2.8 (4.9)	0.7 (1.2)	4.8 (8.3)	0 (0)	0 (0)
Polycarbonate (PC)	0 (0)	0 (0)	0.3 (0.6)	11.1 (19.2)	0 (0)	0 (0)
Polyethylene (PE)	2.4 (4.1)	21.9 (38)	1.4 (2.4)	9.9 (17.1)	0.1 (0.2)	0.7 (1.2)
Polyethylene Terephthalate (PET)	0.9 (1)	13 (16.5)	0.1 (0.2)	0.7 (1.3)	0 (0)	0 (0)
Polypropylene (PP)	0.9 (1.6)	8.3 (14.4)	1.6 (0.6)	11.8 (20.4)	4.2 (7.4)	29.8 (51.5)
Polystyrene (PS)	1.3 (1.5)	13.8 (12.8)	0.7 (0.6)	13.5 (17.5)	1.7 (1.5)	20.8 (19.1)
Polyurethane (PU)	0.4 (0.7)	6.8 (11.8)	0 (0)	0 (0)	0.1 (0.1)	0.6 (1)
Polyvinyl alcohol	0.7 (1.2)	10.7 (18.5)	0 (0)	0 (0)	0 (0)	0 (0)
Rubber	0 (0)	0 (0)	0.3 (0.6)	11.1 (19.2)	1.3 (2.3)	16.7 (28.9)
Total per slide	**9.6 (1.9)**		**6.4 (6.5)**		**10.1 (3.6)**	
Total per gram	**1.9 (0.6)**		**1.3 (1.3)**		**2.0 (0.7)**	

Experimental samples

Table S13. Abundance of MP particles identified in the blank samples and their respective correction factors.

Polymer Identification	B_1		B_2		B_3		B_4		B_5		Mean (SD)	
	n	CF	n	CF	n	CF	n	CF	n	CF	n	CF
Polylactic Acid (PLA)	0	0	0	0	1	0.0011	0	0	0	0	0.2 (0.4)	0.0002
Polyethylene (PE)	2	0.0010	1	0.0002	2	0.0021	2	0.0015	7	0.0078	2.8 (2.4)	0.0025
Polyethylene Terephthalate (PET)	3	0.0015	1	0.0002	0	0	9	0.0067	0	0	2.6 (3.8)	0.0017
Total	5		2		3		11		7		5.6 (3.6)	
Total particles per slide	2064		4135		934		1350		896			

Table S14. Raw counting of MP particles in replicates of experimental samples.

Soil	Layer	FTC treat.	Replicate	Polymer	n
S1	1	FTC	1	PLA	8
S1	1	FTC	1	PE	52
S1	1	FTC	1	PET	71
S1	1	FTC	1	Total	131
S1	1	FTC	2	PLA	13
S1	1	FTC	2	PE	59
S1	1	FTC	2	PET	89
S1	1	FTC	2	Total	161
S1	1	FTC	3	PLA	5
S1	1	FTC	3	PE	105
S1	1	FTC	3	PET	53
S1	1	FTC	3	Total	163
S1	1	NoFTC	1	PLA	10
S1	1	NoFTC	1	PE	75
S1	1	NoFTC	1	PET	85
S1	1	NoFTC	1	Total	170
S1	1	NoFTC	2	PLA	19
S1	1	NoFTC	2	PE	64
S1	1	NoFTC	2	PET	63
S1	1	NoFTC	2	Total	146
S1	1	NoFTC	3	PLA	20
S1	1	NoFTC	3	PE	57
S1	1	NoFTC	3	PET	79
S1	1	NoFTC	3	Total	156
S1	2	FTC	1	PLA	0
S1	2	FTC	1	PE	7
S1	2	FTC	1	PET	1
S1	2	FTC	1	Total	8
S1	2	FTC	2	PLA	1
S1	2	FTC	2	PE	13
S1	2	FTC	2	PET	6
S1	2	FTC	2	Total	20
S1	2	FTC	3	PLA	0
S1	2	FTC	3	PE	33
S1	2	FTC	3	PET	17
S1	2	FTC	3	Total	50
S1	2	NoFTC	1	PLA	0
S1	2	NoFTC	1	PE	0
S1	2	NoFTC	1	PET	0
S1	2	NoFTC	1	Total	0
S1	2	NoFTC	2	PLA	0
S1	2	NoFTC	2	PE	4
S1	2	NoFTC	2	PET	0
S1	2	NoFTC	2	Total	4
S1	2	NoFTC	3	PLA	0

S1	2	NoFTC	3	PE	8
S1	2	NoFTC	3	PET	0
S1	2	NoFTC	3	Total	8
S1	3	FTC	1	PLA	0
S1	3	FTC	1	PE	2
S1	3	FTC	1	PET	0
S1	3	FTC	1	Total	2
S1	3	FTC	2	PLA	0
S1	3	FTC	2	PE	7
S1	3	FTC	2	PET	0
S1	3	FTC	2	Total	7
S1	3	FTC	3	PLA	0
S1	3	FTC	3	PE	5
S1	3	FTC	3	PET	0
S1	3	FTC	3	Total	5
S1	3	NoFTC	1	PLA	0
S1	3	NoFTC	1	PE	0
S1	3	NoFTC	1	PET	0
S1	3	NoFTC	1	Total	0
S1	3	NoFTC	2	PLA	0
S1	3	NoFTC	2	PE	0
S1	3	NoFTC	2	PET	0
S1	3	NoFTC	2	Total	0
S1	3	NoFTC	3	PLA	0
S1	3	NoFTC	3	PE	2
S1	3	NoFTC	3	PET	0
S1	3	NoFTC	3	Total	2
S2	1	FTC	1	PLA	14
S2	1	FTC	1	PE	67
S2	1	FTC	1	PET	70
S2	1	FTC	1	Total	151
S2	1	FTC	2	PLA	13
S2	1	FTC	2	PE	60
S2	1	FTC	2	PET	47
S2	1	FTC	2	Total	120
S2	1	FTC	3	PLA	8
S2	1	FTC	3	PE	92
S2	1	FTC	3	PET	75
S2	1	FTC	3	Total	175
S2	1	NoFTC	1	PLA	15
S2	1	NoFTC	1	PE	46
S2	1	NoFTC	1	PET	55
S2	1	NoFTC	1	Total	116
S2	1	NoFTC	2	PLA	14
S2	1	NoFTC	2	PE	48
S2	1	NoFTC	2	PET	65
S2	1	NoFTC	2	Total	127
S2	1	NoFTC	3	PLA	8

S2	1	NoFTC	3	PE	134
S2	1	NoFTC	3	PET	82
S2	1	NoFTC	3	Total	224
S2	2	FTC	1	PLA	0
S2	2	FTC	1	PE	3
S2	2	FTC	1	PET	2
S2	2	FTC	1	Total	5
S2	2	FTC	2	PLA	0
S2	2	FTC	2	PE	4
S2	2	FTC	2	PET	2
S2	2	FTC	2	Total	6
S2	2	FTC	3	PLA	0
S2	2	FTC	3	PE	13
S2	2	FTC	3	PET	16
S2	2	FTC	3	Total	29
S2	2	NoFTC	1	PLA	0
S2	2	NoFTC	1	PE	3
S2	2	NoFTC	1	PET	4
S2	2	NoFTC	1	Total	7
S2	2	NoFTC	2	PLA	0
S2	2	NoFTC	2	PE	3
S2	2	NoFTC	2	PET	4
S2	2	NoFTC	2	Total	7
S2	2	NoFTC	3	PLA	0
S2	2	NoFTC	3	PE	0
S2	2	NoFTC	3	PET	0
S2	2	NoFTC	3	Total	0
S2	3	FTC	1	PLA	0
S2	3	FTC	1	PE	1
S2	3	FTC	1	PET	0
S2	3	FTC	1	Total	1
S2	3	FTC	2	PLA	0
S2	3	FTC	2	PE	1
S2	3	FTC	2	PET	0
S2	3	FTC	2	Total	1
S2	3	FTC	3	PLA	0
S2	3	FTC	3	PE	1
S2	3	FTC	3	PET	1
S2	3	FTC	3	Total	2
S2	3	NoFTC	1	PLA	0
S2	3	NoFTC	1	PE	2
S2	3	NoFTC	1	PET	0
S2	3	NoFTC	1	Total	2
S2	3	NoFTC	2	PLA	0
S2	3	NoFTC	2	PE	1
S2	3	NoFTC	2	PET	1
S2	3	NoFTC	2	Total	2
S2	3	NoFTC	3	PLA	0

S2	3	NoFTC	3	PE	3
S2	3	NoFTC	3	PET	0
S2	3	NoFTC	3	Total	3
S3	1	FTC	1	PLA	18
S3	1	FTC	1	PE	74
S3	1	FTC	1	PET	84
S3	1	FTC	1	Total	176
S3	1	FTC	2	PLA	25
S3	1	FTC	2	PE	106
S3	1	FTC	2	PET	76
S3	1	FTC	2	Total	207
S3	1	FTC	3	PLA	17
S3	1	FTC	3	PE	124
S3	1	FTC	3	PET	114
S3	1	FTC	3	Total	255
S3	1	NoFTC	1	PLA	11
S3	1	NoFTC	1	PE	86
S3	1	NoFTC	1	PET	77
S3	1	NoFTC	1	Total	174
S3	1	NoFTC	2	PLA	12
S3	1	NoFTC	2	PE	92
S3	1	NoFTC	2	PET	68
S3	1	NoFTC	2	Total	172
S3	1	NoFTC	3	PLA	24
S3	1	NoFTC	3	PE	82
S3	1	NoFTC	3	PET	98
S3	1	NoFTC	3	Total	204
S3	2	FTC	1	PLA	4
S3	2	FTC	1	**PE**	47
S3	2	FTC	1	**PET**	36
S3	2	FTC	1	Total	87
S3	2	FTC	2	PLA	30
S3	2	FTC	2	PE	135
S3	2	FTC	2	PET	133
S3	2	FTC	2	Total	298
S3	2	FTC	3	PLA	5
S3	2	FTC	3	PE	73
S3	2	FTC	3	PET	65
S3	2	FTC	3	Total	177
S3	2	NoFTC	1	PLA	11
S3	2	NoFTC	1	PE	46
S3	2	NoFTC	1	PET	32
S3	2	NoFTC	1	Total	89
S3	2	NoFTC	2	PLA	3
S3	2	NoFTC	2	PE	23
S3	2	NoFTC	2	PET	9
S3	2	NoFTC	2	Total	35
S3	2	NoFTC	3	PLA	15

S3	2	NoFTC	3	PE	80
S3	2	NoFTC	3	PET	81
S3	2	NoFTC	3	Total	176
S3	3	FTC	1	PLA	0
S3	3	FTC	1	PE	11
S3	3	FTC	1	PET	0
S3	3	FTC	1	Total	11
S3	3	FTC	2	PLA	0
S3	3	FTC	2	PE	19
S3	3	FTC	2	PET	0
S3	3	FTC	2	Total	19
S3	3	FTC	3	PLA	0
S3	3	FTC	3	PE	2
S3	3	FTC	3	PET	0
S3	3	FTC	3	Total	2
S3	3	NoFTC	1	PLA	0
S3	3	NoFTC	1	PE	24
S3	3	NoFTC	1	PET	0
S3	3	NoFTC	1	Total	24
S3	3	NoFTC	2	PLA	0
S3	3	NoFTC	2	PE	5
S3	3	NoFTC	2	PET	0
S3	3	NoFTC	2	Total	5
S3	3	NoFTC	3	PLA	0
S3	3	NoFTC	3	PE	2
S3	3	NoFTC	3	PET	1
S3	3	NoFTC	3	Total	3

Table S15. Mean levels of microplastic particles abundance for environmental samples after correcting the raw counting with the correction factor calculated with the blank samples.

Soil	Layer	FTC treat.	Polymer	Mean n corrected (SD)
S1	1	FTC	PE	70 (27.9)
S1	1	FTC	PET	69.6 (18.6)
S1	1	FTC	PLA	8.5 (4.1)
S1	1	FTC	Total	148.1 (17.4)
S1	2	FTC	PE	14.2 (14.8)
S1	2	FTC	PET	6.5 (7.8)
S1	2	FTC	PLA	0.3 (0.5)
S1	2	FTC	Total	21.0 (22.5)
S1	3	FTC	PE	3.2 (2.5)
S1	3	FTC	PET	0 (0)
S1	3	FTC	PLA	0 (0)
S1	3	FTC	Total	3.2 (2.5)
S1	1	NoFTC	PE	61.6 (9.1)
S1	1	NoFTC	PET	73.1 (11)
S1	1	NoFTC	PLA	16 (5.5)
S1	1	NoFTC	Total	150.8 (11.3)
S1	2	NoFTC	PE	2.3 (2.9)
S1	2	NoFTC	PET	0 (0)
S1	2	NoFTC	PLA	0 (0)
S1	2	NoFTC	Total	2.3 (2.9)
S1	3	NoFTC	PE	0 (0)
S1	3	NoFTC	PET	0 (0)
S1	3	NoFTC	PLA	0 (0)
S1	3	NoFTC	Total	0 (0)
S3	1	FTC	PE	98.3 (26.1)
S3	1	FTC	PET	89.3 (20.4)
S3	1	FTC	PLA	19.8 (4.4)
S3	1	FTC	Total	207.3 (41.1)
S3	2	FTC	PE	79.9 (43.4)
S3	2	FTC	PET	74.5 (48.6)
S3	2	FTC	PLA	12.6 (14.6)
S3	2	FTC	Total	167.1 (106)
S3	3	FTC	PE	7.2 (7)
S3	3	FTC	PET	0 (0)
S3	3	FTC	PLA	0 (0)
S3	3	FTC	Total	7.2 (7)
S3	1	NoFTC	PE	80 (7.1)
S3	1	NoFTC	PET	76.4 (15.2)
S3	1	NoFTC	PLA	15.1 (7.3)
S3	1	NoFTC	Total	171.6 (19)
S3	2	NoFTC	PE	43.9 (31.8)
S3	2	NoFTC	PET	36.8 (38.8)
S3	2	NoFTC	PLA	9.2 (6.4)

S3	2	NoFTC	Total	89.9 (76.6)
S3	3	NoFTC	PE	7.4 (10.7)
S3	3	NoFTC	PET	0 (0)
S3	3	NoFTC	PLA	0 (0)
S3	3	NoFTC	Total	7.4 (10.7)
S2	1	FTC	PE	69.9 (16.4)
S2	1	FTC	PET	61.9 (14.6)
S2	1	FTC	PLA	11.4 (3.2)
S2	1	FTC	Total	143.3 (26.7)
S2	2	FTC	PE	5.1 (5.8)
S2	2	FTC	PET	5.6 (8.3)
S2	2	FTC	PLA	0 (0)
S2	2	FTC	Total	10.7 (14)
S2	3	FTC	PE	0 (0)
S2	3	FTC	PET	0 (0)
S2	3	FTC	PLA	0 (0)
S2	3	FTC	Total	0 (0)
S2	1	NoFTC	PE	71.9 (50.1)
S2	1	NoFTC	PET	64.5 (13.1)
S2	1	NoFTC	PLA	12 (3.8)
S2	1	NoFTC	Total	148.4 (58.9)
S2	2	NoFTC	PE	0.8 (0.9)
S2	2	NoFTC	PET	1.9 (1.7)
S2	2	NoFTC	PLA	0 (0)
S2	2	NoFTC	Total	2.7 (2.5)
S2	3	NoFTC	PE	0.2 (0.4)
S2	3	NoFTC	PET	0.1 (0.2)
S2	3	NoFTC	PLA	0 (0)
S2	3	NoFTC	Total	0.3 (0.4)

8.2.2 Positive control for microplastic analysis: recovery rate

The positive control for microplastic analysis was used to estimate the recovery rate of the method used. For this purpose, a known number of microplastic particles of different polymeric compositions were counted, aided by a stereomicroscope and the ImageJ software (version 1.53; Figure S4), and spiked to soil samples (5.0 g) that underwent the same analytical processing as the environmental/experimental samples. These spiked samples were then analyzed and the number of microplastic particles identified in the final count was compared with the number of particles initially added, following the equation:

Equation S3: $Recovery\ Rate\ (\%) = (N_{recovered} - N_{S1})\ (N_{added})^{-1}$,

where $N_{recovered}$ is the number of plastic particles analyzed after the whole analytical processing, N_{S1} is the background level of plastic particles present in sample S1, and N_{added} is the number of plastic particles added to the positive control sample.

The procedure was performed separately for environmental samples and experimental samples considering the time frame for sample processing.

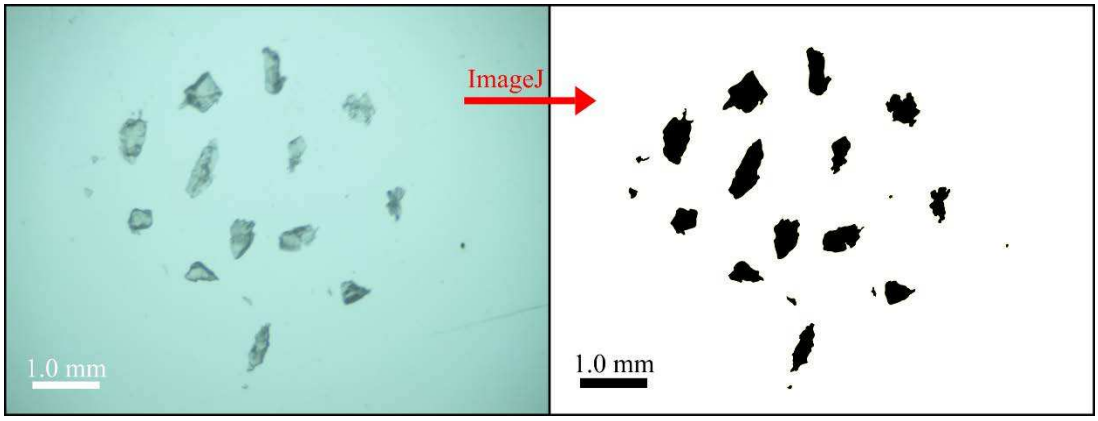

Figure S4. Example of micrograph processing in ImageJ software for counting and spiking microplastic particles in positive control samples.

Environmental samples

Table S16. Estimation of the recovery rate for microplastic analysis on environmental samples.

Sample		PE	PLA	PET	Total
Spike_1	**N_{added} (n)**	24	12	23	59
	$N_{recovered} - N_{S1}$ (n)	25	12	18	55
	Recovery Rate	104%	100%	78%	93%
Spike_2	**N_{added} (n)**	31	16	23	70
	$N_{recovered} - N_{S1}$ (n)	30	15	14	59
	Recovery Rate	97%	94%	61%	84%
Spike_3	**N_{added} (n)**	20	10	9	39
	$N_{recovered} - N_{S1}$ (n)	17	11	8	36
	Recovery Rate	85%	110%	89%	92%
Spike_4	**N_{added} (n)**	11	14	9	34
	$N_{recovered} - N_{S1}$ (n)	7	13	6	26
	Recovery Rate	64%	93%	67%	76%
Mean Recovery Rate (SD)		**87% (15%)**	**99% (7%)**	**74% (11%)**	**87% (7%)**

Experimental samples

Table S17. Estimation of the recovery rate for microplastic analysis on experimental samples.

Sample		PE	PLA	PET	Total
Spike_1	**N_{added} (n)**	59	48	57	164
	$N_{recovered}$ - N_{S1} (n)	59	18	26	103
	Recovery Rate	100%	38%	46%	63%
Spike_2	**N_{added} (n)**	31	35	42	108
	$N_{recovered}$ - N_{S1} (n)	34	26	29	89
	Recovery Rate	110%	74%	69%	82%
Spike_3	**N_{added} (n)**	33	30	31	94
	$N_{recovered}$ - N_{S1} (n)	22	17	22	61
	Recovery Rate	67%	57%	71%	65%
Spike_4	**N_{added} (n)**	40	18	19	77
	$N_{recovered}$ - N_{S1} (n)	26	11	16	53
	Recovery Rate	65%	61%	84%	69%
Spike_5	**N_{added} (n)**	26	31	40	97
	$N_{recovered}$ - N_{S1} (n)	28	29	26	83
	Recovery Rate	108%	94%	65%	86%
Mean Recovery Rate (SD)		**90% (22%)**	**65% (21%)**	**67% (14%)**	**73% (10%)**

FINAL CONSIDERATIONS

Antarctic periglacial environments are sensitive indicators of climate change and hold ecological niches interacting with abiotic components to maintain the ecosystem stability. These environments coexist with MP contamination, and continued research is needed to better understand the resulting consequences. This thesis provides the first screening of the effects of MPs in Antarctic periglacial soils and their interaction with active periglacial pedogenic processes, highlighting potential implications.

Our results showed that MPs can affect in physical, chemical and microbial properties in periglacial soils of Maritime Antarctica, even at short-term scale. While MPs in general decrease soil CEC and increase microbial activity, it became evident that different types and concentrations of MPs induce distinct responses in soil physical properties, with high levels of MP fibers increasing porosity and favoring aeration (CO_2 fluxes). The interactions of MP particles with soil structure were elucidated by micromorphological analyses, indicating that cryoturbation processes possibly mediate the observed effects by favoring particle coating, physical weathering, and characteristic structural microfeatures (planar/vesicular porosity). In turn, processes associated with FTCs were shown to favor the vertical migration of MP particles preferentially in fine-textured weathered acidic soils. In addition to MP characteristics (polymeric composition and size), soil characteristics such as mineralogy, pH, texture and organic matter content are indicated to affect the mobility of MP particles. These findings highlight the potential of MP contaminants to modify the Antarctic soil environment and interact with active periglacial pedogenic processes, which may lead to ecological consequences.

In a climate change scenario increasing soil exposure and the frequency of FTCs, the effects observed here may be intensified, further favoring dispersion and impacts of MPs in deep soil layers. Therefore, future studies are encouraged to explore long-term effects of climate change on the impacts promoted by MPs in Antarctic periglacial soils, considering the interaction of multiple factors, such as: cumulative impacts of MPs and FTCs on microbiota and gas emissions; interaction of MPs with ornithogenic processes; specific mechanisms and rate MP transport by FTCs; role of MP shape in migration promoted by FTCs.